PREFACE

Hot H atoms (H^*) from the photodissociation of HI in the gas phase react with N_2O according to the equation

$$H^{\cdot *} + N_2O \rightarrow N_2 + OH^{\cdot}$$

This reaction is also attended by a moderation process between H^* and N_2O molecules,

$$H^{\cdot *} + N_2O \rightarrow H^{\cdot} + N_2O$$

Experimental yields of H_2, N_2 and I_2 from the reactions

$$H^{\cdot\prime} + HI \xrightarrow{k_2} H_2 + I^{\cdot} \qquad (2)$$

$$H^{\cdot\prime} + N_2O \xrightarrow{k_3} N_2 + OH^{\cdot} \qquad (3)$$

$$H^{\cdot\prime} + I_2 \xrightarrow{k_7} HI + I^{\cdot} \qquad (7)$$

were analyzed kinetically and the specific rate constant ratios of $\frac{k_7}{k_2}$ and $\frac{k_2}{k_3}$ were determined. Variation of temperature at which reactions (2), (3) and (7) were allowed to proceed, also permitted us to determine the corresponding apparent activation energies E_2-E_7 and E_3-E_2. ($H^{\cdot\prime}$ represents a hydrogen atom having some average translational kinetic energy, ranging from thermal to E_{ex}, where $E_{ex} = h\nu_{(\lambda)} - D_{(H-I)}$ kcal mole^{-1}).

Effects of added carbon dioxide and helium to the HI photochemical system allowed an estimation of the number

of collisions needed to cool H^* down to normal thermal energy. By accounting for the moderating effects of N_2O, CO_2 and He semiquantitatively, fractions of hot H atom reactions were estimated. In the case of CO_2 and He, cross-section ratios of reaction relative to moderation $(\frac{\sigma_R}{\sigma_M})$, were also determined.

ACKNOWLEDGEMENT

The author wishes to express his appreciation to his research supervisor, Professor J. L. Holmes, for his invaluable advice, his encouragement and his continuous guidance throughout the course of this research. Additional acknowledgement is made to Professor Holmes for providing the author with a grant made possible under the kind auspices of the National Research Council of Canada. Appreciation is also extended to Professors M. H. Back and K. J. Laidler and to Mr. E. Kristoff for many helpful suggestions on issues surrounding this research.

Finally the author wishes to thank Mrs. W. Storto for her patience and understanding during the typing of this thesis.

TABLE OF CONTENTS

LIST OF TABLES

LIST OF FIGURES

ABSTRACT

A study of the photolysis of HI in the presence of N_2O was carried out at low conversions at temperatures of 25°C, 5°C and -20.5°C using the 2537 Å, 3130 Å and 3660 Å wavelengths. The main products of the photolysis were H_2, N_2, I_2 and H_2O, and the stoichiometric relationship between H_2, N_2 and I_2 was such that $H_2 + N_2 \equiv I_2$.

N_2O reduced the quantum yield of H_2 (ϕ_{H_2}); it was further observed that the reduction in ϕ_{H_2} was influenced by the iodine and hydrogen iodide concentrations and also by the $\frac{[N_2O]}{[HI]}$ ratio. However, the H_2 quantum yield attained a limiting value at a certain $\frac{[N_2O]}{[HI]}$ ratio and beyond this ratio, the ratio of H_2 to N_2 became constant. To account for the limiting behaviour of H_2 and N_2 production, the theory of constant partitioning of hot hydrogen atoms between reaction and moderation with N_2O when a certain level of N_2O was reached, was put forward.

The reactions

$$H^{\cdot} + HI \xrightarrow{k_2} H_2 + I^{\cdot}$$

$$H^{\cdot} + N_2O \xrightarrow{k_3} N_2 + OH^{\cdot}$$

$$H^{\cdot} + I_2 \xrightarrow{k_7} HI + I^{\cdot}$$

constituted the pertinent chemical processes occurring within the photochemical system, and the steady state derived equation

$$\frac{dH_2}{dt}\cdot\frac{1}{I_a} = \frac{1}{1 + \frac{k_7}{k_2}\frac{[I_2]}{[HI]} + \frac{k_3}{k_2}\frac{[N_2O]}{[HI]}}$$

or $$\frac{1}{\phi_{H_2}} = 1 + \frac{k_7}{k_2}\frac{[I_2]}{[HI]} + \frac{k_3}{k_2}\frac{[N_2O]}{[HI]}$$

afforded a number of predictions which were all borne out experimentally. $\frac{k_7}{k_2}$ and $\frac{k_2}{k_3}$ were both dependent on the wavelength used, being largest at 3660 Å and smallest at 2537 Å. However, $\frac{k_7}{k_2}$ showed little change with temperature at any one particular wavelength ($E_2-E_7=.42\pm.4$ kcal mole^{-1} for λ = 2537 Å) whereas $\frac{k_2}{k_3}$ changed appreciably with temperature at 3130 Å ($E_3-E_2=2.88\pm.31$) and at 3660 Å ($E_3-E_2=3.69\pm.44$). The values of $\frac{k_7}{k_2}$ (e.g. 3.1, 7.0 and 11.0) compared well with previously recorded values, while the $\frac{k_2}{k_3}$ values (e.g. 18.0, 28.0 and 50.0) were new.

Experiments in which the incident light intensity (I_o) was varied for constant values of [HI], [I_2] and [N_2O] resulted in $\frac{dH_2}{dt}\cdot\frac{1}{I_o}$ being constant.

A study of the effect of moderator pressure on N_2 production revealed that the $H^{\cdot} + N_2O \rightarrow N_2 + OH^{\cdot}$ reaction is a very sensitive indicator of the presence of hot H atoms. An assessment of the role of hot H atoms in the HI/N_2O photochemical system indicated that the ratio of hot H atom reactions to hot H atom moderation is nearly twice as large for the 2537 Å wavelength.

GLOSSARY OF SYMBOLS

$D_{(H-I)}$	Bond dissociation energy of HI.
ε	Extinction coefficient.
E_{abs}	Radiation energy absorbed.
E_{ex}	Excess energy.
$E(I^*)$	Excitation energy of iodine atom.
γ	Fraction of hot H atom reactions.
h	Planck's constant.
$H^{\cdot\prime}$	Hydrogen atom having some average translational kinetic energy.
$H^{\cdot *}$	Hot hydrogen atom.
$h\nu$	Energy of radiation of frequency ν.
$[HI]_f$	Final concentration of HI.
$[HI]_i, [HI]_o$	Initial concentration of HI.
$[I_2]_f$	Final concentration of iodine.
$[I_2]_i$	Concentration of added iodine.
$[I_2]_p$	Concentration of iodine produced.
$[I_2]_T$	Total concentration of iodine.
I_o	Intensity of incident radiation.
I_a	Intensity of absorbed radiation.
k_2	Specific rate constant for the reaction $H^{\cdot} + HI \rightarrow H_2 + I^{\cdot}$.
k_3	Specific rate constant for the reaction $H^{\cdot} + N_2O \rightarrow N_2 + OH^{\cdot}$.
k_7	Specific rate constant for the reaction $H^{\cdot} + I_2 \rightarrow HI + I^{\cdot}$.

$(\frac{k_7}{k_2})_\infty$	Specific rate constant ratio at large concentration of inert gases.
λ	Wavelength of exciting radiation.
η	Non-bonding orbital.
N	The number of moderating collisions occurring between initial and final energies.
$[N_2O]_o$	Initial concentration of N_2O.
P	Probability of the occurrence of the $H^\cdot + N_2O \rightarrow N_2 + OH^\cdot$ reaction.
π	Pi-bonding orbital.
R	k_7/k_2 ratio.
σ	Sigma-bonding orbital.
σ_M	Moderation cross-section.
σ_R	Reaction cross-section.

CHAPTER 1

INTRODUCTION

The study of photochemistry deals with an unique type of chemical reaction. It is concerned with the interaction of a light quantum with a molecule and the subsequent chemical and physical changes resulting from this interaction.

Four important photochemical rules or laws of general application have evolved over the years. These may be stated as follows:

1. Only the light absorbed by a system is effective in producing a photochemical change - Grotthus-Draper Law (1).
2. Each photon absorbed activates one molecule in the primary excitation step of a photochemical sequence - Stark-Einstein Law of Photochemical Equivalence (2).
3. Each photon absorbed by a molecule has a certain probability of populating either the lowest excited singlet state S_1, or the lowest triplet state T_1.
4. The lowest excited singlet and triplet states are the starting points (in solution) of many photochemical processes particularly organic photochemical processes.

Generally, photochemical reactions can be very complex in nature, and the measured chemical change is rarely

that directly produced by the light. It is necessary, therefore to distinguish between the 'primary' effect of the light and the 'secondary' thermal reactions which follow. If there were only primary processes then the quantum yield, ϕ, which is defined as the number of molecules reacting per quantum absorbed, should be unity. In most cases, owing to secondary processes taking place, the quantum yield is greater or less than one. Thus according to Bodenstein (3) who measured the quantum yield of a large number of reactions, the values of ϕ range from 0.002 for the decolouration reactions of certain dyes to $>10^6$ for the reaction of chlorine with hydrogen.

Absorption of Light

According to Planck, the absorption of electromagnetic energy by a molecular (or atomic) species involves only stepwise transitions. The Planck equation, $E = h\nu$, shows that the energy of these stepwise or quantized absorptions is related directly to the excitation frequency, ν, (and hence the wavelength). It was proposed that during the process of electromagnetic radiation absorption, the energy of the electromagnetic wave is transferred to the molecule by a mechanism involving excitation of the overall molecule to some higher motional frequency and (or) electronic energy state. These processes are quantum processes, energetically distinct and stepwise, and as such require radiation of a particular wavelength. For a molecule to absorb a quantum of

energy $h\nu$, it depends on whether there is an energy difference between two energy levels in the molecule equal to $h\nu$, and on whether a transition between these two states is allowed by symmetry and momentum conservation rules.

The energy in a molecule can be divided into translational, vibrational, rotational and electronic contributions; electronic transitions require the greatest energies. Changes in electronic energy are of the order of 100 kcal $mole^{-1}$, giving an absorption spectrum in the visible or ultraviolet region. The associated vibrational energy changes are about 5 kcal $mole^{-1}$, and they produce the coarse 'vibrational' and the finer 'rotational' structure of the electronic spectral band. In comparison with the above energy values it may be noted that the average translational kinetic energy of a molecule at the ordinary temperature is 3/2 RT or about 1.0 kcal $mole^{-1}$ and since the probability of a molecule possessing energy > E is proportional to $\exp(-E/RT)$, it is evident that high temperatures are necessary to produce electronic transitions by heat alone, and that at ordinary temperatures all but a few molecules will be in their lowest vibrational level. Most of the molecules will however have several quanta of rotational energy.

The immediate product of absorption of a photon is an excited state of the absorbing molecule, with energy in excess of the normal state equal to the energy of the photon which it absorbed. The excited molecule may then react with

another molecule, since its reactivity is greatly increased, or it might dissociate or following a collisional encounter cause another molecule to dissociate into free radicals, the radicals subsequently react in diverse ways. Visible and ultra-violet light are of chemical importance because photons in this range are capable of rupturing the molecule.

Apart from dissociation of molecules into neutral particles, one of which may be excited, Terenin and Popov (4) observed cases of photo-ionization consisting of the decomposition of a molecule into oppositely charged ions. This type of photo-ionization was detected during the exposure of halide salts of univalent thallium which decomposes as,

$$T\ell X + h\nu \rightarrow T\ell^{+} + X^{-}$$

The absorption at very low wavelengths may lead entirely to the ionization of a molecule. Photons may ionize a molecule much more readily than dissociate it, even if its ionization potential is higher than its dissociation energy. The process may be represented as

$$M + h\nu \rightarrow M^{+} + e^{-}$$

This is a particular case of the photoelectric effect, but in ordinary photochemical reactions, it apparently does not play a particularly important part since the ionization potential is usually 10 eV (230.5 kcal/mole) and higher which corresponds to a wavelength ($\lambda < 1200$ Å) in the vacuum U.V. region of the

spectrum. A number of experimental procedures have been described to determine ionization potentials in the vacuum ultra-violet using more or less conventional photolysis techniques, with windows of LiF(5), artificial sapphire or very thin quartz separating the lamp from the photolysis vessel. Below 1000 Å, the transparency of these window materials becomes extremely poor and hence windowless apparatus have been designed (6) which utilize the principle of a fast-flow separation system. By these methods, ionization potentials have been measured for a number of compounds (7). These ionization potentials are very useful parameters for correlating many physicochemical properties, like electronegativity, heterolytic bond dissociation energy, strain in cyclic rings, etc.

The position of an absorption band is often expressed by its wavelength (λ) in angstroms or its wave number ($\bar{\nu} = 1/\lambda$) in reciprocal centimeters. For example, 3000 Å is equivalent in wave numbers to

$$\bar{\nu} = \frac{1}{3000\ \text{Å}} = \frac{1}{3\times10^{-5}\ \text{cm}} = 3.33\times10^{4}\ \text{cm}^{-1}$$

or in frequency to

$$\nu = \frac{c}{\lambda} = \frac{3\times10^{10}\ \text{cm/sec}}{3\times10^{-5}\ \text{cm}} = 10^{15}\ \text{sec}^{-1}$$

The energy required to produce an excited state is obtained by inspection of the absorption or emission spectrum of the molecule in question together with the application of the

equation

$$E_2 - E_1 = h\nu \qquad (1.1)$$

where h is Planck's constant, ν is the frequency (sec^{-1}) at which absorption occurs, and E_2 and E_1 are the energies of a single molecule in the final and initial states. Equation (1.1) may be rewritten as

$$E_2 - E_1 = h\bar{\nu}c = 2.86 \times 10^{-3}\ \bar{\nu} \qquad (1.2)$$

or $E_2 - E_1 = \frac{2.86 \times 10^5}{\lambda}$, $E_2 - E_1$ is the energy difference between the initial and final states in kcal/mole.

The amount of energy produced through the absorption of one mole of photons by a compound at a given wavelength is equivalent to the energy of 6.02×10^{23} photons. This energy is called an einstein. Thus an einstein of 6,000 Å (16,670 cm^{-1}) light is equal to

$$E_2 - E_1 = \frac{2.86 \times 10^5}{6{,}000\ \text{Å}} = 47.7 \text{ kcal}$$

For a photochemical reaction to occur, the energy of the quantum must be equal to or greater than the energy required to produce activation or dissociation. It does not necessarily follow, however, that such dissociation will occur merely because sufficient energy has been provided.

Nature of Photochemical Reactions

Photochemical reactions may be classified as direct or sensitized. In a direct photochemical reaction one or more

of the substances undergoing reaction absorb the light. In a sensitized reaction some substance absorbs light and induces a reaction in which it does not participate. Many compounds like hydrogen, nitric oxide and hydrocarbons, absorb light in the far ultra-violet region which is difficult to study, though McNesby and co-workers (8), with improved experimental techniques, have studied the photolysis of hydrocarbons in the far ultra-violet. However, mixing with a foreign substance - a sensitizer - which absorbs light in a more accessible spectral region, and using the possibility of collisional transfer of excitation energy of the sensitizer to reactant molecules, makes it possible to carry out photochemical reactions of compounds which do not absorb in this spectral region. Photosensitization by mercury, cadmium and zinc has received considerable attention in recent years (9-16). In the case of mercury photosensitization, the mechanism involves the following processes,

$$Hg(6\ ^3P_1) \leftarrow^{2537\ \mathring{A}} \rightarrow Hg(6\ ^1S_0) \qquad (1.3)$$

The $Hg(6\ ^3P_1)$ either radiates back to the $(6\ ^1S_0)$ ground state (radiative life time 10^{-7} sec) (10), returns to the ground state by giving up its energy to a colliding partner,

$$Hg(6\ ^3P_1) + M \rightarrow Hg(6\ ^1S_0) + M^* \qquad (1.4)$$

or is transformed by a collision-induced radiationless transition to the metastable $(6\ ^3P_0)$ state.

$$Hg(6\ ^3P_1) + M \rightarrow Hg(6\ ^3P_0) + M\dagger$$

The latter cannot return to the ground state by emission since the transition is doubly forbidden with J=0 → J=0 and ΔS=1. The $Hg(6\ ^3P_0)$, thus, has a very long radiative lifetime ($\approx 10^{-3}$ sec) (11) and the probability of its suffering a collision before radiating is very great. Examples of mercury photosensitized reactions are,

$$Hg(6\ ^3P_0) + X_2 \rightarrow Hg(6\ ^1S_0) + 2X(^2S_{1/2}) \qquad (1.5)$$

$$Hg(6\ ^3P_1) + X_2 \rightarrow Hg(6\ ^1S_0) + 2X(^2S_{1/2}) \qquad (1.6)$$

where X_2 in this case is a diatomic molecule. In the case of the other resonance line of mercury, the mechanism is:

$$Hg(6\ ^1S_0) + h\nu(1849\ \text{Å}) \rightarrow Hg(6\ ^1P_1) \qquad (1.7)$$

Since there are no metastable singlet states near $Hg(6\ ^1P_1)$, photosensitization by 1849 Å can only occur if $Hg(6\ ^1P_1)$ transfers its energy before radiating. This is to be regarded as a low probability process since the radiative lifetime is small relative to the time between collisions. Very little work has been done on $Hg(6\ ^1P_1)$ sensitized decomposition, mostly because it has not been easy to produce the $(6\ ^1P_1)$ species without also generating the $(6\ ^3P_1)$ variety. This difficulty is due to the inevitability of the appearance of the 2537 Å line as well as the 1849 Å line in mercury discharge lamps. One approach to the problem takes advantage of the fact that mercury absorbs 1849 Å radiation much more strongly

than the 2537 Å radiation, provided the vapour pressure of mercury is maintained at the -10°C saturation pressure (12).

Mori (13) has studied the Hg($6\ ^1P_1$) sensitized decomposition of CO_2 whose decomposition is only very slowly sensitized (14,15) by Hg($6\ ^3P_1$). He found CO to be the only gaseous product. It has also been found that the Hg ($6\ ^1P_1$) sensitized decomposition of NO gives, mainly, N_2 and N_2O_3 (16).

The study of photochemical reactions may be divided into two main parts: (i) a study of the immediate effect of the light on the absorbing molecule which is the primary process, and (ii) a study of the reactions of the molecules, atoms or radicals produced by the primary process.

Photochemical Primary Processes

Noyes et al (17) defined the primary process as 'one which comprises the series of events beginning with the absorption of a photon by a molecule and ending with the disappearance of that molecule or with its conversion into a state such that its reactivity is statistically no greater than that of similar molecules in thermal equilibrium with their surroundings.'

In the primary photochemical process there are usually a variety of paths for degradation of electronic energy of excitation. Chemical paths include intramolecular rearrangements (18-20) or the formation of free radicals and excited molecules which may react in secondary processes to

form new products of chemical interest. However, also usually included in the overall photochemical reactions are radiative and non-radiative photophysical processes which do not lead to a net chemical change, yet are alternate paths for the loss of the absorbed energy. Such processes involving electronically excited states are of great interest to the spectroscopist and photochemist alike. Thus, as Noyes et al (17) point out, "The complete elucidation of a primary photochemical process must include an understanding of all that transpires, whether or not a chemical reaction occurs."

The majority of the unexcited molecules will be in the ground electronic and vibrational states and during an electronic transition the nuclei of the molecule can be considered to be stationary, since the transition occurs within about 10^{-15} sec. Thus a transition on an energy level diagram is approximately vertical. This statement, due to Franck and elaborated by Condon (21) is known as the Franck-Condon principle. The nature of photoexcitation is determined by this principle, by the energy of incident radiation and by the relative positions of the potential energy surfaces (22). Electronic transitions in a molecule are also subject to spin conservation rules first postulated by Wigner (23) according to which, transitions involving change in multiplicity are forbidden. This rule is well obeyed by small molecules, but in the case of large molecules, perturbation of the energy levels leads to a partial breakdown of this selection rule and the transition can occur.

The excitation energy, which a molecule A acquires upon absorption of a photon, may be dissipated by any one of the three general processes given in equations (1.8), (1.9), and (1.10):

$$A^*(\text{EXCITED}) \xrightarrow{\text{EMISSION}} A_o + h\nu \qquad (1.8)$$

$$A^*(\text{EXCITED}) \xrightarrow{\text{RADIATIONLESS CONVERSION}} A_o + \text{HEAT} \qquad (1.9)$$

$$A^*(\text{EXCITED}) \xrightarrow{\text{CHEMICAL REACTION}} \text{PRODUCT} \qquad (1.10)$$

Energy diagrams such as Figure 1.1 illustrate the important processes involving electronically excited states. The figure indicates the lowest singlet (spin paired) S_1 and the lowest triplet (spins unpaired) T_1 excited states. The horizontal lines indicate the electronic excitation energy (relative to the ground state) of the various states in their lowest vibrational level. Radiative processes are indicated by a solid arrow and radiationless processes are indicated by a broken arrow.

The radiative lifetime of an excited state may be often defined in terms of a first-order decay processes. It is important to differentiate the 'true' or inherent radiative lifetime T^o of a state - i.e., the reciprocal of the rate constant for the disappearance of this state if emission were the only path of energy dissipation - and the 'actual' or measured lifetime T, which is the reciprocal of the sum of the rate constants of a number of competing first-order (or pseudo-first-order) processes.

Figure 1.1

Electronic energy state diagram showing typical unimolecular rate constants in sec^{-1} for radiative and non-radiative transitions (continuous and broken lines respectively) for organic molecules with lower $\pi^*-\pi$ states (values in brackets refer to molecules with low $\pi^*-\eta$ states).

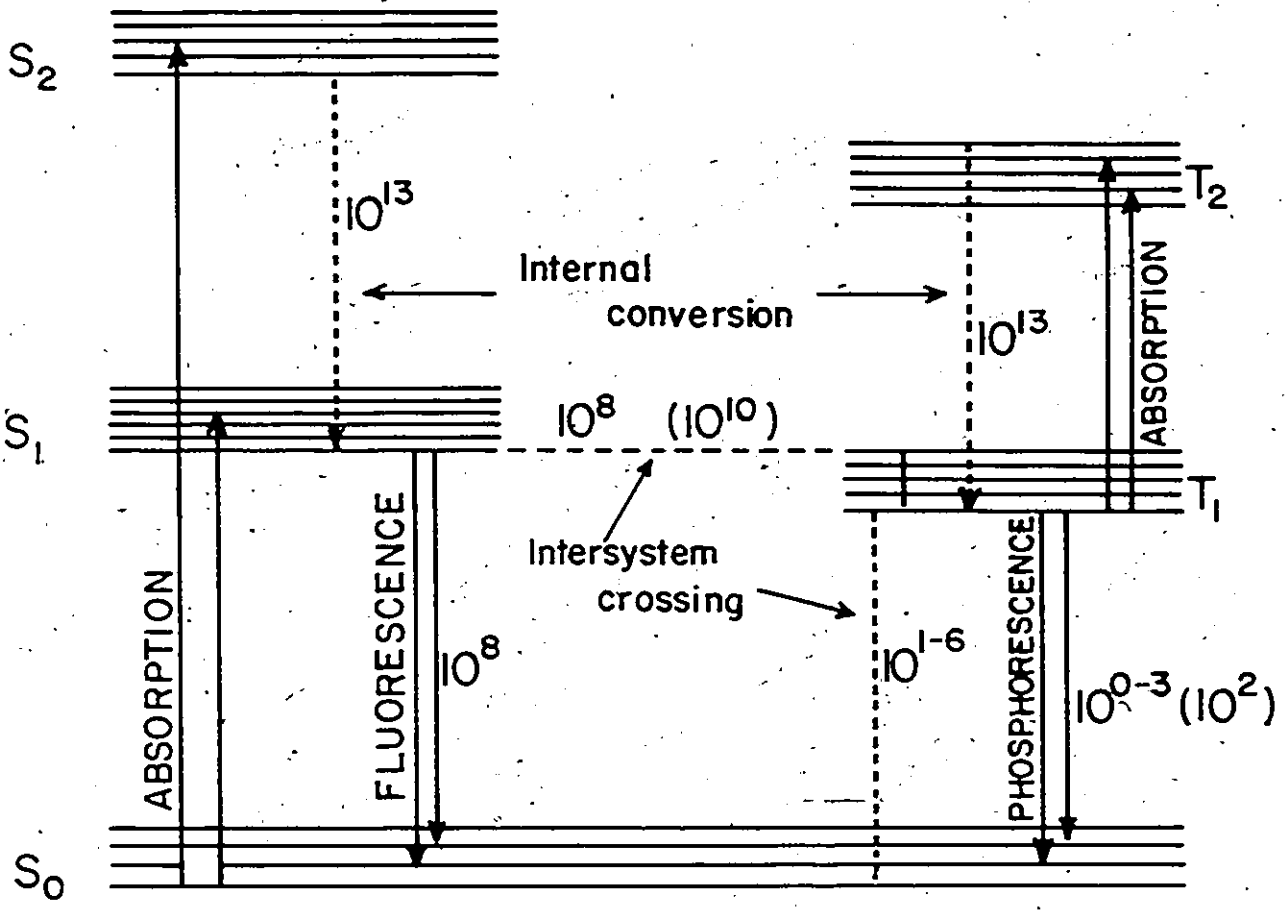
S_2
S_1
S_0
T_2
T_1
10^{13}
Internal conversion
10^{13}
ABSORPTION
10^8 (10^{10})
Intersystem crossing
ABSORPTION
FLUORESCENCE
10^8
10^{1-6}
PHOSPHORESCENCE
10^{0-3} (10^2)

FIGURE 1·1

The time scale of a photochemical sequence is set by the rate of spontaneous radiative emission to the ground state S_o, from S_1 and/or T_1 - i.e., no reaction which competes for deactivation of these states can require much longer time than T^o for emission, or the latter process will dominate.

When a molecule in the ground singlet state absorbs a photon, the resulting excited molecule will also be in a singlet state and may do one of the following things:

(i) Fluoresce: The vibrational quanta possessed by the electronically excited molecules will be quickly degraded into thermal energy through intermolecular collisions. Since the undisturbed lifetime of the excited state is of the order of 10^{-8} seconds, it being assumed that the transition back to the ground state is allowed, emission of the absorbed quantum as fluorescence will occur from the lowest vibrational level of the upper state to upper levels of the ground state, or to put it alternatively, the fluorescence emission spectrum will be of longer wavelengths than the absorption spectrum and will bear an approximately 'mirror-image' relationship to the absorption.

(ii) Undergo Internal Conversion: In many cases, the electronically excited state of the molecule, although potentially fluorescent, is deactivated before it can emit its energy as fluorescence. This can occur, amongst other ways, when there is crossing of potential energy surfaces of the excited and ground electronic states. A radiationless transi-

tion can then occur from the excited state to high vibrational levels in the ground state. The vibrational energy is then quickly degraded into thermal energy through molecular collisions. Usually the term internal conversion refers to a non-radiative transition between states of the same multiplicity and inter-system cross-over refers to a non-radiative transition between states of different multiplicity (24).

(iii) Undergo intersystem cross-over to a triplet state: These are schematically illustrated in Figure 1.1. Figure 1.2 indicates more clearly these primary processes on a potential energy diagram.

(iv) Undergo energy transfer through collision: Here two kinds of collisions can be visualized, 'elastic' collisions in which there is no transfer of energy from the excited to the unexcited molecule, and 'inelastic' collisions in which there is an energy transfer. These collisions are sometimes called 'collisions of the second kind.' The most likely conditions for an energy transfer are obtained when there is resonance between the corresponding energy levels which may be either electronic, vibrational or rotational. The smaller the amount of energy which appears as kinetic energy in a transfer, the more likely it is that the transfer will occur. Electronic energy transfer may lead to the phenomenon of sensitized fluorescence, as well as the possibility of dissociation of the acceptor molecule.

(v) Undergo dissociation: As was mentioned earlier, the

Figure 1.2

Potential energy diagrams showing radiative and non-radiative transitions (continuous and broken lines respectively).

A vibrational deactivation

B internal conversion

C fluorescence

D intersystem crossing and phosphorescence

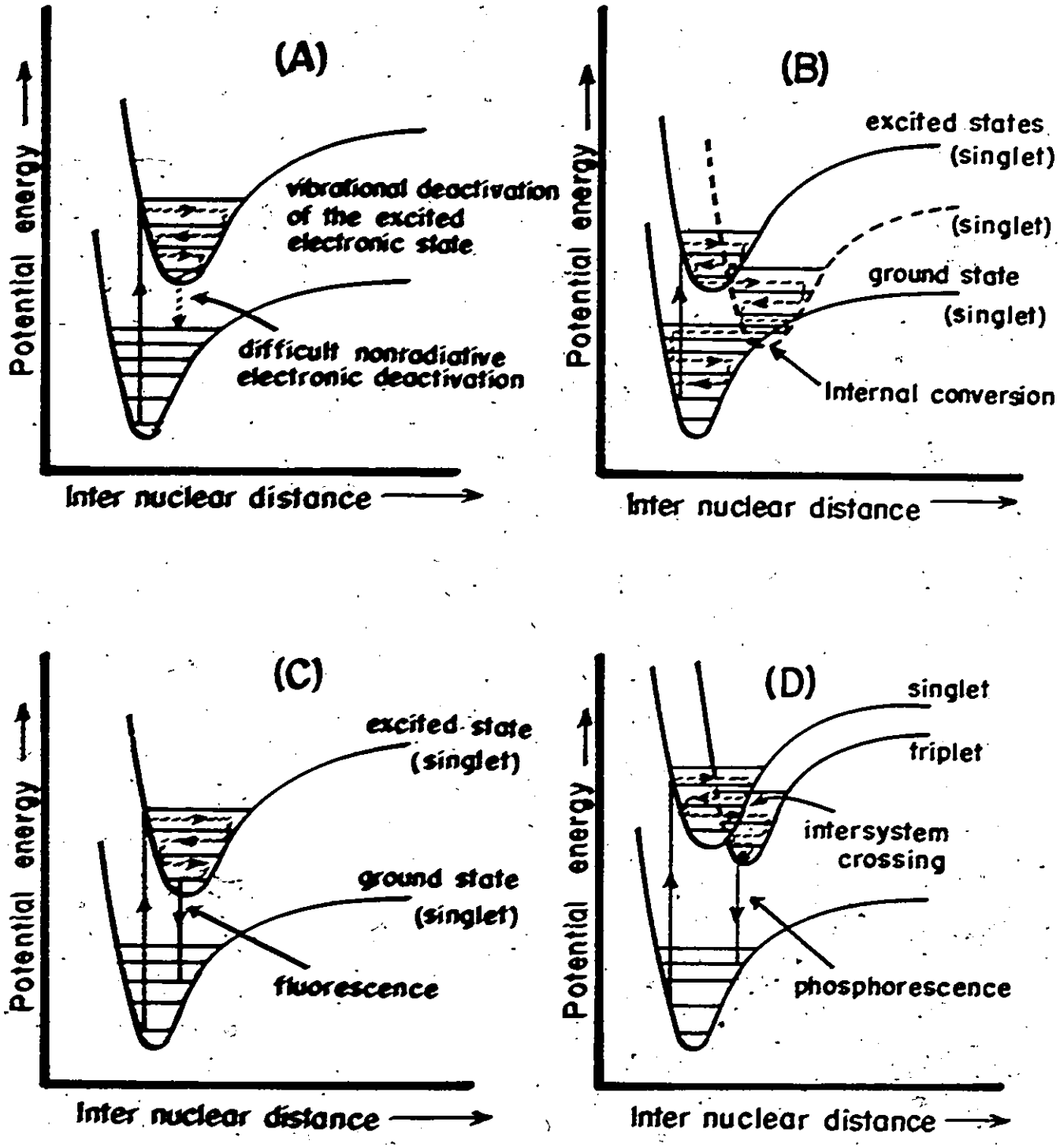
(A)
Potential energy
vibrational deactivation of the excited electronic state
difficult nonradiative electronic deactivation
Inter nuclear distance
(B)
Potential energy
excited states (singlet)
(singlet)
ground state (singlet)
Internal conversion
Inter nuclear distance
(C)
Potential energy
excited state (singlet)
ground state (singlet)
fluorescence
Inter nuclear distance
(D)
Potential energy
singlet
triplet
intersystem crossing
phosphorescence
Inter nuclear distance

FIGURE 1-2

absorption of a photon of visible or ultra-violet light by a molecule can, in some instances, lead to its rupture. This can occur either through the excited molecules being in a repulsive state as in the case of HI (25) at longer wavelength or through its having sufficient vibrational energy in either its upper or lower state to cause it to dissociate. Generally the bond broken is the same as that responsible for light absorption (disulphides, some simple olefines). Sometimes, however, when the bond energies in the chromophoric group are greater than that of the absorbed quantum, this energy may find its way to another, weaker bond in the molecule through resonance energy transfer, and this bond is broken. For example, the irradiation of acetone leads to the production of a methyl and an acetyl radical, although the light is absorbed by the carbonyl group. This process can be thought of as an internal energy transfer.

(vi) Chemical quenching: The excited state can lose its energy, not only through a physical energy transfer on collision, but also through chemical reaction with the quencher molecule. In many cases self-quenching of the excited state may occur, either as a physical effect analogous to solvent quenching or else through dimerization.

Quenching of fluorescence consists of the weakening of the intensity of fluorescence in the presence of foreign admixtures or during increase in pressure (or concentration) of the fluorescent substance itself. The method of measuring the

absolute quenching efficiencies of gases have been fully set out by Mitchell and Zemansky (26) and are not elaborated here. Much work has been done on the quenching of $Hg(6\ ^3P_1)$. When $Hg(6\ ^3P_1)$ atoms interact with molecules of a foreign gas, a transfer of energy may occur with the return of the Hg atoms to the ground state $(6\ ^1S_0)$ by means of a non-radiative transition. The $(6\ ^3P_1) \rightarrow (6\ ^1S_0)$ fluorescence is thus quenched. Absolute values of quenching cross sections which are a measure of the probability of quenching processes have been reported (22,27). The simplest kinetic system of this type may be represented by the following scheme,

$$\text{Absorption} \quad A + h\nu \xrightarrow{I_a} A^* \tag{1.11}$$

$$\text{Deactivation} \quad A^* + A \xrightarrow{k_2} 2A + \text{Heat} \tag{1.12}$$

$$\text{Quenching} \quad A^* + M \xrightarrow{k_3} A + M^* \tag{1.13}$$

$$\text{Emission} \quad A^* \xrightarrow{k_4} A + h\nu \tag{1.14}$$

Here A denotes the atom or molecule which is excited electronically to A^* by the absorption of radiation and M is a substance which can quench by reaction (1.13). I_a is the rate of light absorption (in einsteins $\text{litre}^{-1}\ \text{sec}^{-1}$) = rate of formation of A^* (which may be singlet or triplet). The kinetic equations for this system were worked out by Stern and Volmer (28) whose results can be expressed by the following equations:

$$\frac{\phi_o}{\phi_M} = 1 + \frac{k_3}{k_2 + k_4}[M] \tag{1.15}$$

$$\text{or} \qquad \frac{I}{I_o} = \frac{1}{1 + k_2\tau[A] + k_3\tau[M]} \qquad (1.16)$$

$$\text{where} \qquad \tau = \frac{1}{k_2 + k_4} \qquad (1.17)$$

ϕ_o is the quantum yield for emission from A^* in the absence of M, and ϕ_M is the quantum yield for emission from A^* in the presence of M. I is the intensity of emitted radiation in einsteins per second, I_o is the intensity of emitted radiation in the absence of foreign gas [M]. Here τ is the measured lifetime of A^* in the absence of M. If the assumed mechanism above is operating, then a plot of (ϕ_o/ϕ_M) vs [M] will produce a straight line with a slope of $k_3\tau$. Since the value of τ can be measured in the absence of M, k_3, the bimolecular quenching constant for deactivation of A^* by M through energy transfer, can be derived. If such a Stern-Volmer plot is found experimentally, we have obtained 'prima facie' evidence that a mechanism in which there is competition between a bimolecular quenching process and unimolecular processes (e.g., emission) for deactivation of A^* is operating. It has been shown recently (29) that for the Stern-Volmer equation of (1.16) to be valid, both the pressure of the fluorescent substance and the pressure of the quenching gas must be small (<0.1 cm Hg).

Measurement of light emission may be used to determine the extent of fluorescence. A detailed study of the system will in principle provide information about the extent

of dissociation. Unless there exists some way of determining the number of triplet state molecules formed, there is no way to distinguish clearly between internal conversion and intersystem cross-over (30). Evidence for internal conversion in most polyatomic molecules is far from conclusive. In principle, such conversions might occur as either kinetically first order or as second order processes. Under most experimental conditions, ground state molecules with very large amounts of vibrational energy which might be formed by internal conversion would be hard to detect. Fortunately, internal conversions seems to be of negligible importance (31,32).

There are several methods for determining the presence of triplet state molecules. These may be summarized briefly as follows: (i) character of the emission, that is, the emission must be demonstrated clearly to be characteristic of the triplet state either by analysis of the spectrum or by determination of the mean lifetime of the emission (33). In this connection it may be pointed out that an excited singlet state can be converted to a triplet state through a radiationless intersystem crossover, as shown in Figure 1.2. Emission can then take place from triplet to ground state, which is a spin forbidden transition, with a longer mean life than that from the corresponding singlet state. This is often called phosphorescence. (ii) by energy transfer to other molecules on collision, thus leading to a preferential emission or reaction from the triplet state of the colliding partner (29,

34). There are indirect and much less reliable methods available in some instances. For example, triplet states are at lower energies than the corresponding singlet states. This means frequently that dissociation from such states will require more activation energy than from corresponding singlet states.

The triplet state molecules may go back to the excited singlet state by intersystem cross-over, which may then lead to emission. This is known as 'delayed fluorescence' and is similar to ordinary fluorescence but the emission occurs only after a certain interval of time.

Electronic Excitations in Organic Compounds

Molecular Orbitals: Five types of molecular orbitals are of interest to the organic photochemist. These are pi-bonding (π), pi-antibonding (π^*), non-bonding (η), sigma-bonding (σ) and sigma-antibonding (σ^*) orbitals. Single bonds between two atoms involve σ orbitals and the σ-electrons located in these orbitals are strongly bonding and essentially localized. Consequently, σ electrons require greater excitation energy than π electrons which occupy the π or multiple-bond orbitals. For each σ and π orbital there corresponds a σ^*- and π^*-antibonding orbital, respectively. Certain hetero-atoms (e.g., oxygen, nitrogen) introduce the possibility of η orbitals which are essentially localized on the particular atom and have no antibonding counterpart. Figure 1.3 shows an energy level diagram for bonding and non-bonding orbitals.

Figure 1.3

Energy level diagram for bonding and non-bonding orbitals.

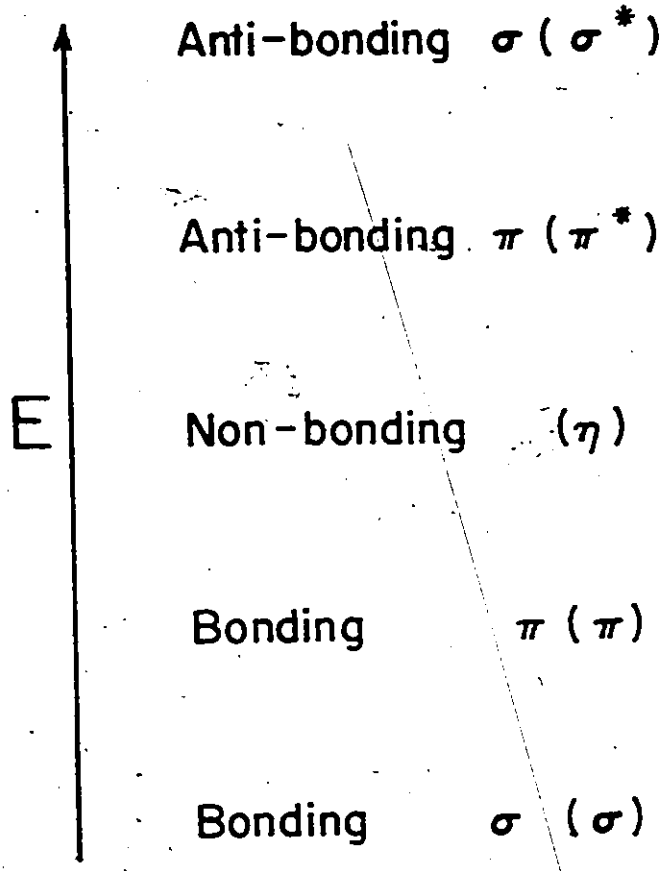
Anti-bonding σ (σ*)
Anti-bonding π (π*)
E
Non-bonding (η)
Bonding π (π)
Bonding σ (σ)

FIGURE 1-3

Typical η Orbitals: The η orbital is often involved in the lowest energy electronic transitions possible for molecules containing heteroatoms. The form of such orbitals is shown for a carbonyl group in Figure 1.4(a). These orbitals are called 'non-bonding' because they take little part in the actual bonding and concentrate very little electron density between nuclei. In the case of the carbonyl group, the η orbital is assumed to be an essentially pure p orbital localized on the oxygen atom; in the case of pyridine (not shown) the η orbital is a sp^2 hybrid. For both molecules the η orbital is located in the plane of the molecule and is perpendicular to the π orbitals of the molecule.

Electrons in η orbitals are characterized by (a) a low ionization potential required to remove them from the molecular system, (b) a relative insensitivity of the (spectroscopic) vibrational constants of the molecule from which this electron is removed - i.e., since η electrons contribute little to the bonding between atoms, removal of the η electron has little effect on the vibrations between atoms.

π and π* Orbitals: π and π* orbitals are delocalized over two or more nuclei. The π orbitals of interest to the organic photochemist are usually pictured as some combination of p orbitals as, for example, the carbonyl group shown in Figure 1.4(b). Corresponding to each π orbital there is a π* orbital which has a node between the carbon and oxygen atoms, as shown in Figure 1.4(b).

The relatively greater electronegativity of oxygen versus carbon causes the mobile π electrons to undergo a considerable displacement from carbon to oxygen. In contrast, the π^* orbital has charge displacement from oxygen to carbon. Both the π and π^* orbitals possess a plane of antisymmetry which coincides with the molecular plane. Virtually all electronic transitions of interest to the organic photochemist involve a π or π^* orbital.

σ and σ^* Orbitals: Since the σ-bonding orbitals σ are usually of low energy with respect to π and n orbitals and the σ-antibonding orbitals σ^* are of relatively high energy, compared to π^* orbitals, neither of these σ orbitals will be encountered very often. Both the σ and σ^* orbitals are cylindrically symmetrical about the inter-nuclear axis of the atoms forming the σ bond (Figure 1.4(c)). The σ^* orbital has a node between the atoms forming the σ bond, which causes the bond to break when an electron is promoted to a σ^* orbital.

Besides the Kasha notation (35) of σ, σ^*, π, π^* and n, specifying different molecular states, there are other types of notation which have been employed when describing an electronic transition of a polyatomic molecule (36,37). One of these is the classification introduced by Mulliken (37). In this classification, states are represented by different capital letters N, Q, V, T, R, etc., where N (normal) stands for the ground state and V (valence) stands for an excited state having large ionic character. Thus the process

$HI + h\nu \rightarrow H^+I^-$ at ~2100 Å represents a V ← N transition (Chapter 2, Figure 2.1). Such transitions have high intensities and in organic molecules are generally designated as $\pi \rightarrow \pi^*$ transition. Transitions in which the transition moment is at right angles to the inter-nuclear axis, are designated Q ← N transitions and the bands (e.g., for the hydrogen halides) typically have low intensities (as do $\eta \rightarrow \pi^*$ transitions in polyatomic molecules).

In formaldehyde, which has both η and π electrons, two types of transitions are observed. The $\pi \rightarrow \pi^*$ transition occurs around 1850 Å and has a high intensity, while the $\eta \rightarrow \pi^*$ transition, with a low intensity is observed at 2700 Å. All organic iodides have absorption bands in the ultra-violet region. Methyl, ethyl and propyl iodides in water have maxima around 2500 Å and the bands have been interpreted as arising from $\eta \rightarrow \sigma^*$ transition, in which one of the lone-pair electrons on iodine is promoted into the antibonding orbital.

Both Q ← N and V ← N transitions occur without a change in the principal quantum number and are 'valence shell' transitions.

In Rydberg transitions, R ← N, a change in the principal quantum number does occur. The electron is promoted from a bonding MO to an MO of sufficiently high energy that the excited orbital is essentially atomic in character. This results in an atomic like absorption spectrum of high absolute intensity, usually lying in the vacuum ultra-violet region.

Figure 1.4

(a) Form of the η orbital of a carbonyl group.

(b) Form of a π orbital (i) and a π^* orbital (ii) of a carbonyl compound.

(c) Form of a σ orbital (i) and a σ^* orbital (ii) of a carbonyl group.

(a)

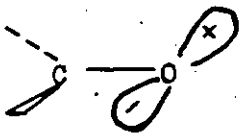

p orbital

(b)

(i) (ii)

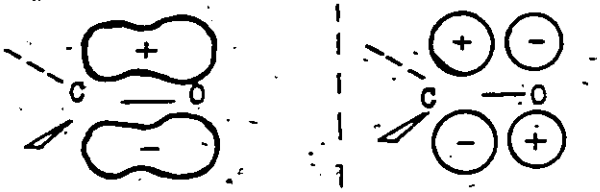

(c)

(i) (ii)

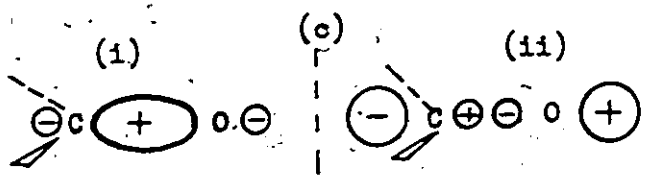

The intensities in these electronic transitions are expressed in terms of molar absorption coefficient ε, which can be obtained from the experimentally measured value of absorbance. The relation between the two is given by Lambert-Beer's law which can be mathematically represented as

$$A = \log\left(\frac{I_o}{I}\right) = \varepsilon c x \qquad (1.18)$$

where 'A' is the absorbance measured spectrophotometrically, c is the concentration in moles liter^{-1}, and x is the cell length in cms. The units of the molar absorption coefficient ε are liters mole^{-1} cm^{-1}. This is related to the oscillator strength f, a theoretically derived quantity obtained from the transition moment and often used to express the intensity of transition (32), by the relation

$$f = 4.32 \times 10^{-9} \int \varepsilon d\nu \qquad (1.19)$$

The integration is performed graphically by plotting the extinction coefficient as a function of ν, the frequency. The area under the curve gives the value of integral from which f can be calculated. This can be compared with the value of f obtained from the transition moment.

The transition moment is a wave mechanical quantity which is proportional to the square root of the intensity of a transition and is given by the integral

$$\sqrt{I} \propto \sqrt{D} = \int \Phi_i \, M \, \Phi_f \, d\tau \qquad (1.20)$$

where Φ_i and Φ_f are the total wave functions of the initial and final states respectively, $d\tau$ represents the product of volume elements in the coordinates of all the nuclei and electrons, D is the dipole strength and M is the so-called dipole moment vector. The dipole moment vector M is given by

$$M = e \sum_i r_i \qquad (1.21)$$

where r_i is the vector which corresponds to the dipole moment operator for electron i and e is the electronic charge.

Equation (1.20) permits the evaluation of the intensity, provided the total wave function Φ_i and Φ_f are known. This is, however, never the case, and a long series of approximations are required. First, it is assumed that rotational and vibrational wave functions can be factorized out and the above equation reduces to

$$\sqrt{D} = \int \Psi_i \, M \, \Psi_f \, d\tau \qquad (1.22)$$

where Ψ_i and Ψ_f are the total electronic wave functions of the initial and final states respectively and $d\tau$ is the product of the volume elements in terms of coordinates of all the electrons. Integrals of the form of Equation (1.22) can be evaluated and the calculations have been performed for a series of simple molecules (37). The relation between the transition moment and the oscillator strength f is given by

$$f = 1.08 \times 10^{11} \nu D \qquad (1.23)$$

where ν is the frequency of emission and 'D' is the square of the transition moment. Mulliken (37) has, in a series of papers, compared the theoretical values of f calculated from transition moment and 'f' calculated from extinction co-effients for a number of compounds and they seem to agree fairly well.

The most useful property of integrals of the type of Equation (1.22) is that they frequently vanish identically; that is, the integral is equal to zero. If this is the case, the transition is called forbidden, and should, according to the approximate theory, not occur at all. Actually, forbidden transitions do occur because calculation by more refined theories give small, non-vanishing values for the intensities. Observed intensities of forbidden transitions are generally quite small, much smaller than those of allowed transitions (for which Equation (1.22) gives non-vanishing intensities).

Fortunately, it is usually possible to tell, from the symmetry properties of the wave functions whether or not Equation (1.22) will vanish. Relatively simple rules can be established which predict the vanishing or non-vanishing of the intensity integral; these rules are referred to as selection rules.

The first selection rule is concerned only with molecules which have a centre of symmetry. All wave functions (orbitals) are either symmetric or anti-symmetric with respect

to the centre (that is either gerade (g) or ungerade (u)), and all components of vector M are of necessity ungerade. The product of two functions is ungerade only if one is gerade and the other ungerade. Hence the integrand of Equation (1.22) can be gerade only if M is multiplied by an ungerade quantity, which can happen only if Ψ_i, the ground state wave function (orbital) and Ψ_f the excited state wave function, are of unequal parity. Hence the selection rule $g \nrightarrow u$ or $u \nrightarrow g$; but $g \not\rightarrow g$ and $u \not\rightarrow u$. The crossed arrows indicate the transitions are forbidden.

The integrals of the above Equation (1.22) vanish if there is change in electron spin on excitation and hence transitions involving change in multiplicity are forbidden. Transitions involving no change in parity are also forbidden. A rotational level is called positive or negative depending on whether the total eigen-function remains unchanged or changes sign for such a reflection. The property positive or negative is also called parity. According to the above selection rule, positive levels combine only with negative and vice versa. Transitions between two positive levels or between two negative levels are forbidden. This selection rule may be written symbolically:

$$+ \nrightarrow -, \quad - \nrightarrow +, \quad + \not\rightarrow +, \quad - \not\rightarrow -$$

Other examples involving special cases are outlined by Herzberg (38). The importance of the selection rule lies in

the fact that from a knowledge of allowed transitions, the symmetry of the molecule can be ascertained, which in turn leads to the geometry of the molecule.

Secondary Reactions: In the great majority of photochemical reactions which have been studied in detail, it has been found that the primary process consists of a dissociation of the absorbing molecule into free radicals or atoms. The free radicals or atoms then take part in secondary reactions. These reactions may lead to stable molecules which, in turn, take part in further reactions. The secondary reactions are thermal and are independent of the means by which the reactants concerned are produced. However, if the radicals or atoms so produced have excess of thermal energy, then they react at a different rate from that of normal atoms. Such examples have been reported in the literature (39,40), and are known as 'hot atom' reactions. The energy distributed in the fragments are given by

$$E_1 = \left(\frac{hc}{\lambda} - D_{12}\right)\left(\frac{M_2}{M_1 + M_2}\right) \qquad (1.24)^*$$

$$E_2 = \left(\frac{hc}{\lambda} - D_{12}\right)\left(\frac{M_1}{M_1 + M_2}\right) \qquad (1.25)^*$$

where E_1 is the energy present in the radical or atom of mass M_1, E_2 the energy of M_2, hc/λ the energy of a photon of a given wave length λ and D_{12} is the bond dissociation energy of the bond being broken. These reactions were found to pro-

*These equations apply only to translational energy.

ceed with no activiation energy. The excited species must carry this excess energy, if they are atoms, as electronic and translational energies, or if they are not atoms as rotational and vibrational energies as well. In all these cases there are restrictions on the type of energy and the way in which it can be divided between the two products of reaction.

The restrictions are (a) conservation of the momentum of the product fragments, which determines the partition of translational energy, that is, in the inverse ratio of the masses, $\frac{E_1}{E_2} = \frac{M_2}{M_1}$. (b) Conservation of spin, although this rule seems of questionable validity for any species containing atoms of atomic number in excess of ten. If the excess of energy is electronic, there is a chance that it may be emitted within a time of 10^{-6} to 10^{-8} sec as radiation if the transition is possible. Otherwise such electronic energy may be degraded by inelastic collisions to other forms of energy, usually vibrational. Generally, it is found that the electronic states produced in chemical reactions are metastable, so that one may expect electronically excited species to follow the path of collisonal de-excitation. The rare cases of allowed transitions result in what are referred to as chemiluminescent reactions.

For excess energy distributed in other degrees of freedom, namely rotation, vibration and translation, only collisional degradation is possible. However, it is known that degradation of vibrational energy is a slow process and

so a considerable fraction of vibrationally excited species thus formed may be expected to persist for some time. Evidence has been presented for the presence of vibrationally excited species in the new bond that is formed by such collisions (41). On the other hand rotational and translational energy appear to be exchanged very readily on collision, so that the species thus excited may be expected to be thermalized very rapidly.

The transfer of energy to translational motion during molecular collisions without change in the form of energy takes place in accordance with the laws governing the collisions of elastic spheres. It follows from these laws that in the simplest case of an oblique impact of a rapidly moving particle of mass M_1 on a stationary particle of mass M_2, the average fraction $\frac{\Delta E}{E}$ of energy transferred to the stationary particle on impact is given by

$$\frac{\Delta E}{E} = \frac{2\, M_1 M_2}{(M_1 + M_2)^2} \qquad (1.26)$$

Thus the amount of energy transferred depends on the masses of the colliding particles, and the most favourable case for energy transfer occurs when the masses of both particles are the same. Therefore, the addition of inert gas, to a system containing hot radicals or atoms, should remove the excess energy by collisions. The atoms or radicals thus thermalized react at a different rate and were found to be temperature

dependent (39). If the radicals or atoms produced in a primary photochemical act are thermalized atoms or radicals, then the secondary reactions that follow are the usual thermal or dark reactions which are common to any kinetic system.

Light Sources

The lamps generally utilized for photochemical studies are mercury resonance lamps of varying intensities although for qualitative studies, ordinary sun lamps or just sunlight are sometimes adequate. The advantages of the mercury resonance lamp are numerous. If operated under properly controlled conditions its output is fairly constant; it emits, if made of quartz, a number of intense lines from 1849 Å to the two yellow lines at 5683 Å and 5688 Å, which may be separated satisfactorily for most purposes by simple filters. Ordinary glass is opaque below 3300 Å and quartz below 2000 Å. Thin films of glass (10μ) are transparent above 1500 Å. Owing to absorption by oxygen below 2000 Å, a vacuum technique must be used for the far ultra-violet region.

The number of designs of mercury lamps described in the literature and manufactured by commercial undertakings is so large that no attempt can be made here to describe them in detail. Roughly, however, three types may be distinguished viz. (a) low-pressure lamps; (b) medium and (c) high pressure arcs. In the first class the mercury vapour pressure is kept as low as practicable, with the result that the intrinsic

brilliance is small. This type, however, has one advantage that much of the energy lies in the first resonance line of the mercury spectrum at 2537 Å and secondly, the line is unreversed. The difference between reversed and unreversed radiation may be explained as follows: A reversed radiation is obtained from a medium pressure arc. In these lamps due to the increase in pressure of mercury vapour, 'pressure broadening' occurs, with the result that the emission line (2537 Å) with the radiation in the middle of 'line' is virtually absent because of self-absorption near the walls. In the case of low pressure lamps there is no pressure broadening and hence the line 2537 Å is a single, intense line. This is known as an unreversed line. Such lamps are suitable where a particularly strong source of resonance light is required, as in mercury photosensitized reactions: usually the amperage is never allowed to go higher than 180 mA. The lamp has another advantage that it may be inserted in a furnace for photochemical experiments at high temperatures, thus permitting the intense irradiation of reaction vessels. Lossing et al (42) has designed an assembly for mass spectrometric study using this type of lamp. It may be noted that the output intensity of a mercury resonance lamp is practically independent of temperature up to 600°C.

Medium pressure arcs: As the pressure in the lamp is raised, the intensity of light weakens in the far ultraviolet and becomes greater in the visible and in the near

ultra-violet regions. Such lamps usually work at a pressure of the order of 100 mm to 10 atmospheres and they carry currents of 1 to 5 A. An inconvenient feature of these lamps is the heat generated, several hundred watts being dissipated. One way out of this difficulty is to surround the lamp by a water jacketed enclosure. Medium pressure arcs give several lines of mercury spectrum but 2537 Å, 3130 Å and 3660 Å are the most intense lines. Even amongst these three, 2537 Å is four times more intense than 3660 Å which is of the same strength as 3130 Å, and these can be isolated by using different filters.

High pressure arcs: High pressure mercury arcs operate at pressures of a few, up to almost 300 atmospheres. At the higher pressures, air or water cooling must be employed. In the event that water is used as a coolant, its purity may be of some significance when the lamp is to be used at wavelengths below 2800 Å. On the other hand, water cooled lamps possess the advantage that a good deal of infra-red radiation is absorbed by the water. These lamps must be so enclosed as to protect from possible explosion. The life time of these arcs is lower than that for medium pressure arcs, and their use for kinetic studies is usually in conjunction with filters or a monochromator.

Vacuum ultra-violet sources: Among the more restrictive features of vacuum ultra-violet photochemistry is the material through which the photon must be propagated and

behind which is contained the gas to be photolysed. Both lamp and reaction vessel usually require such a window. Ideally, the window should be transparent in the wavelength region where the gas absorbs, and should be capable of being affixed to a reaction vessel to make a vacuum-tight seal that can be subjected to extremes of temperature. LiF windows can transmit above 1050 Å, CaF_2 can transmit above 1200 Å and a sapphire window will allow radiation greater than 1450 Å. These are the commonly used window materials.

A major requirement in a photochemical light source is high intensity and it should be monochromatic. A continuum such as obtained in a hydrogen discharge (43) or the rare gas discharges (44) can be useful when used in conjunction with a vacuum monochromator. However, monochromator efficiencies are uniformly poor in the vacuum ultra-violet and hence this arrangement has not been widely employed. Of much more use are the rare gas resonance lamps, which have the twin virtues of high intensity and chromatic purity.

The development of the rare gas resonance lamp began with electrode lamps (45) and evolved recently into the electrodeless lamp powered by microwave energy (46). The great advantage of the microwave powered lamp is simplicity of construction. If one uses a krypton resonance lamp, the wavelengths 1236 Å and 1165 Å are obtained, their intensities being in the ratio of 1:0.28. On the other hand the Xenon resonance lamp gives a powerful line at 1470 Å and a less

intense line at 1295 Å. The most intense krypton resonance lamp was achieved by using 1 mm of a mixture of 10% Kr and 90% He as the filling gas. It was found (46) that 10% H_2 in argon at a total pressure of 1 mm gave an intense, almost pure Lyman α emission (1216 Å). These lamps have been used for studying photoionization.

Filters and Monochromators

When radiation of a specific wavelength is desired, several alternative procedures are applicable. The least accurate, but often satisfactory, results are obtained using filter systems. Filter systems make use of a process of selective absorption. By combining certain filters, wavelength bands can be isolated. These bands are 200 or more Å wide although somewhat narrower bands may be isolated by using certain filter combinations at a limited number of wavelengths. The simplest filter is 'pyrex' glass, which absorbs most radiation of less than 3130 Å. Although the filters absorb a considerable amount of the desired light, they absorb much more of the light in other parts of the spectrum. The transmission curves for typical Corning glass filters are given in their catalogue (47). These filters are ground to a given thickness and polished in standard sizes, 5 cm. square and larger. Many of the glasses have sharp cut-offs. Filter CS-9-53 cuts off light below 2700 Å, while CS-9-54 cuts off below 2200 Å.

Monochromators: In general, the undesired wavelengths can be refracted to one side with a prism more effectively than they can be absorbed in a filter. A spectrometer system which is arranged to supply radiation of a narrow range of frequencies is called a monochromator.

If a continuous light source is used, there may be overlapping of adjacent regions and for this reason a discontinuous spectrum, such as that of a mercury arc, is particularly advantageous for use with a monochromator. Monochromators have the disadvantage, however, of emitting only low intensities at any one individual wavelength. The handicap of low intensity can be offset in part by long exposures, by using larger prisms and lens and by using capillary arcs of greater intensity. Forbes and others (49) have given a good experimental description of setting up a monochromator in conjunction with a lamp and these monochromators are available commercially.

Lasers: To date the laser's position in photochemistry resembles that of a solution for which there is no problem. A broad spectrum of laser emissions are now known, although the intensities of these sources are relatively feeble at wavelengths shorter than 6000 Å. The most remarkable property of lasers - coherence and extreme monochromaticity - has not yet been exploited by photochemists, who seem more intrigued by the potential of lasers as high intensity sources. Presumably, a series of intense lasers spanning the region of

photochemical interest will be developed, and a powerful tool would be added to the armament of the photochemist.

Measurement of Light Intensity

The most distinguishing property of a photochemical reaction is the fact that it is produced by light. All of the various electronic excitation processes can be related in terms of their efficiencies by measuring the number of chemical reactions per impingent light quantum. The tendency of a molecule to undergo a chemical reaction after the absorption process has occurred, gives rise to the concept of the quantum yield. As mentioned earlier, the quantum yield of a photochemical reaction is defined as either the number of moles of reactant consumed or products produced per einstein of absorbed radiation. The primary quantum yield ϕ, measures the number of species that disappear directly as a result of the molecular absorption. It must have values between the limits of 0.0 and 1.0.

The primary quantum yield as distinguished from the total quantum yield, Φ, of a photochemical reaction, measures the efficiency of the one step process giving reaction products immediately from the excited state. The total reaction quantum yield, on the other hand, measures the efficiency of a multiple step process. In practice, the quantum yield for the primary process often cannot be successfully separated from the quantum yield for the total process, and ϕ and Φ become indistinguishable.

It can be shown that the determination of quantum yield will give an indication as to the nature of the most important process or processes in the reaction mechanism. If $\bar{\Phi}$ is large, a chain reaction is indicated; if it is small, either deactivation or recombination is suggested, although the possibilities of isomerization, regeneration or an inner filter effect must not be overlooked. A $\bar{\Phi}$ equal to some small whole number and independent of changing experimental conditions, especially if accompanied by continuous absorption, indicates a rapid and complete dissociation either into stable molecules or radicals which react further by a non-chain process. An example of this is the photolysis of hydrogen iodide with a quantum yield of 2.0. The relative inefficiency of the reactions of certain azo compounds indicates that rearrangements are necessary before decomposition can occur.

Measurement of the quantum yield of a photochemical reaction is generally accomplished by comparison with some standard quantum process. This technique is called 'actinometry' and is more convenient than the direct quantum output measurement of lamp output by photoelectric or thermopile methods (50).

In the measurement of radiation by the use of a thermopile, the instrument is calibrated against a true "black body" which radiates according to Stefan's law. In practice this is rarely done because of the difficulty of setting up a truly black body and when thermopiles are used, they are

usually standardized against standard lamps whose energy output is exactly known. If the response of the thermopile is directly proportional to lamp intensity, this is a reasonably good indication that the thermopile response is independent of wavelength, as it must be. An excellent, brief outline of the construction and use of thermopiles is given by Strong (51). The more commonly used methods for measurement of light intensity involve the use of a photochemical reaction, the quantum yield of which has been well established, in other words a chemical actinometer.

Chemical actinometers: The two most commonly used chemical actinometers are uranyl oxalate (52) and ferric oxalate (53). Chemical actinometry possesses considerable advantages for light intensity measurements, particularly when the source does not involve the use of a monochromator. A chemical actinometer gives the average dose over a given period of time and over a given area. By carrying out actinometry in the reaction vessel itself, one may also eliminate complications resulting from the geometry of the experimental system and avoid corrections due to reflection and absorption losses at the windows of the reaction vessel.

(i) <u>Uranyl oxalate actinometer</u>: This is still the most widely used chemical actinometer, the reaction utilized being the uranyl ion photosensitized decomposition of oxalic acid. It decomposes as

$$H_2C_2O_4 \rightarrow H_2O + CO + CO_2$$

A detailed description of the uranyl oxalate actinometer is given by Noyes and Leighton (54) and by Masson (55) for those cases where actinometry is applied to a light beam emerging from the reacting system. The quantum yield of this photolysis has been determined with great care over the region 5000-2000 Å, (52), the value being 0.62 at 2537 Å, 0.49 at 3660 Å and 0.56 at 3130 Å. The amount of reaction is determined by titration of oxalic acid against standard permanganate solution. Several attempts have been made recently to improve the analytical technique for determining the amount of reaction. Zill (56) followed the reaction manometrically by measuring the amount of carbon monoxide and carbon dioxide liberated during the decomposition of oxalic acid. For studies of photochemical reactions in aqueous solutions using volumes in the range of 1.0 to 10.0 µlitre, Porter and Volman (57) developed a simplified method of uranyl oxalate actinometry. The actinometry is based on the determination of CO by flame-ionization gas chromatography after catalytic hydrogenation to methane (58). This method is more sensitive than any other method or than any other chemical actinometer. However, this method can be useful only on a microscale. The uranyl oxalate actinometer has the advantage that the quantum yield does not vary much with changing wavelength and also has a small temperature coefficient, the coefficient being 1.03 per 10° at 20°C. Since the quantum yield does not vary much with changing wavelength, it is especially useful

if the source of radiation is rendered monochromatic by employing filters instead of a monochromator. The percent decomposition of oxalic acid varies linearly with time provided the decomposition is kept below 20%. Hence knowing the amount of oxalic acid decomposed and its quantum yield, the number of quanta absorbed by the system can be calculated (55).

(ii) Potassium ferrioxalate actinometer: This actinometer has been developed by Parker (53,59) and fulfills the requirements of constant quantum efficiency and high absorption factor over a wide range of operating conditions. The ferrioxalate system is usable in the wavelength region from 2540 to 5780 Å and is quite sensitive for a chemical actinometer. Its other advantages include (a) a small temperature coefficient for the wavelength region 3000 to 5000 Å, which eliminates the need for accurate temperature control between 20 to 30°C; (b) high precision, and (c) ease of operation. The sensitivity of the ferrioxalate actinometer is about one thousand times greater than that of the normal uranyl oxalate actinometer. A concentration of 0.006 M $K_3Fe(C_2O_4)_3 \cdot 3H_2O$ is generally used in this actinometer and the stoichiometry of the reaction is

$$2K_3Fe(III)(C_2O_4)_3 \xrightarrow[H_2O]{h\nu} 2Fe(II)C_2O_4 + 2CO_2 + 3K_2C_2O_4 + H_2O$$

The product ferrous ion and its oxalate complex do not absorb the incident radiation measurably during photolysis. Following exposure, however, it is made highly absorbing by formation of

the red-coloured 1,10-phenanthrolene-Fe(II) complex, which is analyzed spectrophotometrically at 510 mμ. The recommended procedure is given by Hatchard and Parker (59) and the quantum yields at two different wavelengths are $\phi_{2537\text{Å}}^{\circ} = 1.25$ and $\phi_{3660\text{Å}}^{\circ} = 1.21$. Recently Lee and Seliger (60) measured the quantum yield of this actinometer at 3660 Å relative to a calibrated thermopile and their value was essentially the same as determined by Hatchard and Parker (59).

Gaseous actinometers: A number of gaseous actinometers are available for use either at near ultra-violet or far ultra-violet regions. Some of them are used as internal actinometers. Acetone (61) and diethyl ketone (62) have been studied in detail, and were found to have a quantum yield of unity, for ketone decomposition or carbon monoxide formation, at temperatures above 100°C. Carbon monoxide formed can be measured manometrically after condensing the hydrocarbon products. The photolysis of HI is another reliable gaseous actinometer with $\phi_{HI} = 2.0$ over a wide range of experimental conditions. The hydrogen bromide decomposition is less suitable, since, because of a back reaction, the yield decreases with the amount of decomposition. For work in the Schumann region the ozone synthesis may be used (63) where $\phi_{O_3} = 2.0$. In the far ultra-violet region a N_2O gaseous actinometer which has a well established quantum yield for N_2 production of 1.44 at 1849 Å, is often employed (64). Cremer and Margreiter (65) have utilized the hydrogen-chlorine detonation reaction in the presence of oxygen for actinometric purposes.

CHAPTER 2

PHOTOLYSIS OF HYDROGEN IODIDE AND REACTIONS OF PHOTOCHEMICALLY PRODUCED 'HOT' HYDROGEN ATOMS

The spectrum of gaseous hydrogen iodide is continuous in the near ultra-violet, and although the use of wavelengths as long as 4050 Å (66) might bring about dissociation into normal atoms, the detection of absorption is still possible only up to about 3850 Å (67,68). The absorption maximum occurs around 2200 Å. As continuous absorption is displayed during the ultra-violet irradiation of gaseous HI, the absorption coefficients increase with frequency, reaching an approximately constant maximum extending to 50,000 cm^{-1}.

Mulliken (69) made a study of the low-lying electronic states of HI, from which he derived the potential energy diagram shown in Figure 2.1(a). The original excitation of the HI molecule probably involves the promotion of a non-bonding halogen electron to one of several higher molecular orbitals. For HI the electronic states formed are all dissociative; the $^3\pi_1$ and $^1\pi$ states form atoms in their normal ground electronic states $H(^2S_{1/2})$ and $I(^2P_{3/2})$, whereas the $^3\pi_0^+$ state forms an excited $^2P_{1/2}$ iodine atom.

Romand (70) from his study of the absorption spectrum of HI, postulated that the experimental curve which he obtained could be analyzed into two curves. The experimental curve

Figure 2.1(a), (b)

(b) Potential energy curves for the lowest electronic states of HI (Mulliken (69)).

(a) HI absorption curves from the work of Romand (70). Solid portion of curve (1) is the experimental absorption curve, the dotted portion is the postulated continuum curve at lower wavelength. (2) and (3) are the calculated component curves corresponding to two different electronic transitions.

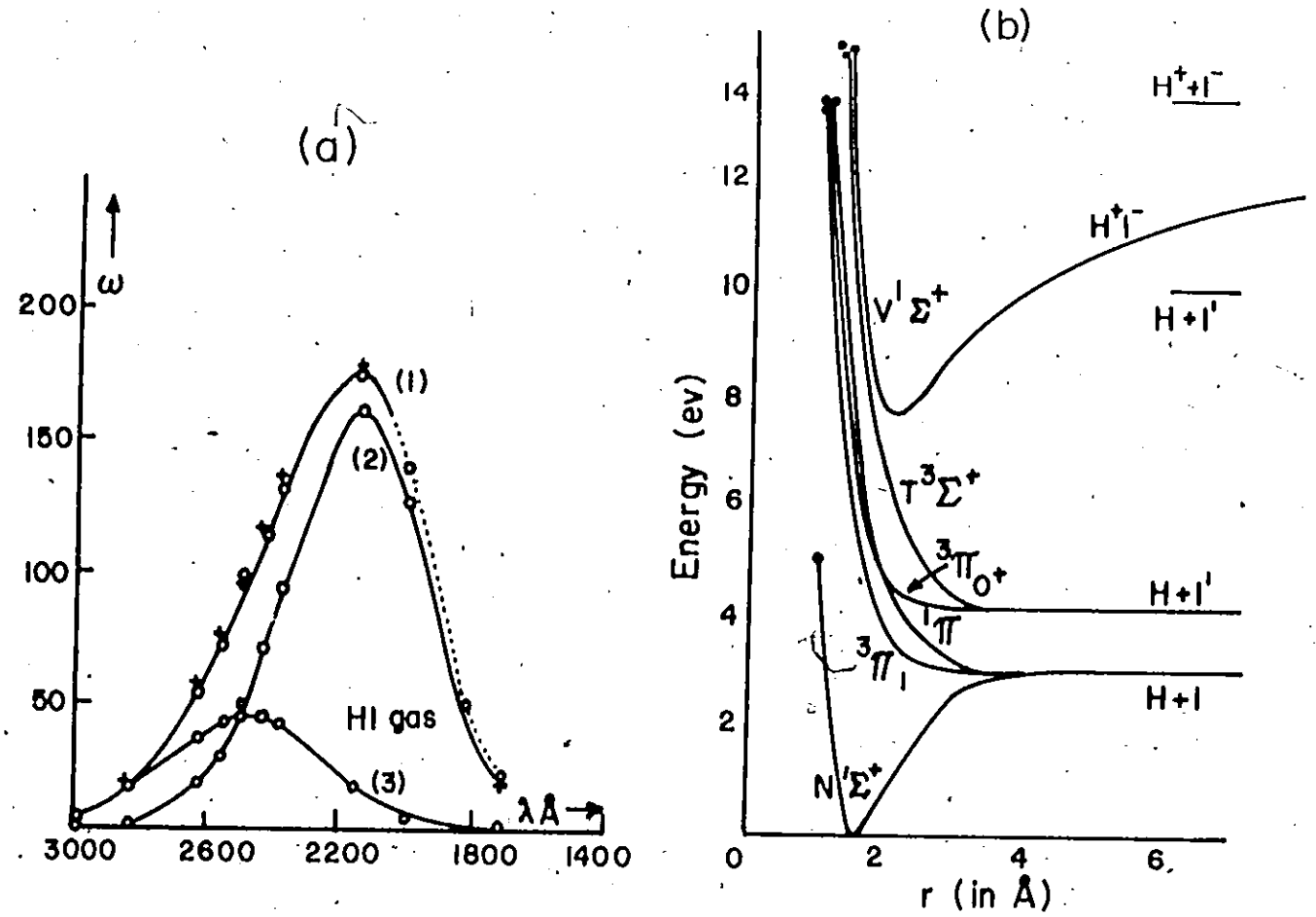
(a)
ω
200
150
100
50
(1)
(2)
(3)
HI gas
λÅ
3000
2600
2200
1800
1400
(b)
Energy (ev)
14
12
10
8
6
4
2
0
2
4
6
r (in Å)
H⁺+I⁻
H⁺I⁻
H+I'
V¹Σ⁺
T³Σ⁺
³Π₀⁺
¹Π
³Π₁
H+I'
H+I
N¹Σ⁺

(1) and the two postulated curves (2) and (3) are shown in Figure 2.1(b). Using the Mulliken notation, curve (2) corresponds to the transition $N\ ^1\Sigma_+ \rightarrow\ ^3\pi_0^+$ and curve (3) corresponds to the transition $^1\Sigma_+ \rightarrow\ ^3\pi_1$ illustrated in Figure 2.1. Curve (2) represents the process in which an excited iodine atom ($^2P_{1/2}$) is produced and curve (3) represents the process involving the production of a ground-state ($^2P_{3/2}$) iodine atom.

It is not very clear as to what fraction of iodine atoms are produced in the $^2P_{1/2}$ state at various wavelengths. However, from the relative positions of the maxima for the $^3\pi_1$, $^3\pi_0^+$, and $^1\pi$ states, Martin and Willard (71) have suggested that the maximum in the $^1\pi$ transition will occur at the shortest wavelength region of the band, the $^3\pi_0^+$ will be favoured at intermediate wavelengths, and the $^3\pi_1$ maximum will occur at the longest wavelengths. Thus formation of the excited iodine atoms ($^2P_{1/2}$) may be favoured to a large extent near the centre of the band, while normal iodine atoms ($^2P_{3/2}$) would be favoured at both extremes of the band.

The positions of the maxima for the three potential energy curves (Figure 2.1) should be in the order $^1\pi$, $^3\pi_0^+$ and $^3\pi_1$, for increasing wavelength if the Frank-Condon principle is obeyed.

Many studies have been made on the photolysis of HI over a number of years (72). Recent work substantiates the earlier view that the decomposition of HI molecules into atoms,

occurs with a quantum yield of two for HI (ϕ_{HI} = 2.00) over a wide range of wavelengths, 1849 Å - 3660 Å. The photolysis of hydrogen iodide provides one of the most striking illustrations of the applicability of the Stark-Einstein law.

Warburg (1918)(73) studied the decomposition of gaseous HI in ultra-violet light of wavelengths 2070, 2350 and 2820 Å; the results obtained are presented in Table 2.1, where the second column gives the number of moles of hydrogen iodide decomposed per kcal of radiation absorbed, and the third column, the quantum yield, that is the number of molecules decomposed per quantum.

In the photolysis of HI, the primary stage is dissociation, thus

$$HI + h\nu \rightarrow H^{\cdot} + I^{\cdot *} \qquad (2.1)$$

a normal hydrogen and an excited iodine atom being formed.

The products may then participate in the following secondary reactions:

$$H^{\cdot} + HI \rightarrow H_2 + I^{\cdot} \qquad (2.2)$$

$$I^{\cdot} + HI \rightarrow H^{\cdot} + I_2 \qquad (2.3)$$

$$H^{\cdot} + H^{\cdot} + M \rightarrow H_2 + M \qquad (2.4)$$

$$I^{\cdot} + I^{\cdot} + M \rightarrow I_2 + M \qquad (2.5)$$

$$H^{\cdot} + I^{\cdot} + M \rightarrow HI + M \qquad (2.6)$$

Reactions (2.4) and (2.6) are so highly exothermic, namely 104 kcal/mole and 71.3 kcal/mole, respectively, that they will occur in three body collisions, and reaction (2.3) is endo-

TABLE 2.1

PHOTOCHEMICAL DECOMPOSITION OF HI (8)

Wavelength	Moles $kcal^{-1}$	Yield
2070 Å	1.44×10^{-2}	1.98
2530 Å	1.85×10^{-2}	2.08
2820 Å	2.09×10^{-2}	2.10

thermic to the extent of at least 11 kcal, and possibly more if the excited iodine atom has lost some energy in collisions, so that it will require a relatively high activation energy. It appears therefore, that reactions (2.2) and (2.5) are the most important secondary chemical processes, and that the net result is

$$2HI + h\nu \rightarrow H_2 + I_2$$

The yield should thus be two molecules of hydrogen iodide decomposed per quantum, as actually found.

The excited iodine atom produced in the first stage is of no special importance, as similar results have been obtained with radiation, viz., 4047 Å wavelength, which gives a normal iodine atom. The reaction

$$H^{\cdot} + I_2 = HI + I^{\cdot}, \qquad (2.7)$$

like the corresponding process with chlorine and bromine, can take place at an appreciable rate, the activation energy being zero. However, if the concentration of molecular iodine is low, this reaction has little effect on the efficiency of photolysis of hydrogen iodide at the beginning of the decomposition. In the later stages it tends to decrease the effective yield.

Not only does the quantum yield of HI remain 2.0 within a considerable range of wavelength variation, but it has also been found by Bodenstein and Lieneweg (74) that this quantum yield is independent of temperature up to 175°C.

In the photolysis of HI, the extent of the secondary reactions depend to a large degree on the nature of the hydrogen atom resulting from the primary action of the splitting of the HI bond. At wavelengths in the region of 3660 Å, the hydrogen atom produced has very little excess kinetic energy and can be expected to react almost like a thermal hydrogen atom. At shorter wavelengths in the region between 1849 Å and 2537 Å, the hydrogen atoms are produced with a considerable amount of kinetic energy, the radiation energy being well in excess of the bond dissociation energy [D(H-I)]. Table 2.2 contains a listing of the translational kinetic energies of H atoms, each TKE corresponding to a particular wavelength.

Besides the use of relatively long wavelengths in the creation of thermal hydrogen atoms, shorter wavelengths in combination with an excess amount of a noble gas within the photochemical system may be employed to achieve the same effect.

In the previous sequence outlining the course of the secondary reactions, the two reactions which were considered to be of major importance were

$$H^{\cdot} + HI \rightarrow H_2 + I^{\cdot}$$

$$I^{\cdot} + I^{\cdot} + M \rightarrow I_2 + M$$

where M could be any third body in the system or the walls of the reaction vessel. Additionally the inhibitory reaction,

$$H + I_2 \rightarrow HI + I$$

TABLE 2.2

ENERGY PARTITION IN HI PHOTOLYSIS

$D(H-I) = 71.3$ kcal mole^{-1}

$E(I^*) = 21.8$ kcal mole^{-1}

λ† Å	State of Iodine Atom (I)	E_λ (kcal mole^{-1})	Translational Kinetic Energy of H Atom (kcal mole^{-1})	Type of H Atom
1849	$^2P_{3/2}$	154.7	83.4	Hot
	$^2P_{1/2}$		61.6	Hot
1942	$^2P_{3/2}$	147.3	76.0	Hot
	$^2P_{1/2}$		54.2	Hot
2537	$^2P_{3/2}$	112.7	41.4	Hot
	$^2P_{1/2}$		19.6	Hot
3130	$^2P_{3/2}$	91.4	20.1	Hot
	$^2P_{1/2}$		0.0	Thermal
3660	$^2P_{3/2}$	78.1	6.8	Hot
	$^2P_{1/2}$		0.0	Thermal

†Prominent lines in the emission spectrum of medium pressure mercury lamps.

does become important, if the photolysis proceeds for a long time to the extent that there is a build-up of I_2, which has a maximum at its S.V.P. at the particular temperature of the reaction.

On application of the steady state treatment to the mechanistic scheme for the production of thermal hydrogen atoms, one obtains the following differential equation,

$$\frac{dH_2}{dt} = \frac{dI_2}{dt} = \frac{I_{abs}}{1 + \frac{k_7}{k_2}\frac{[I_2]}{[HI]}} \qquad (2.8)$$

Here I_{abs} is the concentration of photons absorbed per second and $\frac{k_7}{k_2}$ the specific rate constants ratio is a constant. On integration*, equation (2.8) leads to,

$$I_{abs} \times t - [I_2]_f = \frac{k_7}{k_2}\left|\frac{[HI]_i}{4} \ln \frac{[HI]_i}{[HI]_i - 2[I_2]_f} - \frac{[I_2]_f}{2}\right| \qquad (2.9)$$

where $[I_2]_f$ is the final concentration of iodine, $[HI]_i$ is the initial concentration of hydrogen iodide and $I_{abs} \times t$ is the total quantity of light absorbed, measured actinometrically.

The rate of reaction of hydrogen with iodine in the hydrogen iodide synthesis was studied by Sullivan (75, 76) in the temperature range 667-800°K, and from the experimental results, he calculated the ratio of k_7/k_2 for normal or thermal H atoms, to be 13.0. Because the ratio showed no

*This integration is performed in Appendix 1.

temperature dependency, Sullivan concluded that both activation energies were approximately 0.0 kcal/mole. With the aid of thermodynamic data, Sullivan (76) formulated the following expressions,

$$\log_{10}(k_2/T^{1/2}) = (12.20 \pm 0.20) - \frac{480 \pm 350}{2.303\ RT} \qquad (2.10)$$

$$\log_{10}(k_7/T^{1/2}) = (13.00 \pm 0.20) - \frac{0 \pm 500}{2.303\ RT} \qquad (2.11)$$

At room temperature, a calculation of $\frac{k_7}{k_2}$ from equations (2.10) and (2.11) gives a value of 14.00. The results of Holmes and Sanderam (77) for thermal H atoms in the HI photolysis, also lend support to Sullivan's values for $\frac{k_7}{k_2}$ and for $E_7 - E_2$.

Bonhoeffer (78) in describing the photolysis of hydrogen iodide, had stated that the quantum yield of HI fell from two with increasing conversion, and he attributed this effect to the inhibition by iodine, reaction (2.7). He had estimated $\frac{k_7}{k_2}$ to be approximately 100 and suggested that the photolysis becomes completely self-inhibited by the time 1% decomposition occurs.

In their work, Ogg and Williams (79-81) showed that for the photolysis with 2537 Å radiation, $\frac{k_7}{k_2}$ is independent of HI pressure (50-150 torr), independent of temperature and has the value 3.5 ± 0.3. The effect of cyclohexane (20) as an inert diluent was to increase $\frac{k_7}{k_2}$ to 7.4 ± 0.4 at 155°C, and this value of $\frac{k_7}{k_2}$ remained constant

at high cyclohexane, hydrogen iodide ratios. This result was attributed to collisional thermalization of the 'hot' H atoms produced by the 2537 Å radiation, and this limiting high-pressure value of $k_7/k_2 = (k_7/k_2)_\infty$ was considered to be that for thermally equilibrated H atoms.

These experiments were extended by Hamill et al (82), who used helium, argon and hydrogen as inert diluents. Addition of these gases also resulted in an increase in $\frac{k_7}{k_2}$, which approached a limiting value $(k_7/k_2)_\infty$, at high inert gas pressures. $(k_7/k_2)_\infty$ was independent of the inert gas and was temperature dependent. At a given inert gas pressure, (k_7/k_2) was independent of $\frac{[I_2]}{[HI]}$. These results were explained simply by the 'hot-atom' effect. Values of $(k_7/k_2)_\infty$ were obtained by extrapolation. A plot of $\log(k_7/k_2)_\infty$ versus $\frac{1}{T}$ for the temperature range 114-198°C gave $E_2 - E_7 = 4.5$ kcal/mole. Not only is this large value for E_2 (if $E_7 = 0.0$ kcal/mole) difficult to understand, but Hamill's results are in poor agreement with those of Sullivan (75,76).

Due to the poor agreement of Hamill's results with those of Sullivan for thermalized H atoms in the photolysis of HI, Holmes and Rodgers (83), using He, Ar and H_2 as noble gases, repeated photochemical experiments similar to those of Hamill, in the temperature range 50-200°C, and using the 2537 Å wavelength. The results obtained by Holmes and Rodgers were consistent both with the low value for $E_7 - E_2$ and with the experimental data of Hamill. Figure 2.2 shows Holmes'

Figure 2.2

k_7/k_2 as a function of temperature and inert gas/HI ratio. ▼, X, ●, ▲, Helium as inert gas, temperatures, 53, 69, 102 and 200°C respectively; △, argon 79°C; ■, hydrogen 170°C; 0, from Hamill et al (82), He as inert gas 114°C.

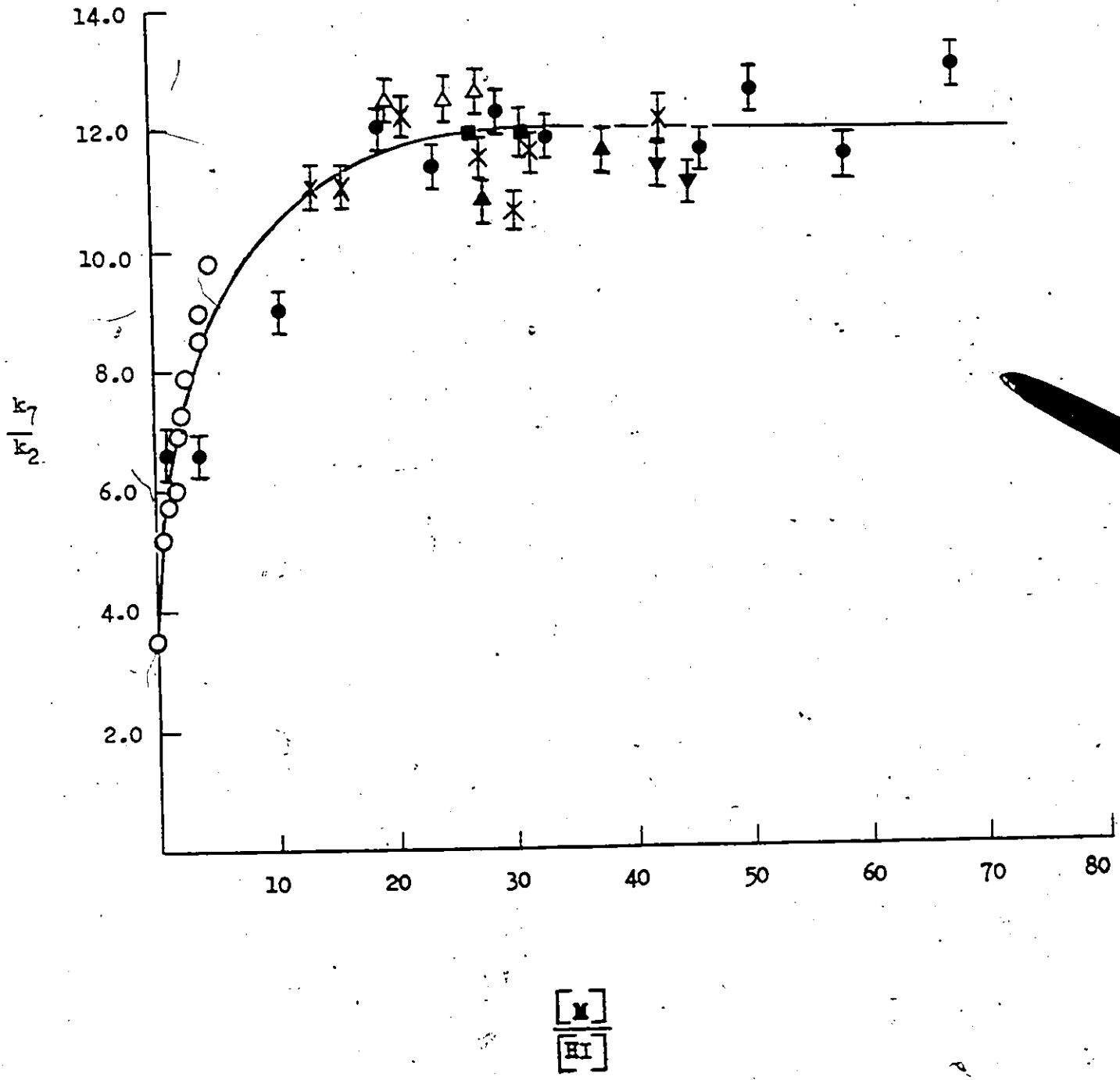

OTTAWA, ONTARIO, CANADA.

results together with those of Hamill, and it is not difficult to see how the latter's extrapolation to high inert gas pressures could be in error. Holmes' value for $E_7 - E_2$ was 0 ± 350 cal/mole.

In the initial investigations of hot hydrogen atoms, by Hamill, Williams et al (82,84) and in some later work (85) photochemically produced hot H atoms were used. These were of relatively low energy (<2 electron volts) and were found to react by the familiar abstraction mode. In 1957 it was reported by El Sayed and Wolfgang (86) that tritium recoiling from nuclear reaction reacts as hot atoms, and that these high energy atoms could undergo efficient high-energy substitution processes. However, as a tool for studying the details of molecular interactions, nuclear activation suffers from the fact that the reactive atoms have initial energies far above those at which they can enter stable combination, and there is no way of determining the probability for reaction in a well-defined region. Also, in cases other than that of tritium, it is generally not possible to state with certainty whether or not the atom is ionized at the time of reaction.

Some evidence has also been obtained by observing the reactions of atoms or radicals formed by the photochemical rupture of bonds by photons of energy considerably in excess of the bond strength. Thus Williams and Ogg (81) found that the ratio of the rate constant for the reaction of H atoms with HI relative to that with I_2 was much larger for atoms

produced from HI by 2537 Å radiation than for thermal H atoms, and subsequent work has extended these results. It has also been shown that D atoms formed by the photolysis of deuterium iodide (DI) at 2537 Å, react much more readily with H_2, CH_4, C_2H_6 and C_5H_{12} than do thermal D atoms (84), the reaction cross section varying with the target molecule.

Probably the best available method for producing hydrogen atoms of known energy in the 2.0 - 92.0 kcal/mole range, is the photo-dissociation of the hydrogen halides. There is a large mass difference between any of the halogens and the three hydrogen isotopes and thus most of the energy of the photon, in excess of the bond energy, minus any electronic excitation of the halogen atoms, must appear as translational energy of the hydrogen atom. For HI, which has the lowest bond energy of the hydrogen halides, this energy is 20.0 kcal/mole for the 3130 Å wavelength (see Table 2.2).

The excess energy of an absorbed quantum remaining after scission of a molecular bond must be carried away by the separating fragments. If the energy is large compared to the normal thermal energies of the fragments, then the species (atoms or radicals) formed, may be quite reactive. Consider for example the molecule Y-X, which dissociates photochemically according to the reaction

$$Y - X + h\nu \rightarrow Y^{\cdot} + X^{\cdot} \qquad (2.12)$$

For the simplest possible case the assumption will be made

that the excess energy is removed as kinetic energy only (no extra vibrational, rotational or electronic excitation of the radicals Y and X are involved). Energy and momentum must be conserved as (2.12) occurs. Let D_{X-Y} be the bond dissociation energy of the molecule XY and M_y and M_x the respective masses of the primary fragments X and Y. The total excess kinetic energy of X and Y in reaction (2.12) will be,

$$E = \frac{hc}{\lambda} - D_{X-Y}$$

The energy taken by X is,

$$E_X = (\frac{hc}{\lambda} - D_{X-Y})(\frac{M_y}{M_x + M_y}) \qquad (2.13)$$

and that by Y is,

$$E_Y = (\frac{hc}{\lambda} - D_{X-Y})(\frac{M_x}{M_x + M_y}) \qquad (2.14)$$

It is shown from (2.13) and (2.14) that for the case of light and heavy fragments formed photochemically, most of the kinetic energy must be carried away by the light fragment. It is in these cases that 'hot' atoms or radicals reactions are most likely. For example, in the CH_3I photolysis at 2537 Å (87), the primary process has been shown to be

$$CH_3I + h\nu \rightarrow CH_3^{\cdot} + I^{\cdot} \qquad (2.15)$$

The observed activation energy for CH_4 formation is nearly zero (88), although its formation arises in the reaction,

$$CH_3^{\cdot} + CH_3I \rightarrow CH_4 + CH_2I^{\cdot} \qquad (2.16)$$

which is considered to have an appreciable activation energy

(approximately 9.0 kcal $mole^{-1}$). If the iodine atom is produced in the ground electronic state ($^2P_{3/2}$), the CH_3 radicals formed in reaction (2.15) in the photolysis of CH_3I with the 2537 Å wavelength, would have about 53 to 59 kcal $mole^{-1}$ total excess energy. This excess energy would be in the form of translational kinetic energy, provided the partitioning of energy between the electronic, vibrational and rotational states of the methyl radical is negligible. The heavy iodine atom would carry the other 6 kcal $mole^{-1}$. If iodine is formed in its $^2P_{1/2}$ state (excited state), then the CH_3 radicals would have an excess energy of about 32 kcal $mole^{-1}$. Therefore it is not surprising that the methane yield from CH_3I photolysis at 2537 Å is relatively insensitive to variations in experimental conditions, for the very 'hot' CH_3 species might be expected to react with CH_3I molecules at the first collision.

The most powerful means of identifying 'hot' H atom or 'hot' radical reactions is by the addition of chemically inert moderators to the system. In general these are noble gases. However, by reducing the number of collisions of the hot atom (radical) with the reactive species, while it is in the appropriate energy range, the moderator will reduce, and in the limit, eliminate hot reactions. With noble gases, energy loss on hot atom collision is elastic (in the relevant energy range) and thus predictable.

Vibrational and rotational excitations are also

likely for separating fragments composed of a large number of atoms. Rotational energy can be converted rather easily into translational energy on collision, but there is much less efficient transfer of vibrational energy. Zener (89) has calculated the probability that a nitrogen molecule in its first vibrational state will transfer its energy in a head-on collision with helium is 6×10^{-8}, and that for transfer to another nitrogen molecule is 4.0×10^{-5}. Evidence from gas phase experiments also favours the interpretation of inefficiency of transfer of vibrational excitation to translational energy. Because of this, a very large ratio of the concentration of inert gas to that of the reactant must be used to ensure thermal equilibration of high energy particles and to test conclusively for 'hot' atom or radical reactions.

'Hot' H atom reactions should be evident at much lower ratios of inert gas to reactant. In the HI photolysis, the mechanistic scheme,

$$HI \xrightarrow{h\nu} H^{\cdot} + I^{\cdot} \qquad (2:1)$$

$$H^{\cdot} + HI \rightarrow H_2 + I^{\cdot} \qquad (2.2)$$

$$2I^{\cdot} + M \rightarrow I_2 + M \qquad (2.5)$$

explains clearly the quantum yield of 1.0 for H_2 formation at wavelengths exceeding 2000 Å. The family of equations does not represent a chain reaction because the reaction

$$I + HI \rightarrow I_2 + H \qquad (2.3)$$

is endothermic by 35 kcal $mole^{-1}$, consequently if an excited

iodine atom ($I\ ^2P_{1/2}$) is formed and enters into an inelastic collision, it cannot cause reaction (2.3).

The translational kinetic energy of the H atoms formed in reaction (2.1) by the 1849 Å - radiation is sufficient to cause the rupture of more than one additional HI bond after the primary process, if used with high efficiency by anyone of several possible mechanisms. This would lead to a quantum yield exceeding two HI molecules fragmented per photon absorbed. The cleavage of more than one HI bond occurring after the primary process would be energetically possible via a direct collisional dissociation of a HI molecule by a 'hot' H atom or 'hot' H_2 molecule, or a collisional activation of a HI molecule by one of these species, enabling it to react with another HI molecule. The first possibly could be represented by,

$$H^* + HI \rightarrow H + H + I \qquad (2.17)$$

$$H_2^* + HI \rightarrow H_2 + H + I \qquad (2.18)$$

and the second by the group of reactions

$$H^* + HI \rightarrow H + HI^* \qquad (2.19)$$

$$H_2^* + HI \rightarrow H_2 + HI^* \qquad (2.20)$$

$$HI^* + HI \rightarrow H_2 + I_2 \qquad (2.21)$$

$$HI^* + HI \rightarrow I + H_2 + I \qquad (2.22)$$

where the 'hot' H_2 molecule is produced in the reaction,

$$H^* + HI \rightarrow H_2^* + I \qquad (2.23)$$

and the H and I atoms formed react according to (2.2) and

(2.5) respectively. An additional possible course of reaction for the H atoms is the inhibition reaction with I_2 as the I_2 concentration gets larger,

$$H + I_2 \rightarrow HI + I \qquad (2.7)$$

The 'hot' H atoms will be formed in the primary process with either 84 or 62 kcal $mole^{-1}$ of kinetic energy. While reactions (2.18) through (2.23) are all energetically possible in either case, reaction (2.17) is however not possible for 62.0 kcal $mole^{-1}$ H atoms, since 71.3 kcal $mole^{-1}$ are required to dissociate a HI molecule. The species HI^* will have its excess energy distributed between the vibrational and rotational modes and H_2^* may have its excess energy distributed between translational, vibrational and rotational modes.

These reactions are all in competition with non-reactive moderation. Such moderation can occur in a number of different ways for the different 'hot' species involved. The greatest fraction of the translational energy of a species B that can be imparted to the HI molecule as translational energy in a single collision is given by,*

$$\frac{4\, M_B\, M_{HI}}{(M_B + M_{HI})^2}$$

which is approximately 1/32 in the case of the H atom and 1/16 in the case of H_2. Energy transfer to vibrational and rotational energy of the HI molecule can also reduce the kinetic energy of the hot species, the rotational quanta being of the order of 0.04 kcal $mole^{-1}$, and the lower

*See Appendix 2

vibrational quanta lying in the 4-6 kcal mole^{-1} range. Theoretical studies by Shuler and Zwanzig (90) and Mies and Shuler (91) suggests that vibrational transitions with $\Delta v > 1$ may be highly probable for highly energetic collisions with strong interactions, an increasingly greater average number of vibrational quanta being transferred per collision as the energy of the impinging particles increases. The vibrational quanta for the transitions $0 \rightarrow 1$, $1 \rightarrow 2$, and $2 \rightarrow 3$ are 6.16, 5.93 and 5.70 kcal mole^{-1}, respectively, so that for H atoms produced with 84 kcal mole^{-1} initially, the transfer of three or more vibrational quanta to the HI molecule would reduce the H atom energy below the 71.3 kcal mole^{-1} needed for HI dissociation. Reaction (2.17) involving the transfer of at least 71.3 kcal mole^{-1} from translational energy of the H atom to vibrational energy of a HI molecule, would in order to be significant, have to have a high probability per collision relative to moderation by transfer of lower energies. Reaction (2.23) which produces the H_2^*, shows an exothermicity of 95 kcal mole^{-1} for a 62 kcal mole^{-1} H atom, and 117 kcal mole^{-1} for an 84 kcal mole^{-1} H atom. In order to conserve momentum, all of this energy must essentially go into the H_2 molecule. The product H_2 molecule may have more or less translational energy than the hot H atom producing it, depending on the distribution of the energy between the translational and vibrational modes of the H_2 molecule.

It is difficult to say very much about the probability

of reaction (2.18), except that it is energetically possible.

The activation energy for the thermal reaction

$$HI + HI \rightarrow H_2 + I_2 \qquad (2.24)$$

has been determined to be 44.3 kcal $mole^{-1}$ from studies in the 550°-750°K range (92,93). At these temperatures, the ratio of the rotational to the translational energy of HI is 2/3, while the ratio of the vibrational to the translational energy is about 1/50. The HI molecules formed in reactions (2.19) and (2.20) are not translationally excited. The thermally determined activation energy and frequency factor therefore may not be applicable to reactions (2.21) and (2.22). The work of Mies and Shuler (91) suggests a significant probability for the transfer of an amount of energy comparable to the activation energy of (2.24) (41 kcal $mole^{-1}$) into the vibrational degree of freedom of a HI molecule upon collision with an H atom or H_2 molecule with two-fold greater energy, such as may be available under the influence of the 1849 Å wavelength. It is quite feasible that because of the slowness of moderation of the hot H atom or hot H_2 molecule in this system by transfer of energy to the translational mode of HI, the production of some vibrationally highly excited HI molecules can occur.

Schwarz et al (82) studied the photolysis of hydrogen iodide and hydrogen bromide in the presence of added inert gases. The inhibiting effect of the free halogens was found to be a function of the concentration of inert gas, the

effect being independent of its nature at large pressure of inert gas. The authors interpreted their results in terms of a hot atom mechanism. Their hot atom mechanism predicted that R_∞, the value of $R(k_2/k_7)$ at infinite inert gas pressure should be the same

$$H^\cdot + HI \xrightarrow{k_2} H_2 + I^\cdot \qquad (2.2)$$

$$H^\cdot + I_2 \xrightarrow{k_7} HI + I^\cdot \qquad (2.7)$$

for all inert gases, and this was observed in their case for hydrogen and helium. Their hot atom mechanism accounted for the lack of a temperature dependence of R_o (the value of R in pure hydrogen iodide), and permitted a temperature dependence in the presence of inert gas. Additionally, the proposed hot atom mechanism predicted that hydrogen should be a slightly better moderator than helium, which in turn should be much better than argon.

Carter et al (84) produced deuterium atoms with large kinetic energy by photolysing gaseous deuterium iodide at 2537 Å. The reaction of these hot deuterium atoms with hydrogen, methane, ethane and neopentane was studied as a function of composition, wavelength, temperature and added rare gas. The reaction of the hot D atoms with methane was much less efficient than the corresponding reaction with hydrogen, ethane and neopentane. This was attributed to the fact that the activation energy for the process (2.25) is 12-13 kcal $mole^{-1}$ (94) while the activation energies of the

$$D^{\cdot} + CH_4 \rightarrow HD + CH_3^{\cdot} \qquad (2.25)$$

corresponding reactions with C_5H_{12}, C_2H_6 and H_2 are much lower, in the region 5-8 kcal mole^{-1}. Therefore, a hot D atom produced originally with some 47 kcal mole^{-1} of kinetic energy falls below the energy threshold for reaction with methane much earlier in its life than with ethane, hydrogen and neopentane.

The relative moderating efficiencies of the various substrates also showed an interesting regularity. Although from the standpoint of elastic collisions alone, hydrogen should have been the best moderator, it was found to be the poorest, while neopentane was the best. This was taken to mean then that the internal degrees of freedom absorb energy in the moderating collisions and that moderating efficiency increases with increasing number of available internal degrees of freedom.

Hydrogen bromide offers several advantages over hydrogen iodide as the source of hot H atoms. Both 84.0 and 52.0 kcal mole^{-1} H atoms are produced from HI when it is dissociated by 1849 Å radiation, and it is not possible on the basis of available information to determine the relative yields of the two. Hydrogen bromide has the same set of transitions as hydrogen iodide, but the $^3\pi_0^+$ transition giving an excited halide atom is believed to be much weaker with hydrogen bromide than with hydrogen iodide, so that an estimated 98% or more of the transitions of hydrogen bromide at

1849 Å should yield ground-state bromine atoms and 66.9 kcal $mole^{-1}$ hydrogen atoms (95). The first excited state of bromine ~~is~~ about 9.22 kcal above the ground state, so transitions giving excited bromine atoms will yield 57.6 kcal $mole^{-1}$ hydrogen atoms.

Martin and Willard (85) made a study of the reaction and moderation probabilities for 69.2 kcal $mole^{-1}$ 'hot' H atoms produced in the photolysis of HBr, in the substrate systems D_2, CD_4, and C_2D_6, and for 69.2 kcal $mole^{-1}$ hot D atoms (by the photolysis of DBr) in the systems H_2, CH_4 and C_2H_6. The 69.2 kcal $mole^{-1}$ H atoms produced in D_2, CD_4 or C_2D_6 could produce HD by hot-atom reaction with the deuterated species, or H_2 by hot reaction with HBr, or may be thermalized by moderating collisions and scavenged by thermal reaction with HBr. Plots of the product ratios, H_2/HD, versus the reactant ratios, HBr/RD, gave straight lines. The values of the intercepts were equal to the ratio of the atoms moderated to those which underwent hot reaction with RD in pure RD. From the slopes and intercepts, it was possible, with plausible assumptions, to deduce approximate values for the average probability of reaction per collision in the hot range and for the average fractional energy loss per moderating collision with the hydrocarbon. The latter value when compared with the calculated loss for elastic collisions gave an indication of the inelasticity of the collisions in the experimental system. These determinations were made for the systems stated and for the isotopically reversed systems of

DBr in H_2, CH_4 and C_2H_6. They indicated that the average probabilities of reaction per collision for the H atoms colliding with D_2, CD_4 and C_2D_6 are 0.18, 0.0034 and 0.019, respectively, while those for the reactions of the D atoms with the corresponding hydrogenated compounds were 0.35, 0.062 and 0.14. The ratio of actual energy loss per collision in this range to loss assuming hard-sphere collisions was estimated to be about 1.0 for H + CD_4, 4.0 for H + C_2D_6, 2.0 for D + CH_4, and 4.0 for D + C_2H_6, based on the assumption that H + D_2 and D + H_2 moderating collisions are completely elastic. If these latter collisions were partially inelastic, both the estimated reaction probabilities and moderating efficiencies given above should have been higher.

Penzhorn and Darwent (96) investigated the photolysis of HI in the gas phase, between 303 and 533°K with the 2537 Å wavelength, and in the presence of varying concentrations of I_2 and CO_2. Their results show: (i) that the efficiency of CO_2 in deactivating the photochemical 'hot' H is given, with reasonable accuracy, by the simple 'billiard ball' calculation; (ii) the ratio of k's for the reactions of thermal H with I_2 and HI is 4.95 exp (640/RT); and (iii) the ratio of the k's for the reactions of 'hot' H with I_2 and HI is approximately the same as that of the pre-exponential factors for the thermal H reactions. Darwent and Penzhorn's value of 640 cal $mole^{-1}$ for the thermal reaction H + HI is in general agreement with Sullivan's value

(75,76) of 480 ± 350 cal/mole, but not with that of Schwarz, Williams and Hamill (82) of 4500 cal $mole^{-1}$. The ratio of the pre-exponential factors A_7/A_2 was found to be 4.95. Both the simple collision theory and the transition-state theory lead to values of about unity for

$$H^{\cdot} + HI \xrightarrow{k_2} H_2 + I^{\cdot}$$

$$H^{\cdot} + I_2 \xrightarrow{k_7} HI + I^{\cdot}$$

the ratio of A_7/A_2. Schwarz et al (82) found by transition-state theory, that the ratio of pre-exponential factors (A_7/A_2) was approximately 10^{-2}. However, they omitted the moment of inertia of the transition state in their calculations. The inclusion of that moment of inertia leads to a value of about unity for (A_7/A_2). A possible explanation for the high value found by Schwarz et al., for k_7/k_2, is that the presence of mercury in their reaction system, which reacts with I_2 to form HgI, may have affected their results.

Penzhorn and Darwent (97) made a study of the photolysis of HI in the presence of C_2D_4 and C_2H_4 at low conversions in the presence of large moderator pressures and at various temperatures. The reaction was followed by the rate of hydrogen production. It was found that HD was produced from the photolysis with C_2D_4. A study of the effect of moderator pressure on the HD/H_2 ratio revealed that this ratio is a very sensitive indicator of the presence of 'hot' reactions.

The observed rate of hydrogen formation was used to evaluate the ratio of rate constants for the following reactions,

$$H^{\cdot} + HI \rightarrow H_2 + I^{\cdot} \qquad (2.26)$$

$$H^{\cdot} + C_2D_4 \rightarrow C_2D_4H^{*\cdot} \qquad (2.27)$$

$$H^{\cdot} + C_2H_4 \rightarrow C_2H_5^{*\cdot} \qquad (2.28)$$

The Arrhenius parameters for k_{28}/k_{27} were found to be 0.30 exp(-845/RT), and, based on previous work (75,76,96), the authors calculated E_{27} as 1.5 ± 0.1 kcal mole^{-1}. It was found that C_2D_4 reacts about 10% faster than C_2H_4 at 30.0°C.

A study of the reaction of hot hydrogen atoms was carried out by photolyzing various C_2D_4-H_2S mixtures. When C_2D_4 and H_2S at a constant ratio of 1.00 were photolyzed, it was observed that $\phi_{(HD\ H_2)}$ and $\phi_{(H_2)}$ were essentially constant from total pressures of 2.0 up to 128 torr. This result, which confirms an earlier finding of Cvetanovic (98), suggests that neither the hot ethyl radicals nor the H atoms are appreciably deactivated by a pressure increase. As the mole fraction x of C_2D_4 approaches unity, all 'hot' H atoms disappear by reaction with C_2D_4 and the rate of HD formation becomes a measure of the abstraction process

$$H^{*\cdot} + C_2D_4 \rightarrow HD + C_2D_3^{\cdot} \qquad (2.29)$$

It was found that the normalized rate of HD formation decreases to 0.015 at x = 0.97, indicating that reaction (2.29) is negligible compared to

$$H^{*} + C_2D_4 \rightarrow C_2D_4H^{**} \qquad (2.30)$$

This result is at variance with Dzantiev's (99,100) finding of $k_{29}/k_{30} = 0.20$ and 0.25.

The HD formation therefore occurs via the following main additional steps

$$C_2D_4H^{**} \rightarrow H^{\cdot} + C_2D_4 \qquad (2.31)$$

$$C_2D_4H^{**} \rightarrow D^{\cdot} + C_2D_3H \qquad (2.32)$$

$$D^{\cdot} + H_2S \rightarrow DH + SH^{\cdot} \qquad (2.33)$$

Since the life time of the $C_2D_4H^{**}$ radicals may be as short as 10^{-11} sec, they will decompose before they can be deactivated at pressures of some hundreds of torr.

Hydrogen sulphide exhibits a continuous absorption spectrum (101) over the region 2700 Å → 1850 Å with a maximum at about 2000 Å. The primary dissociation in this spectral region is to $H(^2S)$ and $HS(^2\pi)$ (102). The bond dissociation energy D(HS-H) is not certain, but 90 ± 2 kcal $mole^{-1}$ (103) is probably realistic. A recent photoionization study (104) gives $D_o(HS-H) = 89.3 \pm 0.5$ kcal $mole^{-1}$ and $D_o(H-S) = 83.2 \pm 0.5$ kcal $mole^{-1}$.

At the 2139 Å exciting wavelength, the excess energy is 39.2 → 48.4 kcal $mole^{-1}$ for the reported range of bond dissociation energies for H-SH (94.5 → 85.3 kcal $mole^{-1}$). The partition of energy between translational motion of the photolysis products and the rotational energy of the SH radical is constrained by the requirements of angular momentum

conservation. Linear momentum conservation requires that ~97% of the translational energy of separation of the photolysis products be located in the hydrogen atom. Therefore, if the products separate with zero impact parameter and the SH radical is generated in the ground vibrational state, the atomic hydrogen will be born with an initial kinetic energy between 34.6-47.3 kcal $mole^{-1}$.

Hot H atoms are formed (105-107) in the H_2S photolysis, but react (105) as thermalized atoms when a large excess of inert gas is present for collisional deactivation. The fate of HS assuming no reaction with substrate, will be either,

$$2HS \rightarrow H_2S + S^{\cdot} \qquad (2.34)$$

or

$$2HS \rightarrow H_2 + S_2 \qquad (2.35)$$

Reaction (2.35) has been postulated (108,109) to explain hydrogen quantum yields in excess of unity, but recently Darwent et al. (105), unable to detect H_2 in a system where only (2.34) and (2.35) can occur, have shown (2.34) to be much faster than (2.35). Reaction (2.36) although fast, will only be

$$H^{\cdot} + HS \rightarrow H_2 + S^{\cdot} \qquad (2.36)$$

significant at low pressures and high light intensities. At pressures in the region 10-30 torr, the quantum yield seems to be close to unity (108,110) and reactions (2.35) and (2.36) are not important. Darwent et al. also showed in experiments

conducted with I_2 and Br_2 in the presence of a large excess of CO_2, that the halogens are much more effective in reducing $\phi_{(H_2)}$ when CO_2 is present. This strongly suggests that the photochemically produced H atom is 'hot' and therefore does not discriminate greatly between its reactions with H_2S and the halogens. When CO_2 is present, the 'hot' atoms are deactivated and thus show a much higher reactivity toward the halogen than to H_2S.

As part of a general investigation of thiyl radical reactions, Steer and Knight (111) examined in detail the photolysis of methanethiol vapour and made a further study on the ethanethiol system. They studied in particular, the reactions of hydrogen atoms produced in the photolysis with added ethylene and inert gas.

The principal products of mercaptan photolysis, hydrogen and disulphide can be accounted for by the established simple scheme,

$$RSH \xrightarrow{h\nu} RS^{\cdot} + H^{\cdot} \qquad (2.37)$$

$$H^{\cdot} + RSH \rightarrow H_2 + RS^{\cdot} \qquad (2.38)$$

$$RS^{\cdot} + RS^{\cdot} \rightarrow RSSR \qquad (2.39)$$

For both methanethiol and ethanethiol, the primary quantum yield of H_2 is unity within experimental error.

The reaction in the presence of olefines has been studied in a variety of systems, and the additional reactions involving hydrogen atoms are:-

$$H^{\cdot} + C_2H_4 \rightarrow C_2H_5^{\cdot} \qquad (2.40)$$

$$C_2H_5^{\cdot} + RSH \rightarrow C_2H_6 + RS^{\cdot} \qquad (2.41)$$

The photolysis of mercaptan in the presence of ethylene and CO_2 with the 2537 Å light led to a significant reduction of H_2 especially at high CO_2 pressures. This behaviour was certainly due to the formation of energetic hydrogen atoms in the primary process. The rate of H_2 production in the high pressure region corresponded to k_{38}/k_{40} ratios of 1.15 ± 0.10 (CH_3SH) and 1.05 ± 0.05 (C_2H_5-SH). Thus the rate constant ratios determined with RSH and C_2H_4 alone are evidently characteristic of hot hydrogen atoms, while those observed with added inert gas indicate the reactivity of thermalized hydrogen atoms.

There are two other reactions producing H_2, not usually considered for thermalized H atoms, but which are energetically possible for 'hot' hydrogen atoms (H^*),

$$H^{*\cdot} + C_2H_4 \rightarrow C_2H_3^{\cdot} + H_2 \qquad (2.42)$$

$$H^{*\cdot} + RSH \rightarrow R'SH + H_2 \qquad (2.43)$$

The methanethiol-ethylene system was also examined at 2288 Å, where a k_{38}/k_{40} ratio for hot hydrogen atoms of 2.1 ± 0.2 was found, which was identical within experimental error to the value at 2537 Å. It is therefore probable that the primary decomposition proceeds via predissociation of the mercaptan yielding hydrogen atoms with excess energy independent of exciting wavelength.

Woolley and Cvetanovic (98) studied the effects of added CO_2, C_2F_6 and Xe on the photolysis of a 1:1 H_2S/C_2H_4 mixture (~11.0 torr of each reactant), using the 2490 Å wavelength. The results, showed that the H_2 yield fell by some 30% with increasing CO_2 and C_2F_6, becoming constant after about 400 torr, while additions of Xe or increasing the reactant pressure at constant H_2S/C_2H_4 ratio had a smaller effect.

The large decrease in the H_2 yield with CO_2 and C_2F_6 additions can be explained in two ways: (a) CO_2 and C_2F_6 moderate 'hot' H atoms and the thermalized atoms formed, have a greater relative tendency to add to olefine than to abstract from H_2S or the olefine; (b) CO_2 and C_2F_6 stabilize the hot alkyl radicals ($C_2H_5^*$ in this case) and prevent their back dissociation into H and the olefine. The trends observed with Xe additions and with increased pressure of the reactants show that the former effect, i.e., moderation of 'hot' H atoms, is responsible for most of the large decrease in H_2 when CO_2 and C_2F_6 are added. The heavy Xe atoms are poor moderators of H atoms while increasing pressures of H_2S and C_2H_4 at a constant ratio cannot have an effect on the reaction probability of the 'hot' H atoms. Only a slight decrease in H_2 is observed in these two instances and this should be ascribed to stabilization of the hot alkyl radicals. The much larger decrease in H_2 due to CO_2 and C_2F_6 is therefore mainly due to a moderation of hot H atoms.

CHAPTER 3

EXPERIMENTAL

Apparatus

The static high-vacuum apparatus employed was of the conventional all pyrex glass type. The essential features of the apparatus are shown in Figure 3.1..

The whole system could be evacuated to about 10^{-5} mm Hg by means of a 'three stage' mercury diffusion pump (P_1) which was backed by a single stage Welch rotary pump (P_2). A single manifold connected all parts of the apparatus. Gases used in the experiments were stored in bulbs V_1, V_2, V_3 and V_4, each having freezing nipples for purification of the gases. Storage bulb V_1 had a capacity of 2 litres and was used to store purified hydrogen iodide. The bulb was blackened in order to prevent photolytic decomposition. Apiezon T stopcock grease was used for greasing the stopcocks in frequent contact with hydrogen iodide, since it had been shown to be resistant to attack by HI. Silicone grease was used for the other stopcocks. The bulb V_2 also had a capacity of 2 litres and was used to store pure N_2O. Bulb V_3 having a capacity of 3 litres was used for storing CO_2, while bulb V_4 was a 1-litre vacuum sealed vessel containing helium. V_5 and V_6 were small calibrated vessels whose volumes were determined by weighing several times with distilled water.

Figure 3.1

Schematic diagram of the apparatus

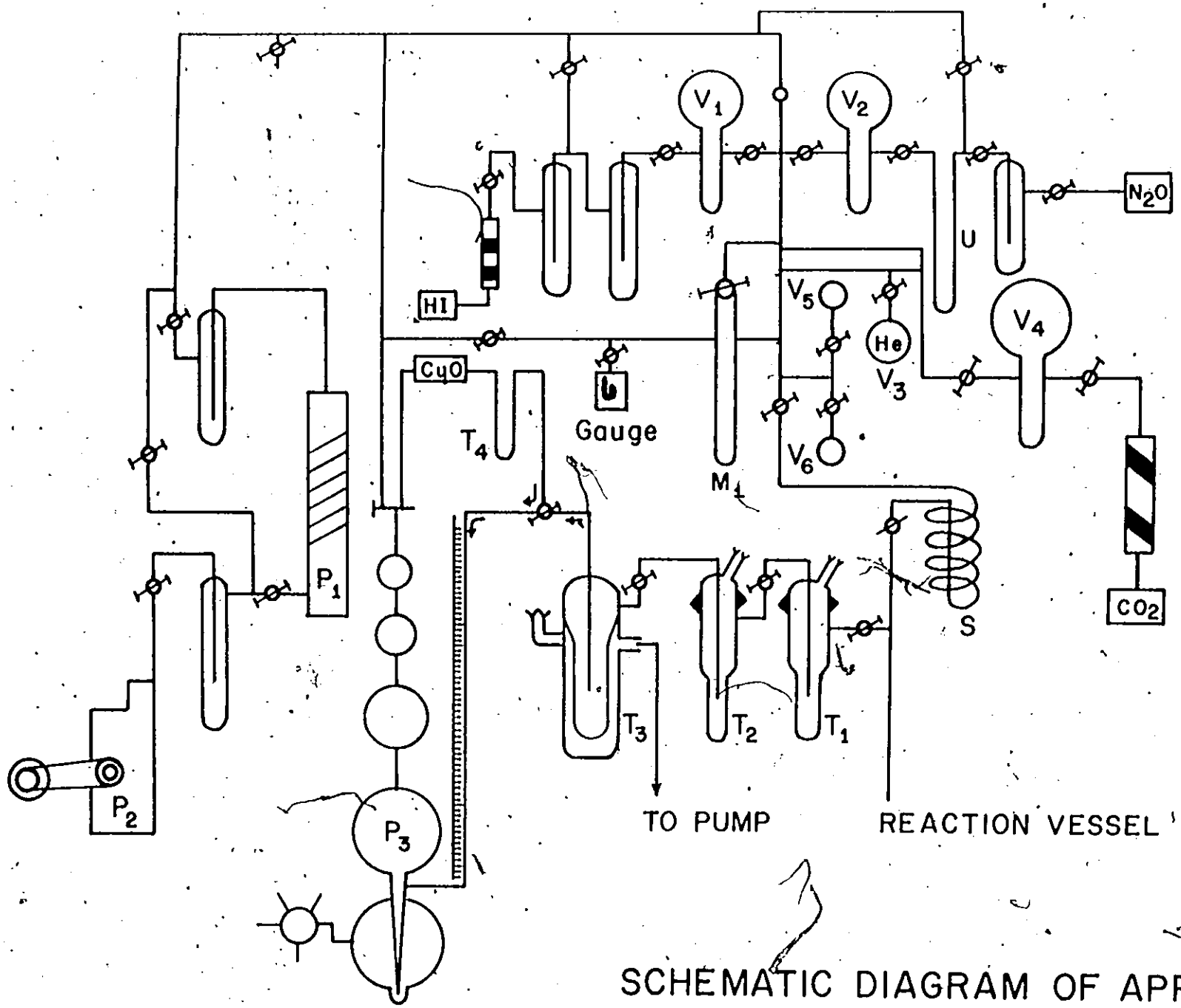

SCHEMATIC DIAGRAM OF APPARATUS

The standard volumes of these bulbs were taken as the mean average of several readings. V_5 had a volume of 151.8 ml and V_6 was 24.9 ml in volume. Pressures in these bulbs were measured with a mercury manometer M_1, which had a three-way stopcock connected to the main manifold. One arm was always used for measuring hydrogen iodide pressures, while the other arm was used for measuring nitrous oxide pressures. The reason for using separate arms for HI and N_2O, was, that hydrogen iodide slowly attacks mercury thereby contaminating it with iodides of mercury. The inlet to each bulb V_1 and V_2 was attached to a purification unit which in turn was attached to the cylinders of the research grade gases. A U-trap (U), approximately 80 cms long and one cm diameter, containing high activity silica gel for the purification of nitrous oxide, was connected between the bulb V_2 and a trap. Each of the storage vessels and the calibrated standard vessels was attached to the reaction vessel (RV) through a spiral (S) which was always maintained at $-78^{\circ}C$ to prevent mercury vapour from entering the reaction system.

The reaction vessel (RV) was a cylindrical quartz tube, 11 cm long and 5.5 cm in diameter, having plane parallel faces. The volume of the reaction vessel including the dead space was calculated as 280 ml. Attached to the reaction vessel was a small cold finger V_7, which was used for freezing the reaction mixtures and for mixing the gases before they were photolyzed. The outlet side of the reaction vessel was

attached to the analytical system, which consisted of two titration traps (T_1) and (T_2) followed by a pump-down solid N_2 trap (T_3) which in turn was attached to a Toplet pump (P_3) and a gas burette. Each volume in the gas burette was calibrated accurately by weighing with mercury and with water. The end of the gas burette was closed by a three-way stopcock, one connecting the main manifold and the second connecting a CuO furnace as illustrated in Figure 3.1. The CuO furnace was used to oxidize H_2 to H_2O and hence to separate H_2 from N_2. The CuO temperature was maintained at 320°C.

The Optical System

The reaction vessel (RV) was enclosed in a well insulated box, one side of which could be removed. The temperature of the box could be raised from room temperature to a greater temperature by heating with an electric coil, and made uniform throughout the box by a fan system. For temperatures lower than room temperature, namely, at 5°C and -20.5°C, only the reaction vessel was cooled. The box had a window of 6.0 x 6.0 cm where a quartz filter was used for wavelength 2537 Å, and a Corning glass filter, colour specification CS #9-53 was used to cut off light below 3000 Å. For the 3660 Å wavelength, a Corning glass filter (7380) of colour specification CS #0-52 was used.

The lamp was a medium pressure Hg arc, Hanovia S-500, which was attached to a transformer. An ammeter was placed in series with the lamp. Since the intensity of the

lamp depends on the amperage and voltage, these two variables were always kept constant. However, once the lamp began to age, the intensity fell; this was indicated by a fluctuation of the voltage. When the output of a lamp became irreproducible it was replaced. The total assembly is schematically pictured in Figure 3.2. The lamp was enclosed in a water cooled metal box which had a light-exit hole of 2.0 cm diameter. A quartz lens of 7.5 cm diameter and of 10 cm focal length was placed between the filter and the lamp so that the light beam falling on the reaction vessel was almost parallel and the total volume of the cell was illuminated.

An actinometer cell of 5.0 cm diameter and 3.0 cm depth was placed as shown in Figure 3.2. The position of the actinometer was adjusted such that all the light passing through the reaction vessel passed through the actinometer solution. In any experiment the volume of the actinometer solution was always kept constant. Reflection and absorption losses at the windows of the reaction vessel were negligible and hence corrections were unnecessary. The amount of oxalate decomposed with the reaction vessel in the path of the actinometer was 99% of that without the vessel.

Low Temperature Assembly

In the experimental work at 5.0 and -20.5°C, the general set up of the apparatus was essentially the same as described for the studies at 25.0°C. The additional apparatus

Figure 3.2

Optical System

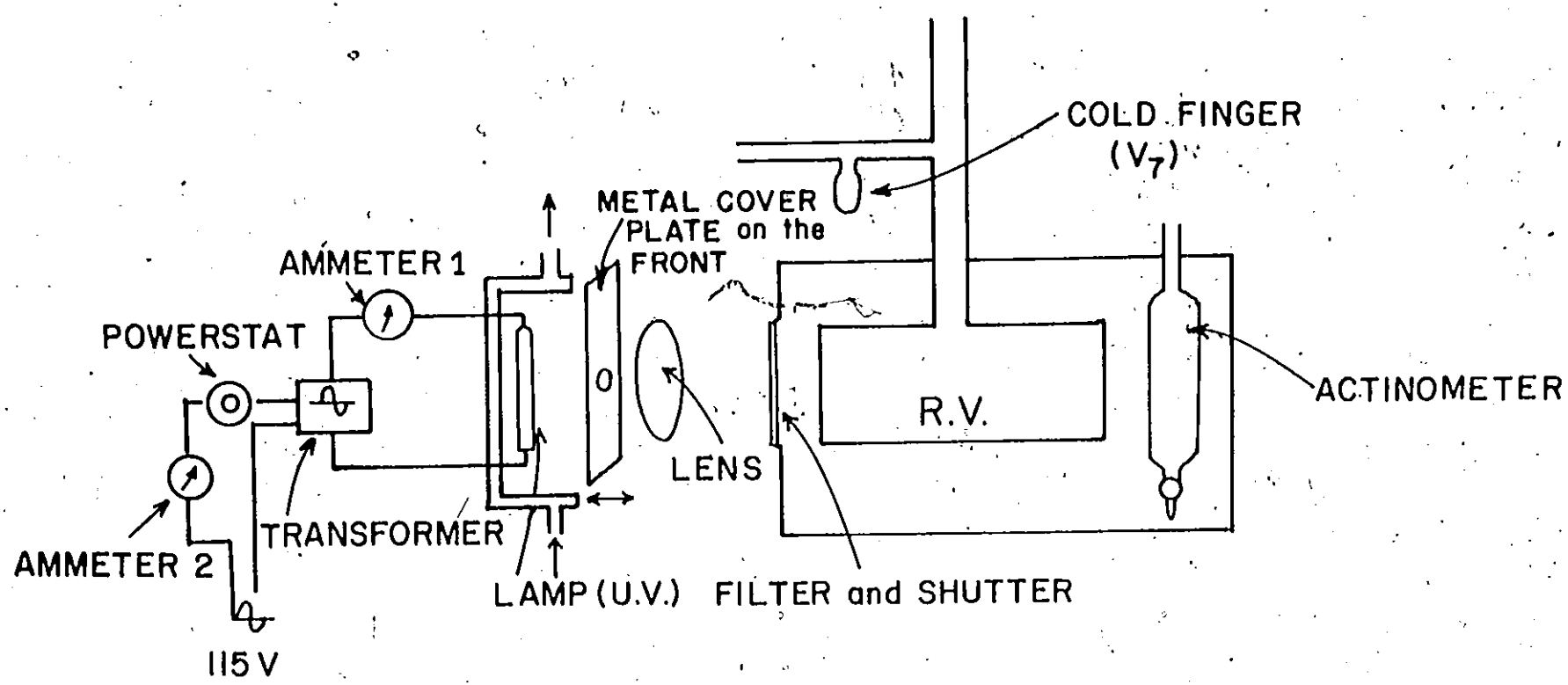

FIGURE 3·2 OPTICAL SYSTEM

incorporated into the main apparatus, consisted of (a) a new type of reaction vessel which was constructed so that only the vessel was cooled to the desired temperature, and (b) a thermostatic and pumping arrangement for maintaining the reaction vessel at the desired temperature.

The reaction cell assembly and thermostat are shown schematically in Figure 3.3. The cell was a cylindrical quartz vessel, 12 cm long and 5.5 cm diameter. The total volume including the dead space was 300.0 ml. The dead space as with the former reaction vessel, was not greater than 5-10% of the total volume.

The vessel was enclosed in an annular jacket, through which cooling liquid could be circulated, and the temperature was read by means of a copper-constantan thermocouple. The windows were enclosed by vacuum jackets (see Figure 3.3). This prevented condensation of water vapour on the windows. The whole assembly was surrounded by a close fitting styrofoam box. During a run, the window of the annular jacket on which the radiation was impinging, was kept free of moisture by passing a steady flow of dry nitrogen over its surface.

A temperature of 5°C was attained by circulating cooled alcohol through the reaction vessel jacket. The ethanol was cooled in a large beaker which was contained in a Dewar flask, by insertion of a metal can containing a mixture of coarse salt and ice. The amount of ice and salt

Figure 3.3

Low temperature assembly

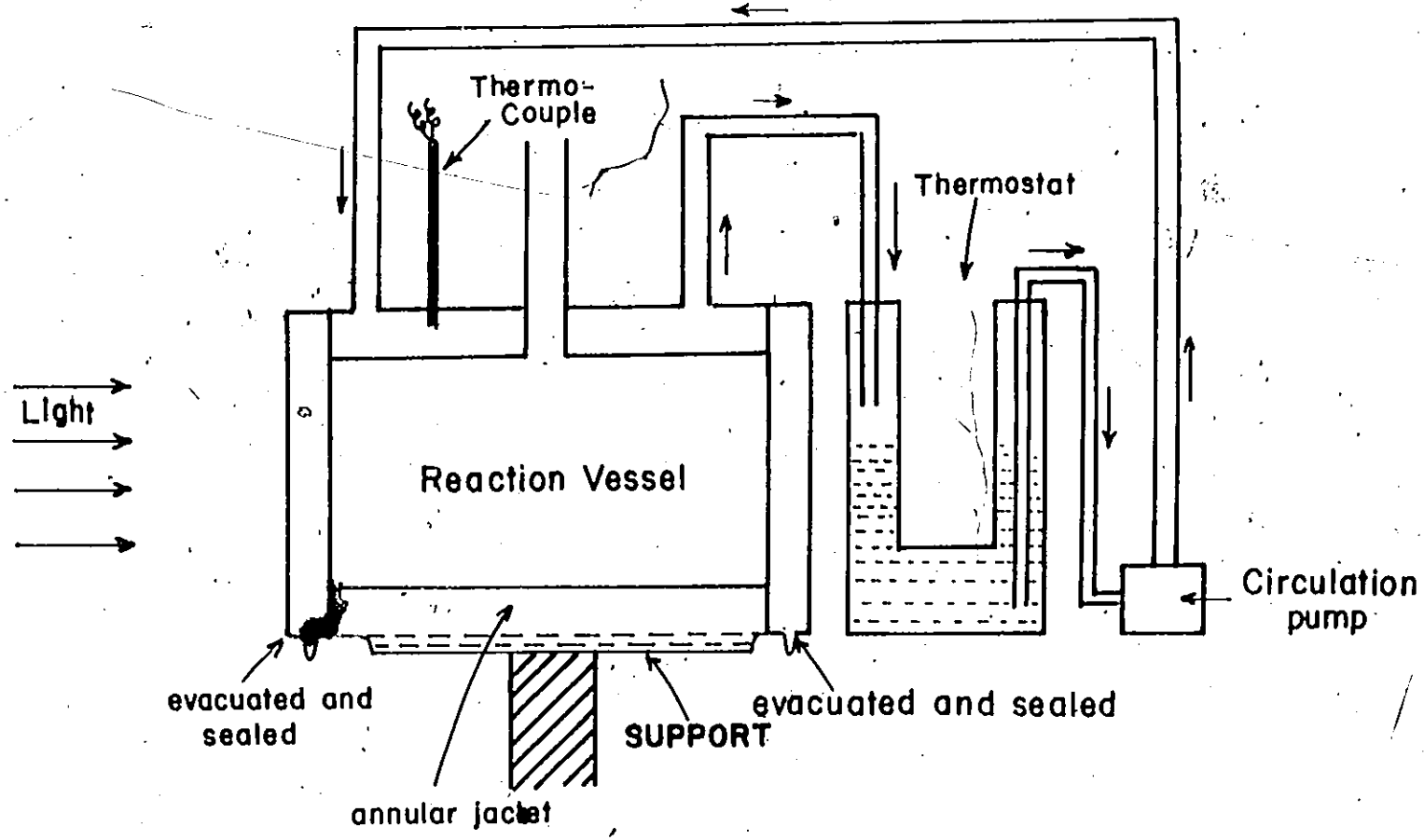
Thermo-
Couple
Thermostat
Light
Reaction Vessel
Circulation
pump
evacuated and
sealed
SUPPORT
evacuated and sealed
annular jacket

FIGURE 3·3

was always kept constant throughout a run and provision was made for draining off the water formed. The circulation of the cooled alcohol was accomplished by means of an electric pump. The whole cooling system was carefully insulated to minimise heat losses. The copper-constantan thermocouple, which was used to read the temperature in the reaction vessel, was calibrated against the boiling point of water and the melting point of ice. The temperature varied within $\pm 1.0^{\circ}C$ from run to run, but stayed constant during a particular run.

To attain $-20.5^{\circ}C$ the above method was slightly modified, by substituting dry ice for the ice and salt mixture in the metal can. By adjusting the amount of dry ice in the can, and keeping this level constant throughout a run, temperature variation during a run was minimised. The temperature varied $\pm 1.0^{\circ}C$ from run to run.

Materials

Hydrogen Iodide: A lecture bottle of hydrogen iodide (>99%) was obtained from the Matheson Co. Any HI taken from the lecture bottle was first condensed in a trap, cooled by liquid N_2. The condensed HI was pumped on for about 15 minutes to remove any H_2 and then after several trap to trap distillations ($-78^{\circ}C$ to $-196^{\circ}C$) the gas was stored in bulb V_1. Before use, the hydrogen iodide was again redistilled and any non-condensible gas at $-196^{\circ}C$ was removed by pumping. When HI is very pure, it is a white solid at

-196°C. HI decomposes very slowly and so before each experiment the HI was degassed and samples were taken at -78°C to avoid contamination by iodine.

Nitrous Oxide: Nitrous oxide gas (>98%) was also obtained from Matheson Co. The gas from the cylinder was condensed in a trap cooled by liquid nitrogen and any contaminating N_2 and O_2 were removed by pumping for a period of 60 minutes. The liquid nitrogen was then removed from the trap thus allowing the trap and the N_2O gas to warm up to room temperature. The N_2O gas was then passed through a column of silica gel (U) immersed in dry ice-acetone mixture at -78°C, to remove moisture. Simultaneously the nipple of the bulb V_2 was immersed in liquid nitrogen and communication was made between the bulb and the U-tube, so that the colder temperature of the liquid nitrogen provided the driving force for the N_2O gas to flow through the silica gel. The N_2O gas collected in the bulb V_2 was a white solid. Before each experiment in which N_2O was used, the N_2O was degassed at -196°C as a precautionary measure.

Carbon dioxide (a 'Linde' specialty gas) was instrument grade (99.99%) and was obtained from Union Carbide of Canada. Helium was pure research grade from Matheson Co. of Canada and was obtained in a 1-litre pyrex flask with a break-seal.

For the volumetric determination of iodine and hydrogen iodide, the following reagents were used: Analar

potassium iodide and Analar potassium iodate from BDH. The potassium iodide contained less than 0.0001% of iodate. Sodium thiosulphate was a Fischer certified reagent chemical.

Sodium oxalate, uranyl oxalate and potassium permanganate which were used in the actinometric determinations, were also Fischer certified reagent chemicals.

General Procedure

In a typical run, a known quantity of HI was taken in the standard vessel V_6 and the connecting dead space (whose volume was precisely known from HI titration), at a known pressure. From this the initial concentration of HI was calculated from the ideal gas law equation ($PV = nRT$). The amount of HI corresponding to a certain initial pressure could also be checked by consulting the titration graph in Figure 3.4. Table 3.1 shows a number of initial HI concentrations obtained from both the ideal gas equation and titrimetric evaluation. From the standard vessel V_6, HI was allowed to expand and then recondensed in the cold finger V_7 after passing through the spiral (S) which was kept at $-78^{\circ}C$. The stopcock attached to the reaction vessel was then closed and HI was allowed to expand into the reaction vessel. In every experiment the lamp was allowed to warm up for at least half an hour before photolysis of the reactant or reactants was commenced. When N_2O was added to the reaction system, a known amount of N_2O (measured in V_5 and attached dead space) was recondensed in

Figure 3.4

HI titration graph for calibrating a segment of the vacuum apparatus (Figure 3.1).

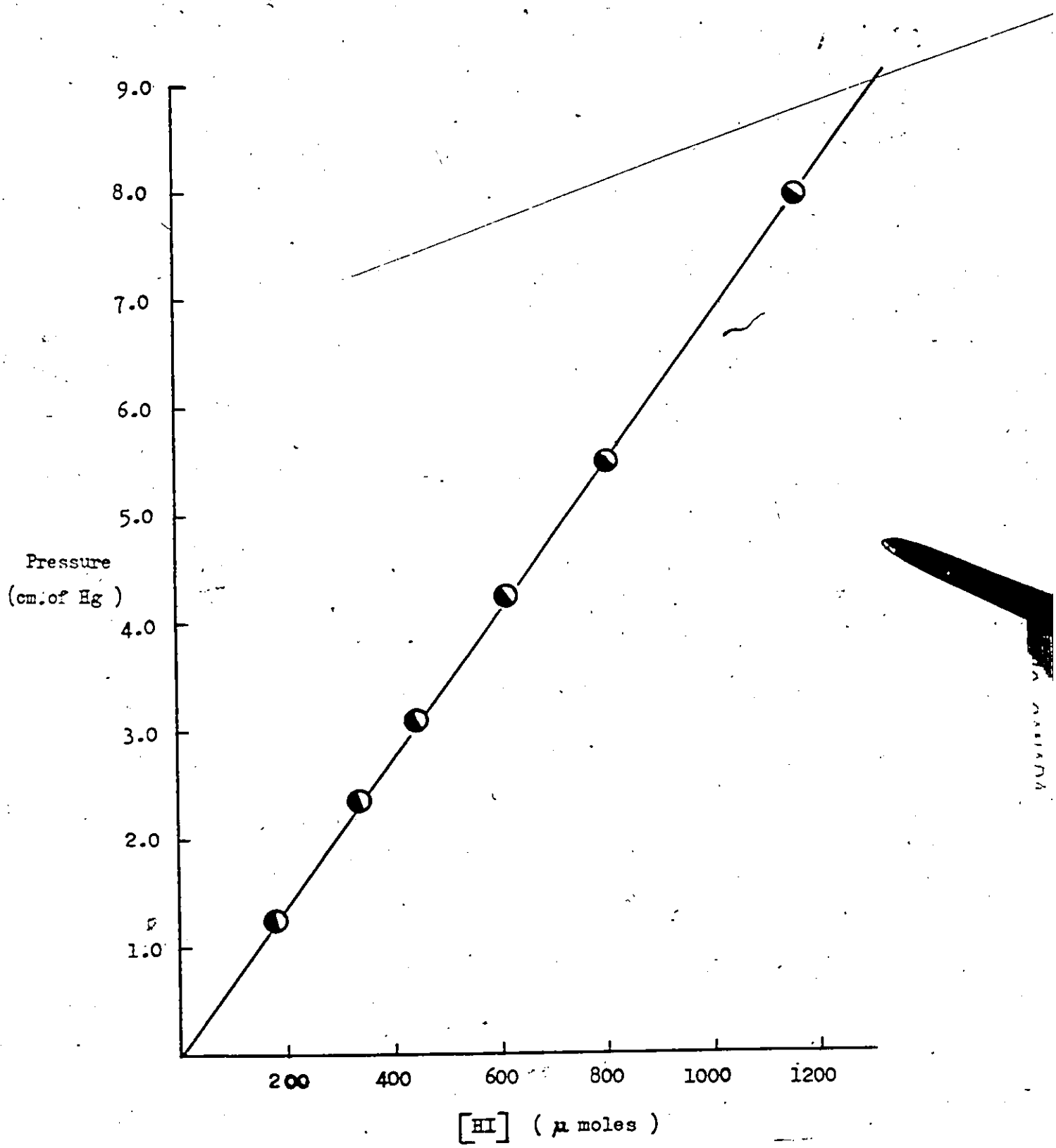
9.0
8.0
7.0
6.0
5.0
4.0
3.0
2.0
1.0
Pressure
(cm. of Hg)
200
400
600
800
1000
1200
[HI] (μ moles)

TABLE 3.1

CALIBRATION OF SECTION OF VACUUM LINE BY TITRIMETRIC EVALUATION OF INSERTED HI GAS

Pressure of HI Gas (cm of Hg)	No. of μ moles of HI (From Formula n = PV/RT) M_1	No. of μ moles of HI (From Titration) M_2
1.25	186.7	186.5
2.35	339.6	339.5
3.10	448.0	447.6
4.25	614.2	613.9
5.50	805.4	805.0
8.00	1176	1165

the cold finger V_7 after passing through (S). In order to ensure complete mixing of HI and N_2O and hence eliminate any errors due to variation in reactant composition, the two gases were condensed in V_7 and evaporated several times before they underwent photolysis. Once the mixture had attained the reaction temperature, it was photolysed for a known interval of time (which varied from 5 minutes to 6 hours). With the addition of CO_2 to the system, the same procedure as in the case of N_2O was followed. However, when helium was being introduced to the reaction vessel, HI and N_2O were kept condensed in the cold finger, and a certain pressure of helium was selected for a given volume (consisting of the reaction cell's volume and minimum volume of dead space connecting the reaction vessel to the helium reservoir). The stopcock attached to the reaction vessel was then closed and the condensed gases were allowed to expand and mingle with the helium gas. The process of recondensing and expansion for a number of times was also effected here, although this process only applied to the condensible gases and not to helium. The helium residing in the space outside the reaction vessel (i.e., beyond the stopcock connecting the reaction vessel to the remainder of the apparatus) was pumped away.

In each case in the photolysis of HI or a mixture, the reaction was allowed to proceed to no more than 7% conversion, except in a few cases, where the inhibition of H_2 production by N_2O, was studied over a prolonged period of

photolysis. At the end of an experiment, the light was shut off, and the reactants and products were condensed in the titration trap (T_1) using liquid N_2. Trap (T_2) was also cooled by liquid N_2, while trap (T_3) had solid N_2 ($-210^{\circ}C$) as coolant. The non-condensible gases H_2 and N_2 were removed at $-210^{\circ}C$ and were measured in the gas burette using the Topler pump. This gave the total amount of H_2 and N_2. All the gas was then displaced into the CuO furnace, which was maintained at $320^{\circ}C$. The displacement of the gas was effected by raising the mercury in the gas burette up to the threeway stopcock (Figure 3.1). The H_2O formed by the oxidation of hydrogen by CuO, was condensed in Trap T_4 which was cooled by liquid nitrogen. After about 30 minutes, the liquid nitrogen coolant was replaced by acetone and dry-ice and after a further 15 minutes, the residual gas was recirculated into the gas burette and its pressure measured. The process of combustion and recirculation was repeated until the gas burette reading was constant. In most cases only two repetitions were necessary. When the pressure was constant, the value was noted; this gave the amount of N_2 present in the mixture. The difference gave the amount of H_2.

After the removal of H_2 and N_2, an attempt was made to separate any nitric oxide present, from HI, by distilling the mixture in trap T_1 at liquid N_2 temperature, to trap T_3 at $-210^{\circ}C$. This distillation was carried on for a period of about 6 hours. However, in all experiments where this pro-

cedure was carried out, no measurable amount of NO was obtained, and moreover the mass balances from each experiment showed invariably that $H_2 + N_2 \not\rightarrow I_2$ and hence nitric oxide (NO) was not a product of the photolysis of HI and N_2O mixtures.

I_2 and HI were separated using acetone-dry ice and liquid N_2. The stopper in the titration trap T_1 was removed and a dilute solution of potassium iodide was introduced through the side tube. The trap was removed and the solution with combined rinsings was titrated with standard sodium thiosulphate solution using starch indicator. Potassium iodide solution was also added to the HI while it was condensed in liquid N_2 in trap T_2. After warming up to room temperature, the trap was removed and its contents and washings were poured into a 100 ml volumetric flask. 10 mls of saturated potassium iodate solution were added to the HI solution and combined rinsings. The iodine so liberated was titrated against standard sodium thiosulphate solution using starch indicator.

Added I_2 at 25.0°C

When it was necessary to introduce I_2 into the reaction vessel before a run, a known amount of HI was photolysed for a given time and the I_2 formed was separated from H_2 and residual HI by condensing the iodine vapour in the reaction vessel with an acetone-dry ice mixture, while

pumping away the H_2 and HI via trap T_1 which was cooled by liquid N_2. HI was collected in trap T_1 and subsequently removed.

Actinometry

The uranyl oxalate actinometer was employed in order to determine the number of quanta absorbed by the reactants. The procedure outlined in Farkas and Melville (112) was adopted. A 0.005 M solution of uranyl oxalate was used in all experiments. The oxalate solution was filled accurately up to the mark in the actinometer cell, the volume of which was exactly known. After the photolysis, all the solution was transferred to a clean dry 250 ml volumetric flask. After shaking well, 10 mls of the solution were pipetted into a conical flask and 10 mls of $6NH_2SO_4$ were added. The titration was then carried out at about 85°C with standard N/50 potassium permanganate solution. The permanganate solution was standardized with a standard sodium oxalate solution, following the procedure outlined in Vogel (113). A portion of the unexposed uranyl oxalate solution was also titrated with N/50 $KMNO_4$ solution. Knowing the volume of the actinometer solution and the quantum yield of the oxalate decomposition, the number of einsteins absorbed by the reactant(s) could be calculated. Suppose C_1 moles litre^{-1} of oxalate are decomposed in time 't' without any reactant in the reaction vessel, and C_2 moles litre^{-1} are decomposed in the same time with the

reactant present, then the fraction of light absorbed by the reactant is proportional to

$$\frac{C_1 - C_2}{C_1}$$

The incident light intensity I_o is proportional to C_1 or in other words, C_1 moles litre^{-1} of oxalate have been decomposed due to the absorption of a certain number of einsteins given out by the lamp. Since the volume of the actinometer solution was V ml and not one litre, the amount of oxalate decomposed would be

$$\frac{C_1 \times V}{1000} \text{ moles}$$

and taking the quantum yield as 0.55 at 25°C, the number of einsteins initially absorbed would be given as

$$E_o = \frac{C_1 \times V}{1000 \times 0.55}$$

or, the number of einsteins absorbed by the reactant

$$= \frac{C_1 - C_2}{C_1} \times \frac{C_1 \times V}{1000 \times 0.55}$$

i.e., $$E_{abs} = \frac{(C_1 - C_2)\ V}{1000 \times 0.55}$$

Therefore, having a knowledge of the number of moles of product formed by the analytical method, and the number of einsteins absorbed by the actinometer, the quantum yield can be calculated.

CHAPTER 4

RESULTS AND DISCUSSION

The kinetics of the HI/N_2O system were studied at three wavelengths, namely 2537 Å, 3130 Å and 3660 Å.

Nitrous oxide (N_2O) does not undergo any photochemical reaction at any of these wavelengths; it shows photochemical activity at much shorter wavelengths. The role of the nitrous oxide throughout all the photochemical investigations in this work, at the three temperatures, 25°C, 5°C and -20.5°C, is as a chemical adduct to hot hydrogen atoms.

In the absence of nitrous oxide, the production of hydrogen for any HI photolysis remains constant. When the photochemical conversion is limited to 7-10% of the initial amount of hydrogen iodide, inhibition by I_2 is minimal.

The addition of N_2O to the HI photolysis has a significant effect on the quantum yield of hydrogen, the effect increasing with increase of nitrous oxide, when the HI concentration and the photolysis time period are both kept constant. Tables 4.1 and 4.2 show the effect of added N_2O on the HI photochemical system. The amount of hydrogen (H_2) formed in each run, divided by the number of microeinsteins absorbed by a constant amount of HI gives the quantum yield ϕ_{H_2}.

TABLE 4.1

ϕ_{H_2} Values at Various $\frac{[N_2O]_o}{[HI]_o}$ Ratios and at Various HI Concentrations

[Series 1][λ → 3130 Å][Time 2700 seconds][Temperature 25°]

$\frac{[N_2O]_o}{[HI]_o}$	$[H_2]$ (μmoles)	$[N_2]$ (μmoles)	$[I_2]$ (μmoles)	$[HI]_o$ (μmoles)	$[HI]_f$ (μmoles)	E_{abs} (μeinsteins)	ϕ_{H_2} (moles einstein^{-1})
0.0	7.40	0.00	7.40	202	187	7.40	1.000
1.0	6.60	0.74	7.39	201	186	7.40	0.891
2.1	6.41	0.93	7.38	204	189	7.39	0.868
3.0	6.36	0.98	7.39	200	184	7.39	0.861
4.0	6.36	0.98	7.38	201	186	7.39	0.861
5.1	6.36	0.98	7.38	201	186	7.39	0.861
6.1	6.36	0.98	7.38	193	179	7.39	0.861
7.0	6.36	0.98	7.40	200	186	7.39	0.861
8.0	6.36	0.98	7.39	193	179	7.40	0.861
9.0	6.36	0.98	7.38	205	191	7.40	0.861
10.0	6.36	0.98	7.39	201	186	7.39	0.861

Table 4.1 - continued

[Series 2]

$\frac{[N_2O]_o}{[HI]_o}$	$[H_2]$ (μmoles)	$[N_2]$ (μmoles)	$[I_2]$ (μmoles)	$[HI]_o$ (μmoles)	$[HI]_f$ (μmoles)	E_{abs} (μeinsteins)	ϕ_{H_2} (moles einstein^{-1})
0.0	11.4	0.00	11.4	369	348	11.4	1.000
1.0	10.4	0.98	11.4	370	347	11.4	0.912
2.1	10.3	1.11	11.4	387	364	11.4	0.900
3.1	10.2	1.22	11.4	385	363	11.4	0.890
4.0	10.2	1.23	11.4	371	349	11.4	0.890
5.1	10.2	1.23	11.4	372	350	11.4	0.890
6.0	10.2	1.22	11.4	373	351	11.4	0.890
7.0	10.2	1.23	11.4	385	362	11.4	0.890
8.1	10.2	1.23	11.4	374	352	11.4	0.891
9.0	10.2	1.22	11.4	362	339	11.4	0.890
10.0	10.2	1.23	11.4	376	352	11.4	0.891
11.0	10.2	1.23	11.4	372	349	11.4	0.890

Table 4.1 - continued

[Series 3]

$\frac{[N_2O]_o}{[HI]_o}$	$[H_2]$ (μmoles)	$[N_2]$ (μmoles)	$[I_2]$ (μmoles)	$[HI]_o$ (μmoles)	$[HI]_f$ (μmoles)	E_{abs} (μeinsteins)	ϕ_{H_2} (moles einstein^{-1})
0.0	14.4	0.00	14.4	511	483	14.4	1.000
1.0	13.4	0.99	14.4	511	482	14.4	0.931
2.0	13.2	1.22	14.4	511	482	14.4	0.915
3.0	13.1	1.35	14.5	507	478	14.4	0.911
4.1	13.1	1.35	14.5	518	489	14.5	0.911
5.0*	13.1	1.35	14.5	500	470	14.5	0.911
6.1	13.1	1.35	14.5	518	489	14.5	0.911
7.1	13.1	1.34	14.5	508	480	14.4	0.911
8.1	13.1	1.35	14.5	508	479	14.4	0.911
9.0	13.1	1.35	14.5	503	474	14.5	0.911
10.0	13.1	1.35	14.5	510	481	14.5	0.911

Table 4.1 - continued

[Series 4]

$\frac{[N_2O]_o}{[HI]_o}$	$[H_2]$ (μmoles)	$[N_2]$ (μmoles)	$[I_2]$ (μmoles)	$[HI]_o$ (μmoles)	$[HI]_f$ (μmoles)	E_{abs} (μeinsteins)	ϕ_{H_2} (moles einstein^{-1})
0.0	16.9	0.00	16.9	674	639	16.9	1.000
1.0	15.8	1.10	16.9	667	632	16.8	0.937
2.0	15.6	1.22	16.9	667	633	16.9	0.928
3.0	15.5	1.41	16.9	666	633	16.8	0.920
4.1	15.5	1.40	16.9	668	634	16.8	0.920
5.0	15.5	1.39	16.9	663	630	16.9	0.920
6.1	15.5	1.39	16.9	652	619	16.9	0.920
7.1	15.5	1.40	16.9	690	655	16.9	0.920
8.1	15.5	1.40	16.9	689	656	16.9	0.920
9.0	15.5	1.40	16.9	646	612	16.9	0.920
10.1	15.5	1.41	16.9	670	635	16.9	0.920
11.1	15.5	1.41	16.9	676	643	16.9	0.920

Table 4.1 - concluded

[Series 5]

$\frac{[N_2O]_o}{[HI]_o}$	$[H_2]$ (μmoles)	$[N_2]$ (μmoles)	$[I_2]$ (μmoles)	$[HI]_o$ (μmoles)	$[HI]_f$ (μmoles)	E_{abs} (μeinsteins)	ϕ_{H_2} (moles einstein^{-1})
0.0	24.2	0.00	24.2	1027	979	24.2	0.999
1.0	22.9	1.23	24.2	1045	997	24.2	0.948
2.1	22.8	1.34	24.2	1028	979	24.2	0.943
3.0	22.7	1.47	24.2	1023	975	24.2	0.937
4.0	22.7	1.46	24.2	1030	983	24.2	0.937
5.0	22.7	1.47	24.2	1028	980	24.2	0.937
6.0	22.7	1.47	24.2	1021	972	24.2	0.938
7.0	22.7	1.47	24.2	1022	974	24.2	0.937
8.0	22.7	1.46	24.2	1031	982	24.2	0.936
10.0	22.7	1.47	24.2	1020	971	24.2	0.937

TABLE 4.2

Variation of ϕ_{H_2} Values at Various $\frac{[N_2O]}{[HI]_o}$ Ratios

and at Various HI Concentrations

[Temp: -20°5C][λ → 3130 Å][Time 2700 seconds]

[Series 1]

$\frac{[N_2O]}{[HI]_o}$	$[H_2]$ (μmoles)	$[N_2]$ (μmoles)	$[I_2]$ (μmoles)	$[HI]_o$ (μmoles)	$[HI]_f$ (μmoles)	ϕ_{H_2} (moles einstein^{-1})
0.0	11.1	0.00	11.1	378	356	1.000
1.0	10.8	0.15	11.1	372	350	0.977
2.0	10.6	0.37	11.1	378	356	0.956
3.0	10.4	0.63	11.1	389	368	0.935
4.0	10.1	0.85	11.1	375	352	0.914
5.0	10.1	0.85	11.1	380	358	0.914
6.0	10.1	0.85	11.1	384	362	0.913
7.0	10.1	0.85	11.1	384	361	0.914
8.0	10.1	0.85	11.1	380	358	0.914
9.0	10.1	0.85	11.1	380	357	0.913
10.0	10.1	0.85	11.1	381	359	0.914
11.1	10.1	0.85	11.1	387	364	0.914

Table 4.2 - continued

[Series 2]

$\frac{[N_2O]}{[HI]_o}$	$[H_2]$ (μmoles)	$[N_2]$ (μmoles)	$[I_2)$ (μmoles)	$[HI]_o$ (μmoles)	$[HI]_f$ (μmoles)	ϕ_{H_2} (moles einstein^{-1})
0.0	23.8	0.00	23.8	1020	973	0.999
1.0	23.3	0.48	23.8	1017	970	0.978
2.0	22.8	0.97	23.8	1006	958	0.957
3.0	22.3	1.46	23.8	1002	955	0.937
4.0	22.3	1.46	23.8	1029	982	0.937
5.0	22.3	1.46	23.8	1018	970	0.937
6.0	22.3	1.46	23.8	1005	957	0.937
7.0	22.3	1.46	23.8	1011	964	0.937
8.0	22.3	1.46	23.8	1027	979	0.937
9.1	22.3	1.46	23.8	1025	977	0.937
10.0	22.3	1.46	23.8	1014	967	0.937

In the presence of N_2O the quantum yield of hydrogen continues to decrease from a value of unity in pure HI, and attains a limiting value which shows no further change despite larger additions of nitrous oxide. The experimental results show that the limiting quantum yield has some dependency on HI concentration. This dependency is illustrated in Figure 4.1 for the 3130 Å radiation. A similar dependency is found for 2537 Å and 3660 Å radiations. Table 4.3 and Figure 4.2 show this for the 2537 Å wavelength.

The N_2 yields showed the opposite behaviour to the H_2 yields. With a fixed concentration of HI and the photolysis time kept constant, the production of N_2 increased with increasing N_2O, the N_2 yield reaching its limiting value concommitantly with H_2 reaching its limiting value.

The yields of both H_2 and N_2 were related to the wavelength of the radiation used. The yields increase with decrease in wavelength, i.e., with increase in the energy of radiation, so that for corresponding runs at the three wavelengths, the largest yields of N_2 were obtained with the 2537 Å radiation and the smallest yields with the 3660 Å radiation.

A change of λ gives a change of excess energy E, where $E = h\nu - D_{(H-I)}$. $D_{(H-I)}$ is the dissociation energy of the H-I bond. The shorter the wavelength, the larger E becomes, and thus the hydrogen atoms produced are hotter. Consequently there is a greater probability of fruitful reactions occurring between the hot H atoms and the other

Figure 4.1

Variation of ϕ_{H_2} as a function of $\frac{[N_2O]}{[HI]}$ at 25°C and 3130 Å

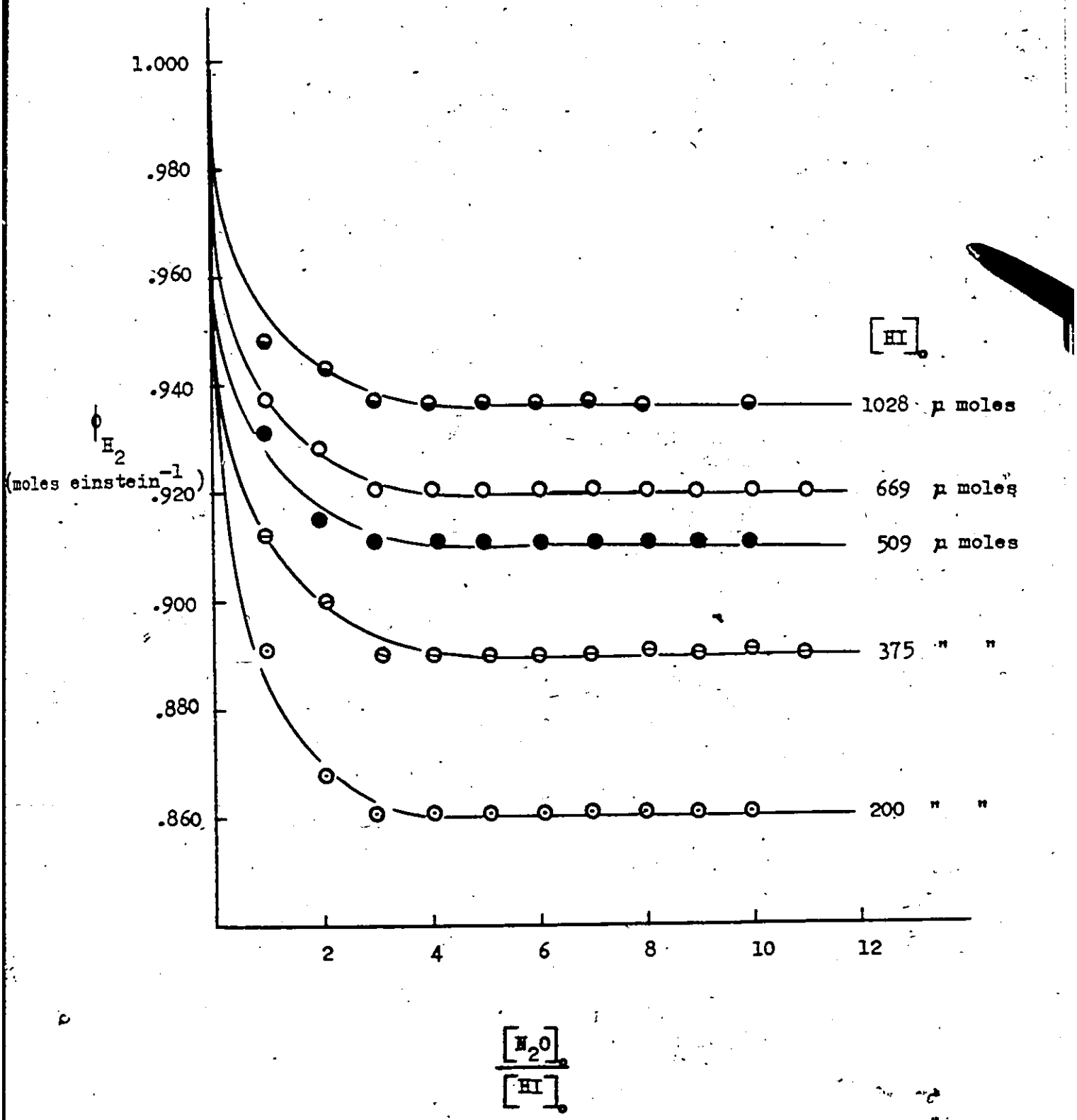
1.000
.980
.960
.940
.920
.900
.880
.860
ϕ_{H_2}
(moles einstein^{-1})
2
4
6
8
10
12
$\frac{[H_2O]_o}{[HI]_o}$
$[HI]_o$
1028 μ moles
669 μ moles
509 μ moles
375 " "
200 " "

TABLE 4.3

ϕ_{H_2} Values at Various $\frac{[N_2O]_o}{[HI]_o}$ Ratios and at Various HI Concentrations

[Series 1][Temp: 25°C][λ = 2537 Å][Time 450 seconds]

$\frac{[N_2O]}{[HI]_o}$	$[H_2]$ (μmoles)	$[N_2]$ (μmoles)	$[I_2]$ (μmoles)	$[HI]_o$ (μmoles)	$[HI]_f$ (μmoles)	E_{abs} (μeinsteins)	ϕ_{H_2} (moles einstein^{-1})
0.0	26.6	0.00	26.6	651	597	26.6	1.000
1.1	24.7	1.80	26.6	652	599	26.6	0.930
2.0	23.7	2.88	26.6	650	598	26.6	0.891
3.0	22.6	3.90	26.5	650	598	26.6	0.851
4.0	21.6	4.91	26.5	652	599	26.6	0.813
5.1	21.0	5.47	26.5	652	598	26.6	0.792
6.1	20.7	5.78	26.5	650	598	26.6	0.780
7.1	20.6	5.87	26.5	650	597	26.6	0.777
8.1	20.6	5.87	26.6	652	599	26.6	0.777
9.0	20.6	5.86	26.6	651	598	26.6	0.778
10.1	20.6	5.87	26.6	650	597	26.6	0.777
11.0	20.6	5.87	26.5	648	594	26.6	0.777

Table 4.3 - continued

[Series 2]

$\frac{[N_2O]_o}{[HI]_o}$	$[H_2]$ (μmoles)	$[N_2]$ (μmoles)	$[I_2]$ (μmoles)	$[HI]_o$ (μmoles)	$[HI]_f$ (μmoles)	E_{abs} (μeinsteins)	ϕ_{H_2} (moles einstein^{-1})
0.0	16.3	0.00	16.3	371	339	16.3	1.000
1.3	15.0	1.25	16.3	374	342	16.2	0.925
2.0	14.4	1.81	16.3	373	341	16.2	0.883
3.0	13.7	2.46	16.2	374	341	16.3	0.844
4.0	13.1	3.12	16.3	371	339	16.3	0.808
5.0	12.6	3.65	16.3	375	343	16.3	0.774
6.1	12.2	4.05	16.3	373	341	16.3	0.750
7.0	12.1	4.11	16.3	371	338	16.3	0.745
8.0	12.1	4.11	16.3	373	340	16.3	0.744
9.0	12.1	4.12	16.3	370	338	16.3	0.745
10.0	12.1	4.10	16.3	376	344	16.3	0.745
11.1	12.1	4.11	16.3	375	343	16.2	0.745

Figure 4.2

Variation of ϕ_{H_2} as a function of $\frac{[N_2O]}{[HI]}$ at 25°C and 2537 Å

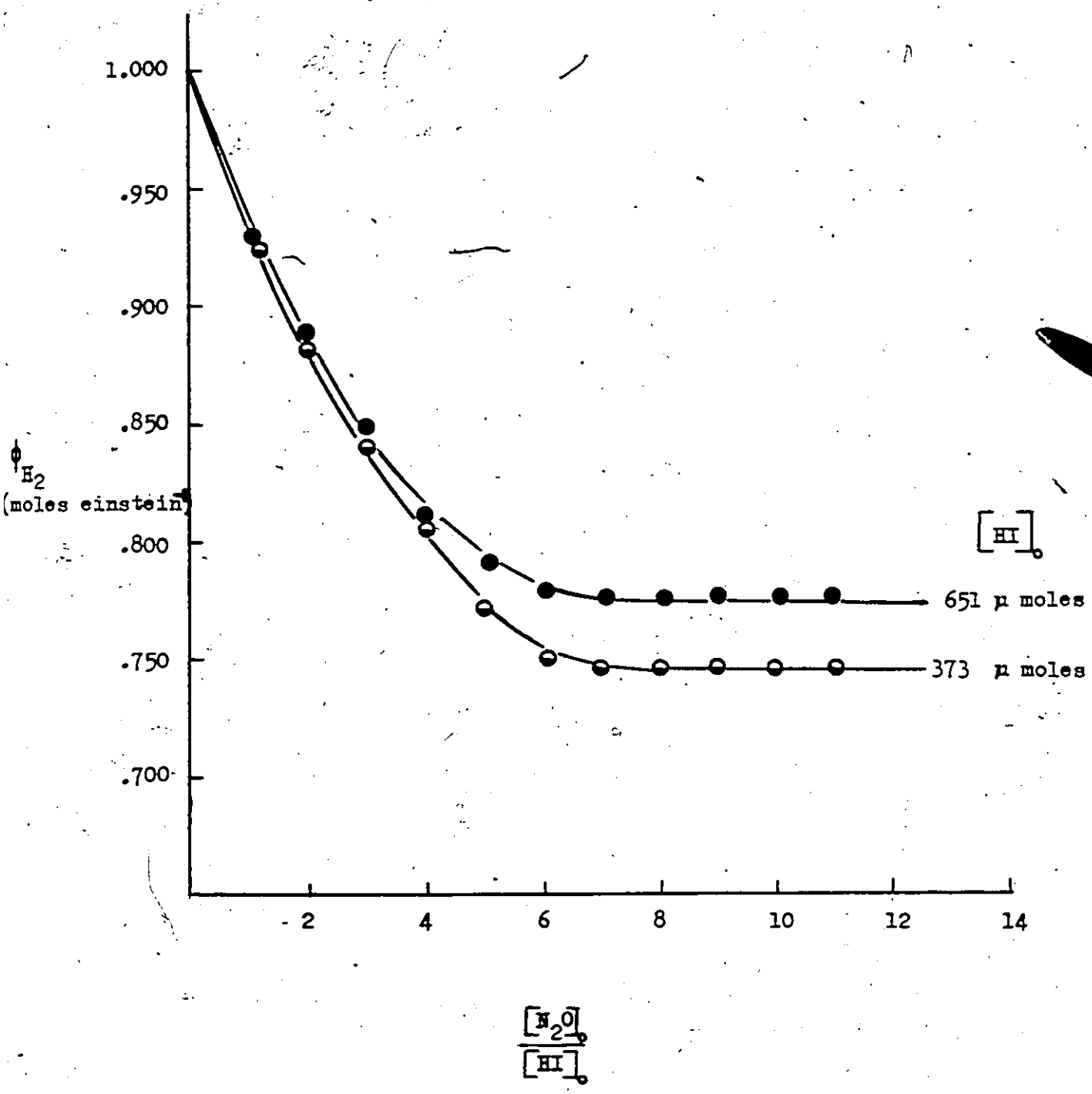

reactive species in the photochemical system. In addition, the intensity of radiation is greater at the shorter wavelength and would also account for the increase in product yields as one passes from the 3660 Å to the 2537 Å wavelength.

In a typical time course run with a constant $\frac{[N_2O]}{[HI]}$ ratio, the rates of H_2 and N_2 production continued to decrease until the saturated vapour pressure of I_2 was reached. Beyond this, limiting values of the rates prevailed. Figure 4.3 shows the time yield plots for H_2 and N_2 production at 25°C while Figures 4.4 and 4.5 show the respective plots for H_2 and N_2 production with time, at 5°C and -20.5°C.

Figures 4.4 and 4.5 show that at both 5°C and -20.5°C, the rates of production of hydrogen and nitrogen are constant and are independent of time. For 198 μmoles of HI and $\frac{[N_2O]_o}{[HI]_o}$ = 3.0 at 5°C, the rate of hydrogen production is 3.3×10^{-9} moles sec^{-1}, and the rate of N_2 production is 2.1×10^{-10} moles sec^{-1} at 3130 Å. For 197 μmoles of HI at -20.5°C, with $\frac{[N_2O]_o}{[HI]_o}$ = 3.1 ($\lambda \rightarrow$ 3130 Å), the rate of hydrogen production is also 3.3×10^{-9} moles sec^{-1}, while the rate of N_2 production is 1.8×10^{-10} moles sec^{-1}. At these lower temperatures, the different saturation vapour pressures (S.V.P.'s) play no effective role in determining the rates of H_2 and N_2 production. The S.V.P. of I_2 at 5°C was calculated as 1.13 μmoles and at -20.5°C the S.V.P. was determined as 0.104 μmoles for the reaction cell volume of 300 cc. The S.V.P. at 25°C corresponded

Figure 4.3

Yield-time plots for the formation of H_2 and N_2 at 25° and 3130 Å

$\frac{[N_2O]_o}{[HI]_o} = 3.08$

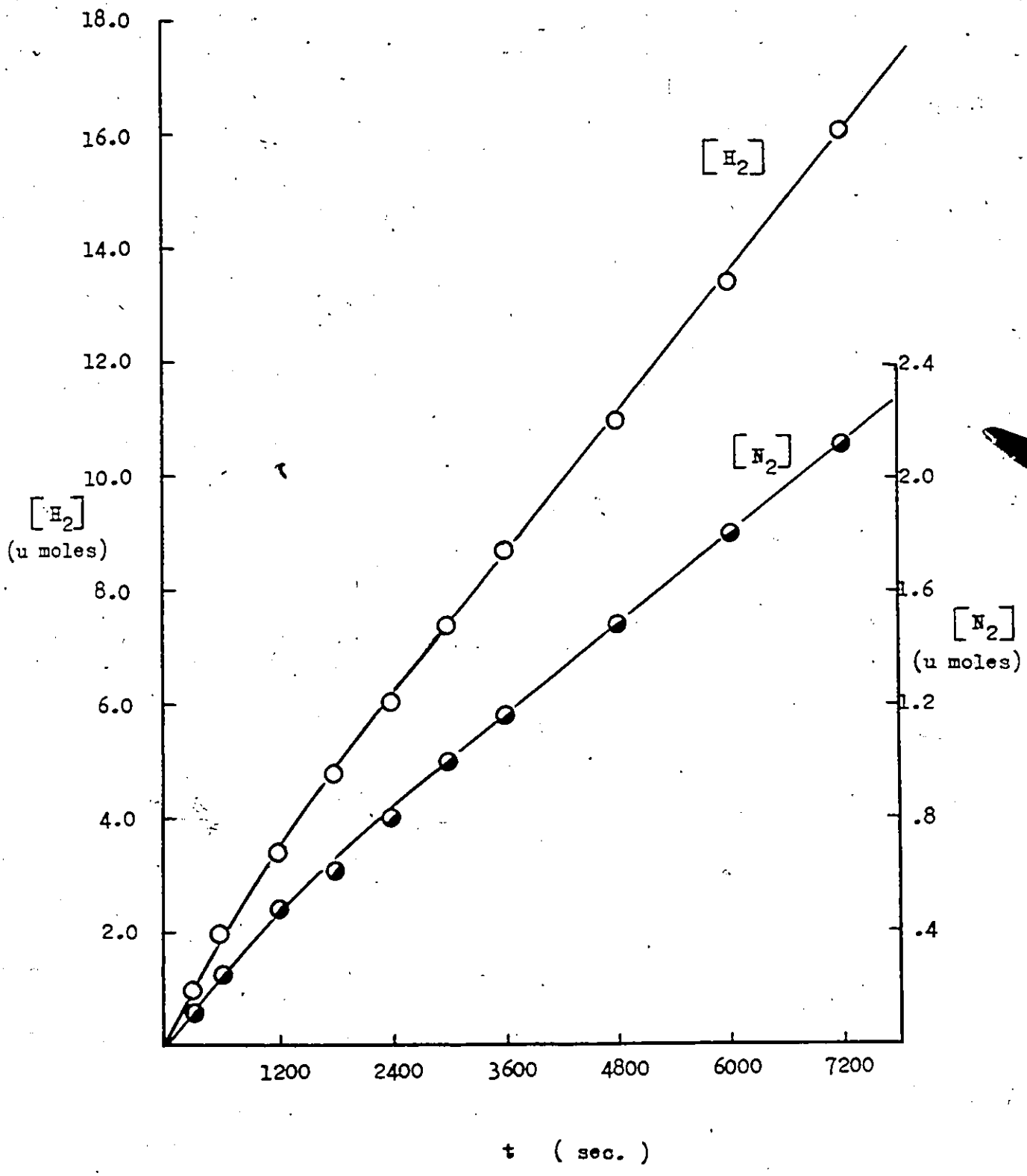
18.0
16.0
14.0
12.0
10.0
8.0
6.0
4.0
2.0
[H2]
(u moles)
2.4
2.0
1.6
1.2
.8
.4
[N2]
(u moles)
[H2]
[N2]
1200
2400
3600
4800
6000
7200
t (sec.)

Figure 4.4

Yield-time plot for the production of H_2 and N_2 at 5°C and 3130 Å

$$\frac{[N_2O]_o}{[HI]_o} = 3.00$$

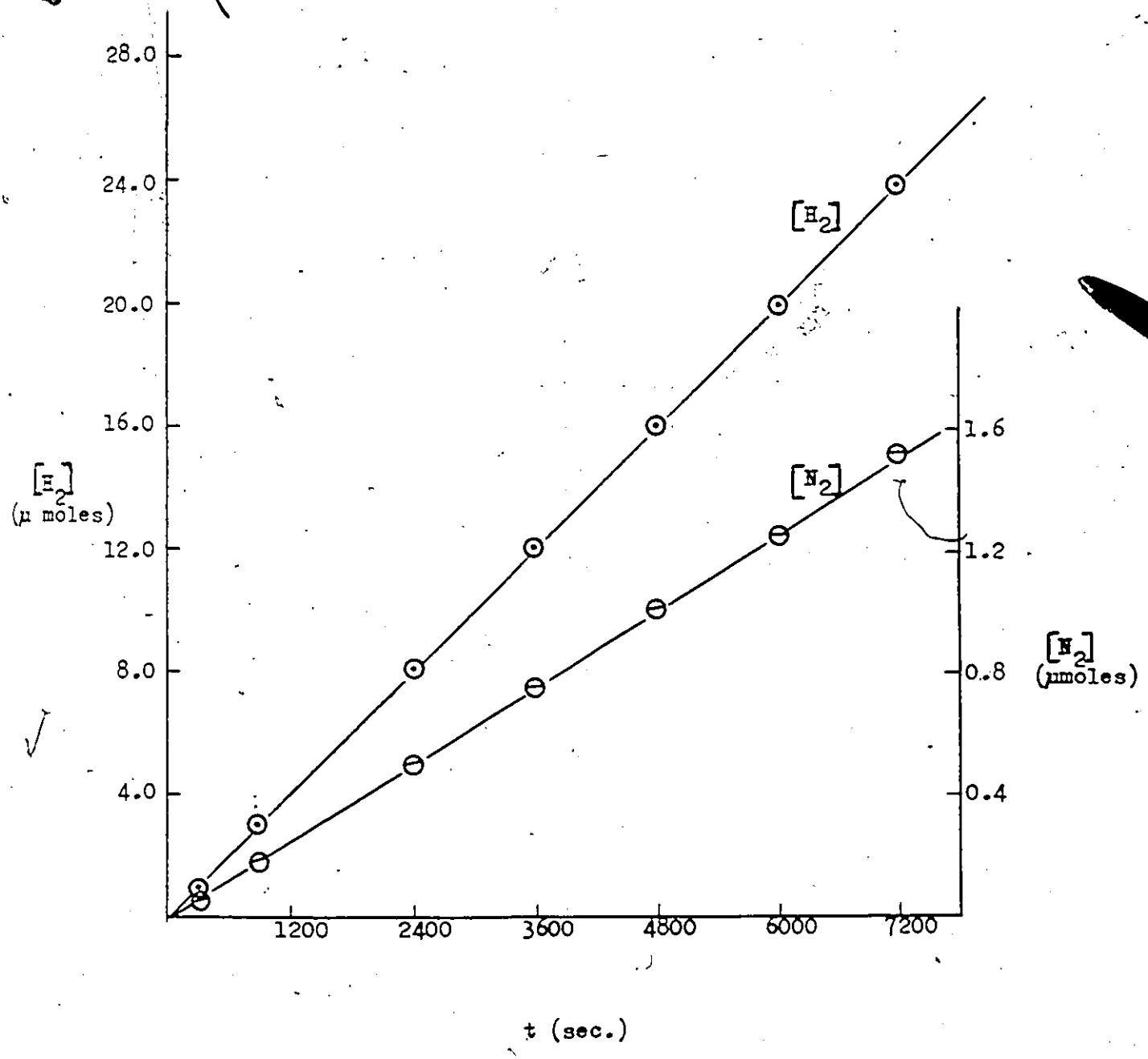
28.0
24.0
20.0
16.0
12.0
8.0
4.0
[H2]
(μ moles)
[H2]
[N2]
1.6
1.2
0.8
0.4
[N2]
(μmoles)
1200
2400
3600
4800
6000
7200
t (sec.)

Figure 4.5

Yield-time plot for the production of H_2 and N_2 at -20.5°C and 3130 Å

$$\frac{[N_2O]_o}{[HI]_o} = 3.05$$

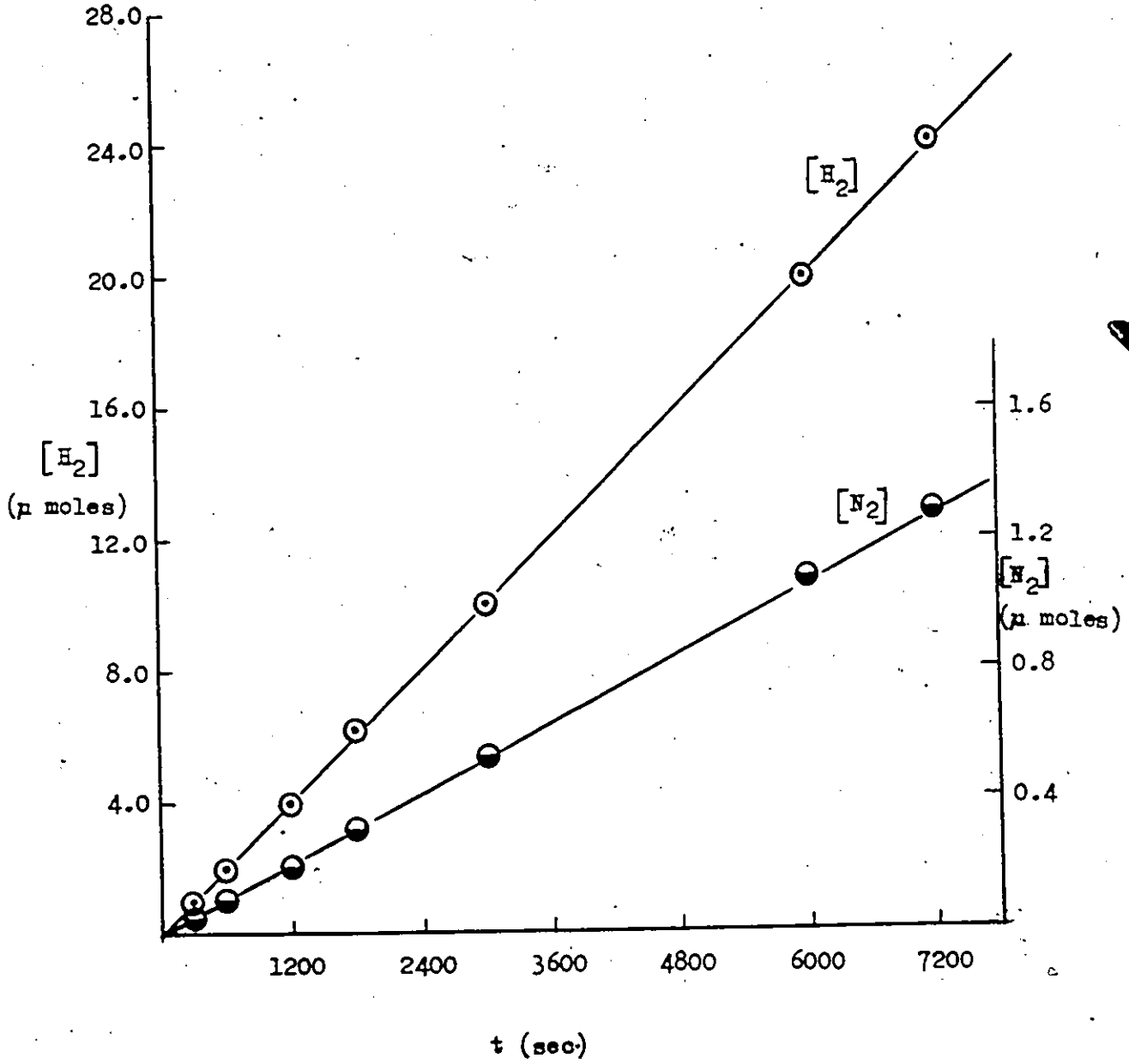

to 5.20 μmoles. These S.V.P. values of I_2 were obtained with the aid of the straight line relationship of $2 + \log p$ versus $\frac{1}{T}$ from Figure 4.6 (114) where p is the saturated vapour pressure of iodine at a given temperature T°K.

At 5°C and -20.5°C the attainment of linearity for H_2 and N_2 production is very rapid because the S.V.P.'s at these temperatures are quickly reached for the concentrations of HI employed, even at the smallest time period of the series of experimental runs.

The quantities of H_2 and N_2 produced at the three temperatures, 25°C, 5°C and -20.5°C, under similar conditions, showed very little variation for the 2537 Å wavelength. However, with the longer wavelengths, the N_2 yield decreased as the temperature was lowered from 25°C to -20.5°C.

The size of the S.V.P. of I_2 helps to regulate the limiting value of the quantum yield of H_2 in the HI/N_2O photochemical system. It was shown that in three series of runs (Tables 4.1, 4.6 and 4.7) where the initial HI concentrations were the same from run to run and from series to series, and the same $\frac{[N_2O]_o}{[HI]_o}$ variation was followed for similar time periods (2700 seconds), the limiting quantum yield of H_2 was the highest at the lowest temperature and lowest at the highest temperature. Thus the larger S.V.P. of I_2 had a greater effect on the fate of the H atoms within the system, via the $H^{\cdot} + I_2 \rightarrow HI + I^{\cdot}$ reaction.

The addition of iodine to the photochemical system

Figure 4.6

Logarithmic plot of saturated vapour pressure of iodine against temperature (114)

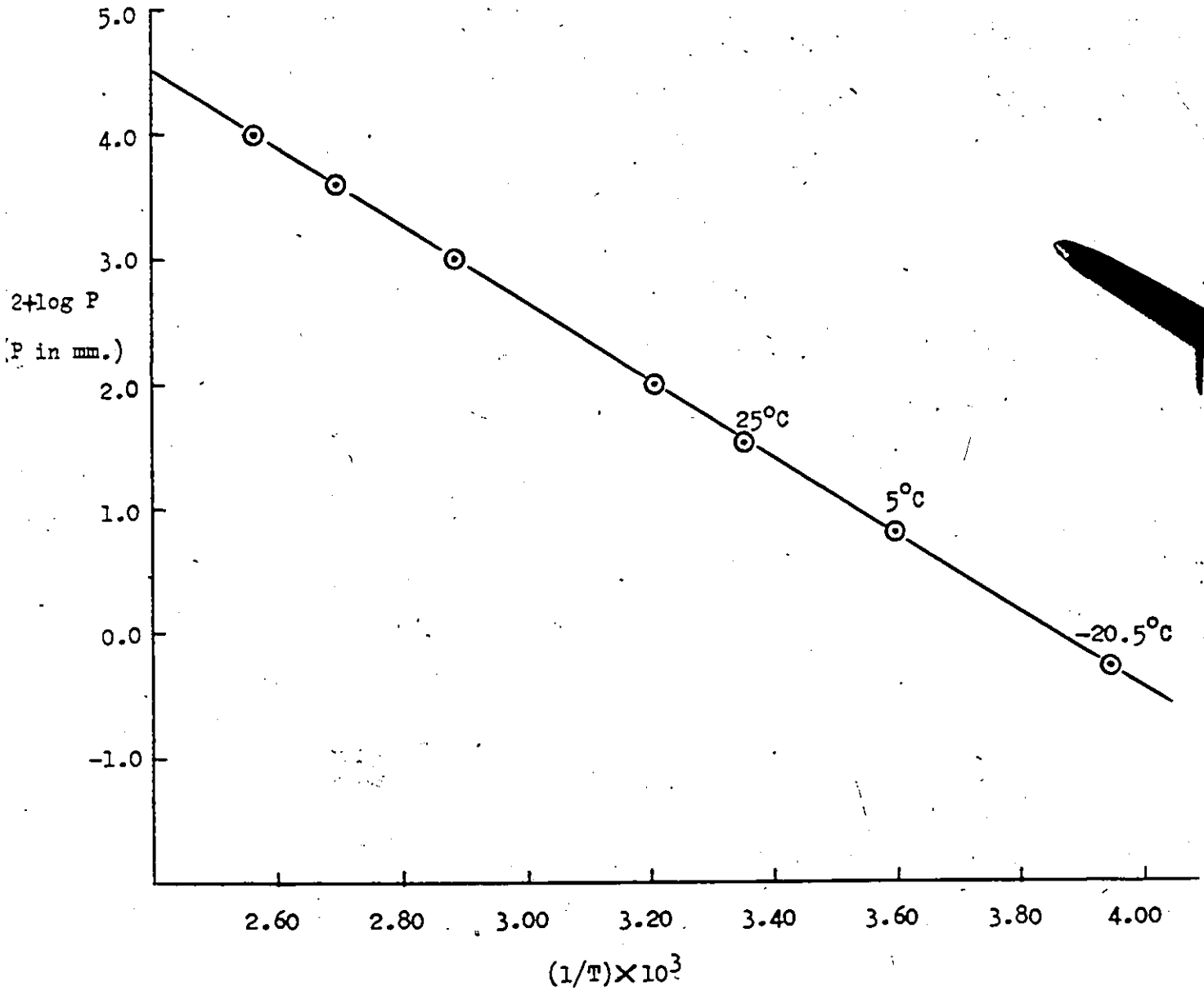
5.0
4.0
3.0
2.0
1.0
0.0
-1.0
2+log P
(P in mm.)
25°C
5°C
-20.5°C
2.60
2.80
3.00
3.20
3.40
3.60
3.80
4.00
(1/T)×10³

TABLE 4.4

Rate of H_2 and N_2 Production at 25°C

[$\lambda \rightarrow 3130$ Å]

$\frac{[N_2O]_o}{[HI]_o}$	Time (seconds)	$[H_2]$ (μmoles)	$[N_2]$ (μmoles)	$[I_2]$ (μmoles)	$[HI]_o$ (μmoles)	$[HI]_f$ (μmoles)	$[N_2O]_o$ (μmoles)
3.1	300	0.99	0.12	1.12	194	191	596
3.1	600	1.97	0.25	2.24	193	188	614
3.0	1200	3.43	0.48	3.94	203	195	617
3.1	1800	4.79	0.62	5.44	195	184	599
3.1	2400	6.05	0.81	6.93	201	187	619
3.1	3000	7.37	0.99	8.40	200	184	617
3.0	3600	8.74	1.16	9.91	201	181	611
3.1	4800	11.0	1.48	12.5	203	178	624
3.1	6000	13.5	1.80	15.3	210	179	646
3.1	7200	16.2	2.12	18.3	194	158	595

TABLE 4.5

Rates of Nitrogen and Hydrogen Production at 5°C and -20.5°C

[$\lambda \rightarrow 3130$ Å]

$\frac{[N_2O]_o}{[HI]_o}$	Time (seconds)	$[H_2]$ (μmoles)	$[N_2]$ (μmoles)	$[I_2]$ (μmoles)	$[HI]_o$ (μmoles)	$[HI]_f$ (μmoles)
A. Temp: 5°C						
3.0	300	1.00	0.06	1.07	195	193
3.0	900	3.01	0.18	3.20	194	188
3.0	2400	8.03	0.50	8.55	202	185
3.0	3600	12.0	0.75	12.8	200	175
3.0	4800	16.0	1.01	17.0	197	162
3.0	6000	20.1	1.25	21.4	199	156
3.0	7200	24.2	1.52	25.8	195	144
B. Temp: -20.5°C						
3.0	300	1.01	0.05	1.10	196	194
3.1	600	2.01	0.10	2.18	192	187
3.1	1200	4.02	0.22	4.35	199	191
3.0	1800	6.29	0.32	6.61	199	185
3.0	3000	10.0	0.54	10.7	197	174
3.0	6000	20.0	1.08	21.4	198	155
3.0	7200	24.2	1.28	25.7	202	151

TABLE 4.6

Variation of H_2 and N_2 Production with $\frac{[N_2O]}{[HI]}$ Ratios

at 5°C

[$\lambda \rightarrow 3130.\overset{\circ}{A}$][2700 seconds]

$\frac{[N_2O]_o}{[HI]_o}$	$[H_2]$ (μmoles)	$[N_2]$ (μmoles)	$[I_2]$ (μmoles)	$[HI]_o$ (μmoles)	$[HI]_f$ (μmoles)	$[N_2O]_o$ (μmoles)	ϕ_{H_2} (moles einstein^{-1})
0.0	7.38	0.00	7.38	201	186	0.00	1.000
1.0	7.13	0.18	7.39	198	184	202	0.964
2.0	6.96	0.24	7.40	205	190	418	0.940
3.0	6.86	0.37	7.39	201	186	603	0.928
4.0	6.82	0.49	7.40	201	187	810	0.922
5.0	6.81	0.49	7.40	205	190	1023	0.920
6.1	6.80	0.49	7.38	206	191	1262	0.920
7.0	6.80	0.49	7.39	205	190	1438	0.921
8.1	6.80	0.49	7.38	205	190	1657	0.920
9.1	6.80	0.49	7.38	205	190	1858	0.920
10.2	6.80	0.49	7.39	204	189	2076	0.920

TABLE 4.7

Variation of H_2 and N_2 Production with $\frac{[N_2O]_o}{[HI]_o}$ Ratios

at -20.5°C

[$\lambda \rightarrow 3130$ Å][Time 2700 seconds]

$\frac{[N_2O]_o}{[HI]_o}$	$[H_2]$ (μmoles)	$[N_2]$ (μmoles)	$[I_2]$ (μmoles)	$[HI]_o$ (μmoles)	$[HI]_f$ (μmoles)	$[N_2O]_o$ (μmoles)	ϕ_{H_2} (moles einstein^{-1})
0.0	7.33	0.00	7.35	203	189	0.00	0.998
1.0	7.16	0.12	7.36	205	190	205	0.973
2.1	7.01	0.24	7.35	203	189	423	0.953
3.1	6.93	0.37	7.35	205	190	630	0.943
4.2	6.91	0.37	7.36	205	190	853	0.939
5.0	6.91	0.37	7.36	204	189	1023	0.939
6.0	6.88	0.37	7.34	203	189	1227	0.938
7.0	6.91	0.37	7.35	205	190	1453	0.940
8.0	6.91	0.37	7.36	204	190	1634	0.939
9.1	6.91	0.37	7.36	206	191	1872	0.939
10.0	6.91	0.37	7.36	204	189	2040	0.939

Figure 4.7

Variation of ϕ_{H_2} with $\frac{[N_2O]_o}{[HI]_o}$ for 25°C, 5°C and -20.5°C at 3130 Å, showing effect of S.V.P. of I_2 on limiting ϕ_{H_2}

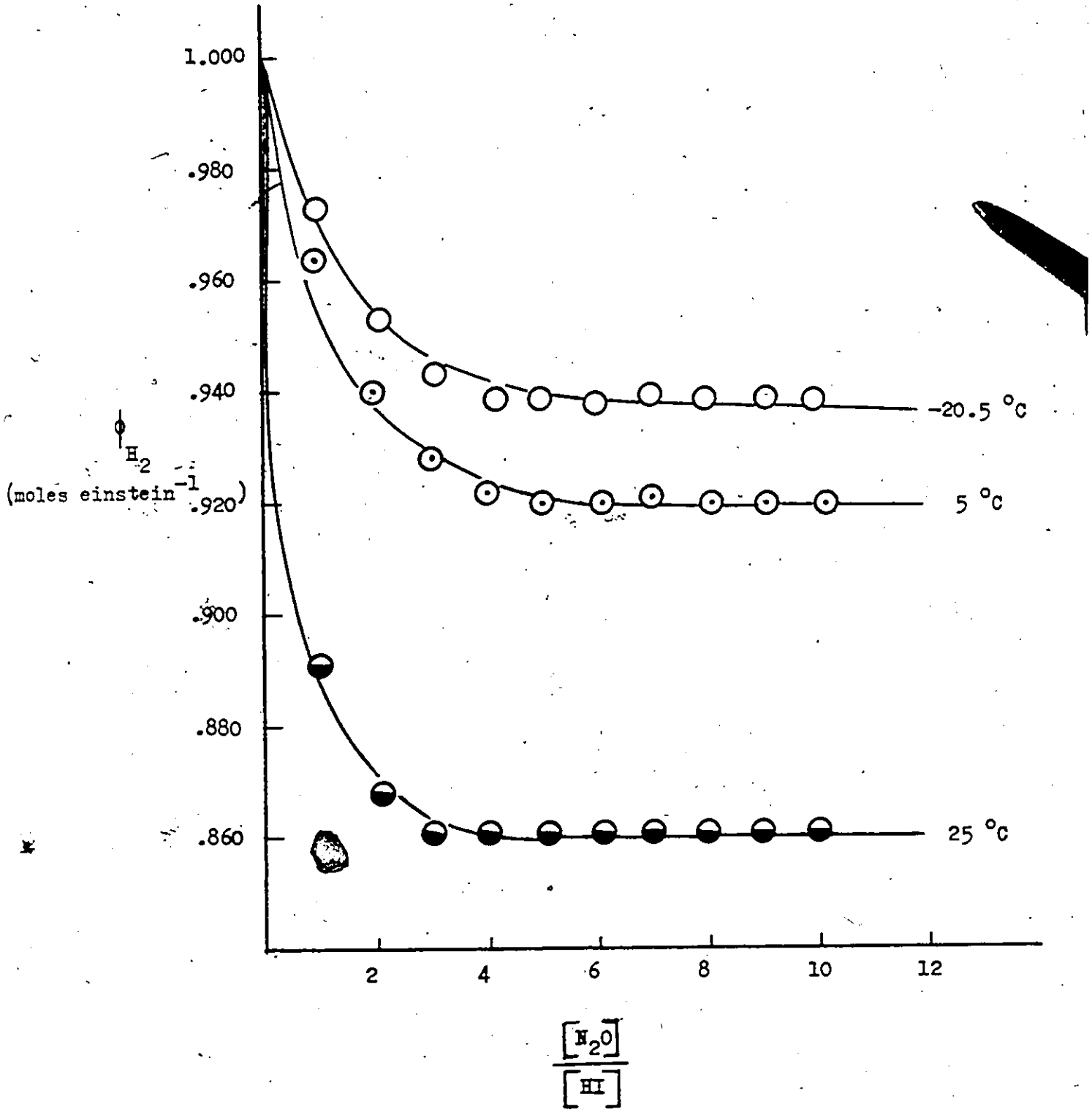
1.000
.980
.960
.940
.920
.900
.880
.860
ϕ_{H_2}
(moles einstein^{-1})
-20.5 °C
5 °C
25 °C
2
4
6
8
10
12
$\frac{[N_2O]}{[HI]}$

caused a noticeable reduction in both the H_2 and N_2 yields. This effect is recorded in Table 4.8.

Inert Gas Effects

The inhibition effects of inert gases such as helium and carbon dioxide were examined. Despite the fact that there is a drawback in employing carbon dioxide in these experiments because of its low efficiency in energy transfer processes, it was preferred to helium for more detailed experiments since it could be frozen out very easily at liquid air temperature and subsequently would offer no interference to the measurement of small quantities of H_2 and N_2. Because of this low efficiency in energy transfer processes, high pressures of CO_2 were used in order to bring about the maximum effect.

The production of N_2 showed a steady decrease with increases in the inert gas concentration for a fixed HI initial concentration and for a fixed photolysis time, and this was more pronounced at the longer wavelengths (Tables 4.9 - 4.12).

The ratio of the rate constants k_2 and k_7 for the reactions

$$H^{\cdot} + HI \xrightarrow{k_2} H_2 + I^{\cdot} \qquad (4.2)$$

$$H^{\cdot} + I_2 \xrightarrow{k_7} HI + I^{\cdot} \qquad (4.7)$$

was also subjected to variations as the transition was made from experiments conducted in the absence of inert

TABLE 4.8

A. The Effect of Added I_2 on the Quantum Yield of H_2

[Temp: 25°][λ → 3130 Å][Time 2700 seconds]

$\frac{[N_2O]_o}{[HI]_o}$	Added I_2 (μmoles)	$[H_2]$ (μmoles)	$[N_2]$ (μmoles)	$[I_2]_f$ (μmoles)	$[HI]_o$ (μmoles)	$[N_2O]_o$ (μmoles)	ϕ_{H_2} (moles einstein^{-1})
8.0	0.00	6.37	1.03	7.41	199	1594	0.861
8.0	4.45	6.00	0.85	11.3	200	1603	0.811
8.0	5.36	5.89	0.82	12.1	201	1606	0.796
8.0	6.30	5.84	0.76	12.9	200	1600	0.789
8.0	7.35	5.78	0.69	13.8	200	1602	0.781
8.0	8.04	5.73	0.64	14.4	202	1617	0.774

B. [Added I_2 without N_2O][λ → 3660 Å]

[Time 6 hours][Temp: 25°C]

$[HI]_o$ (μmoles)	$[I_2]_i$ (μmoles)	$\frac{[I_2]}{[HI]}$	$[H_2]$ (μmoles)	$[I_2]_T$ (μmoles)	E_{abs} (μeinsteins)	ϕ_{H_2} (moles einsteins^{-1})	$\frac{k_7}{k_2}$
600	10.1	0.017	1.40	11.4	1.61	0.870	9.0
1500	15.0	0.010	2.05	17.0	2.26	0.907	10.3
2004	12.2	0.006	2.28	14.5	2.42	0.943	10.0

TABLE 4.9

The Inert Gas Effect of CO_2 at Various Wavelength

A. [$\lambda \rightarrow 3660$ Å][Time 21,600 seconds][Temp: 25°C]

$\frac{[N_2O]_o}{[HI]_o}$	$\frac{[CO_2]}{[HI]_o}$	$[H_2]$ (μmoles)	$[N_2]$ (μmoles)	$[I_2]$ (μmoles)	$[HI]_o$ (μmoles)	E_{abs} (μeinsteins)	$\frac{k_7}{k_2}$
2.0	0.0	0.93	0.18	1.15	988	1.15	-
2.0	9.1	0.72	0.00	0.75	991	1.10	11.2
0.0	10.5	0.70	0.00	0.72	1002	1.20	12.0

B. [$\lambda \rightarrow 3130$ Å][Time 10,800 seconds][Temp: 25°C]

$\frac{[CO_2]}{[HI]_o}$	$[H_2]$ (μmoles)	$[I_2]$ (μmoles)	$[HI]_o$ (μmoles)	$[CO_2]$ (μmoles)	E_{abs} (μeinsteins)	$\frac{k_7}{k_2}$
30	5.19	5.21	81.4	2442	7.18	10.0
66	5.21	5.20	89.4	5849	7.19	11.8
110	5.14	5.15	96.9	11942	7.22	12.2

C. [$\lambda \rightarrow 2537$ Å][Time 1000 seconds][Temp: 25°C]

$\frac{[CO_2]}{[HI]_o}$	$[I_2]_i$ (μmoles)	$[H_2]$ (μmoles)	$[I_2]_T$ (μmoles)	$[HI]_o$ (μmoles)	E_{abs} (μeinsteins)	$\frac{k_7}{k_2}$
2.5	5.70	6.1	11.7	48.2	8.40	3.5
5.0	5.70	6.1	11.8	48.2	8.40	3.5
10.0	5.70	6.0	11.7	48.0	8.40	3.6
15.0	5.70	5.7	11.3	48.2	8.40	4.3
20.0	5.70	5.5	11.2	48.3	8.40	4.9
30.0	5.70	5.1	10.9	48.0	8.40	6.1
50.0	5.70	4.7	10.3	48.3	8.40	7.2
200.0	5.70	3.7	9.4	48.2	8.40	11.6

TABLE 4.10

Effect of CO_2 on N_2 Production at 3130 Å

[Time → 3 hours][Temp: 25°C]

$\frac{[N_2O]_o}{[HI]_o}$	$\frac{[CO_2]}{[HI]_o}$	$[HI]_o$ (μmoles)	$[H_2]$ (μmoles)	$[N_2]$ (μmoles)	$[I_2]$ (μmoles)	$[CO_2]$ (μmoles)
4.1	0.0	97.2	5.83	1.69	7.57	0.00
2.1	0.0	96.7	6.44	1.09	7.56	0.00
1.0	0.0	96.7	6.85	0.66	7.56	0.00
0.0	0.0	96.5	7.55	0.00	7.56	0.00
4.0	29.3	96.2	6.04	0.24	6.30	2822
2.2	54.9	96.7	5.62	0.08	5.74	5307
6.0	30.3	96.3	5.86	0.15	6.04	2916
1.1	109	97.2	5.11	0.06	5.12	10574

TABLE 4.11

Effect of CO_2 on HI/N_2O Photolysis at 2537 Å

[Time 900 seconds][Temp: 25°C]

$\frac{[CO_2]}{[HI]_o}$	$\frac{[CO_2]}{[N_2O]_o}$	$[HI]_o$ (μmoles)	$[H_2]$ (μmoles)	$[N_2]$ (μmoles)	$[I_2]$ (μmoles)	$[HI]_f$ (μmoles)	ϕ_{I_2} (moles einstein^{-1})
0.0	0.0	332	23.4	0.00	23.4	286	1.000
0.0	0.0	332	21.2	2.08	23.4	285	0.999
3.1	1.0	333	20.4	1.35	21.8	289	0.930
6.0	2.0	339	19.3	0.98	20.4	298	0.870
9.0	3.0	334	18.3	0.86	19.2	296	0.820
12.0	4.0	335	17.5	0.73	18.3	299	0.780
18.4	6.1	335	16.2	0.63	16.9	301	0.720
24.0	8.3	336	16.0	0.59	16.6	303	0.710
27.0	9.0	335	15.9	0.57	16.5	302	0.705
30.0	10.0	335	15.7	0.55	16.3	301	0.695
34.5	11.5	335	15.6	0.53	16.2	302	0.690

TABLE 4.12

Effect of Helium on HI/N_2O Photolysis

[$\lambda \rightarrow 2537$ Å][Time 900 seconds][Temp: 25°C]

$[HI]_o$ (μmoles)	$[N_2O]_o$ (μmoles)	$\frac{[He]}{[N_2O]_o}$	$\frac{[He]}{[HI]_o}$	$[I_2]$ (μmoles)	$[HI]_f$ (μmoles)	ϕ_{I_2} (moles einstein^{-1})
334	0.0	0.0	0.0	23.4	288	1.000
333	1011	0.0	0.0	23.4	286	0.999
334	1009	1.0	3.1	17.9	302	0.762
334	1010	2.0	6.2	14.6	304	0.625
327	1006	3.0	9.0	12.3	303	0.527
331	1011	4.0	12.1	11.0	309	0.472
328	1009	6.0	18.3	9.71	309	0.415
332	1012	8.2	24.0	9.34	313	0.400
333	1008	11.0	33.1	9.01	315	0.385

gases to those conducted in the presence of these gases. It was found that

$$\frac{k_2}{k_7} < \frac{k_2}{k_7}$$

(presence of inert gas) (absence of inert gas)

The effects of the addition of CO_2 and He on ϕ_{H_2} are shown in Figure 4.8. For constant $\frac{[N_2O]_o}{[HI]_o}$ ratios, ϕ_{H_2} decreases with increasing CO_2 or He, and becomes constant and independent of He or CO_2 at higher concentrations of the inert gas. When conditions were attained such that ϕ_{H_2} became independent of the concentration of CO_2 or He, it was feasible to assume that, under those conditions, essentially all of the hot H atoms were deactivated.

The N_2O + H reaction was very sensitive to the presence of inert gases, and the effect which these gases exerted on this reaction is shown in Figure 4.9 with CO_2 as the inert gas. Table 4.13 demonstrates the effect which helium (He) has on the photolysis of pure HI.

Discussion

The photolysis of HI in the presence of N_2O may be discussed in terms of the following mechanism:

$$HI + h\nu \rightarrow H^{\cdot} + I^{\cdot} \qquad (4.1)$$

$$H^{\cdot} + HI \rightarrow H_2 + I^{\cdot} \qquad (4.2)$$

$$H^{\cdot} + N_2O \rightarrow N_2 + OH^{\cdot} \qquad (4.3)$$

$$I^{\cdot} + I^{\cdot} + M \rightarrow I_2 + M \qquad (4.4)$$

Figure 4.8

Inhibition plots for ϕ_{I_2} versus $\frac{[\text{inert gas}]}{[HI]_o}$ at 25°C and 2537 Å in the photolysis of $HI + N_2O$.

● CO_2

θ Helium

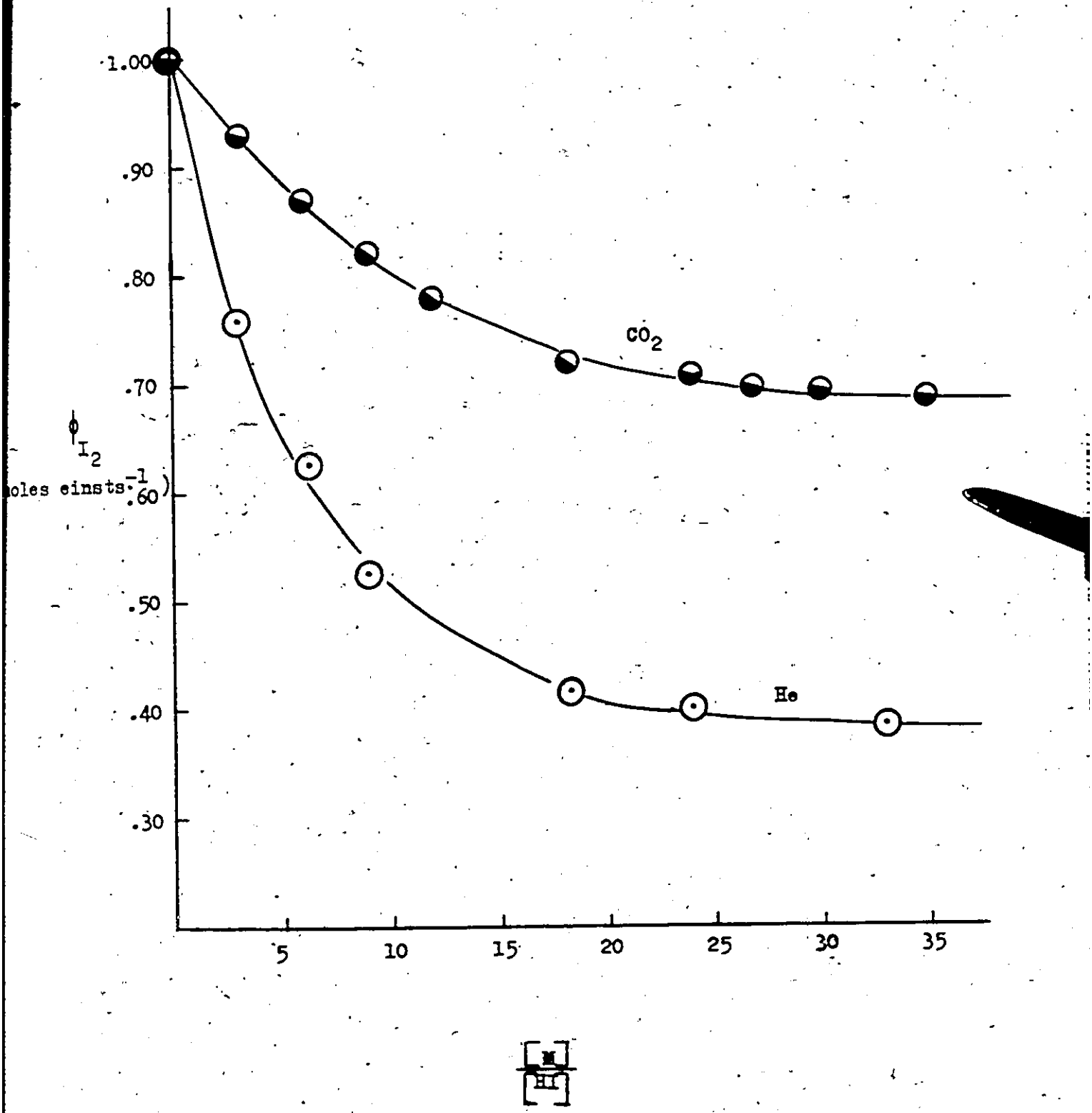
1.00
.90
.80
.70
.60
.50
.40
.30
ϕ_{I_2}
oles einsts^{-1})
CO_2
He
5
10
15
20
25
30
35

Figure 4.9

Inhibition of N_2 production by CO_2 at 25°C and 2537 Å

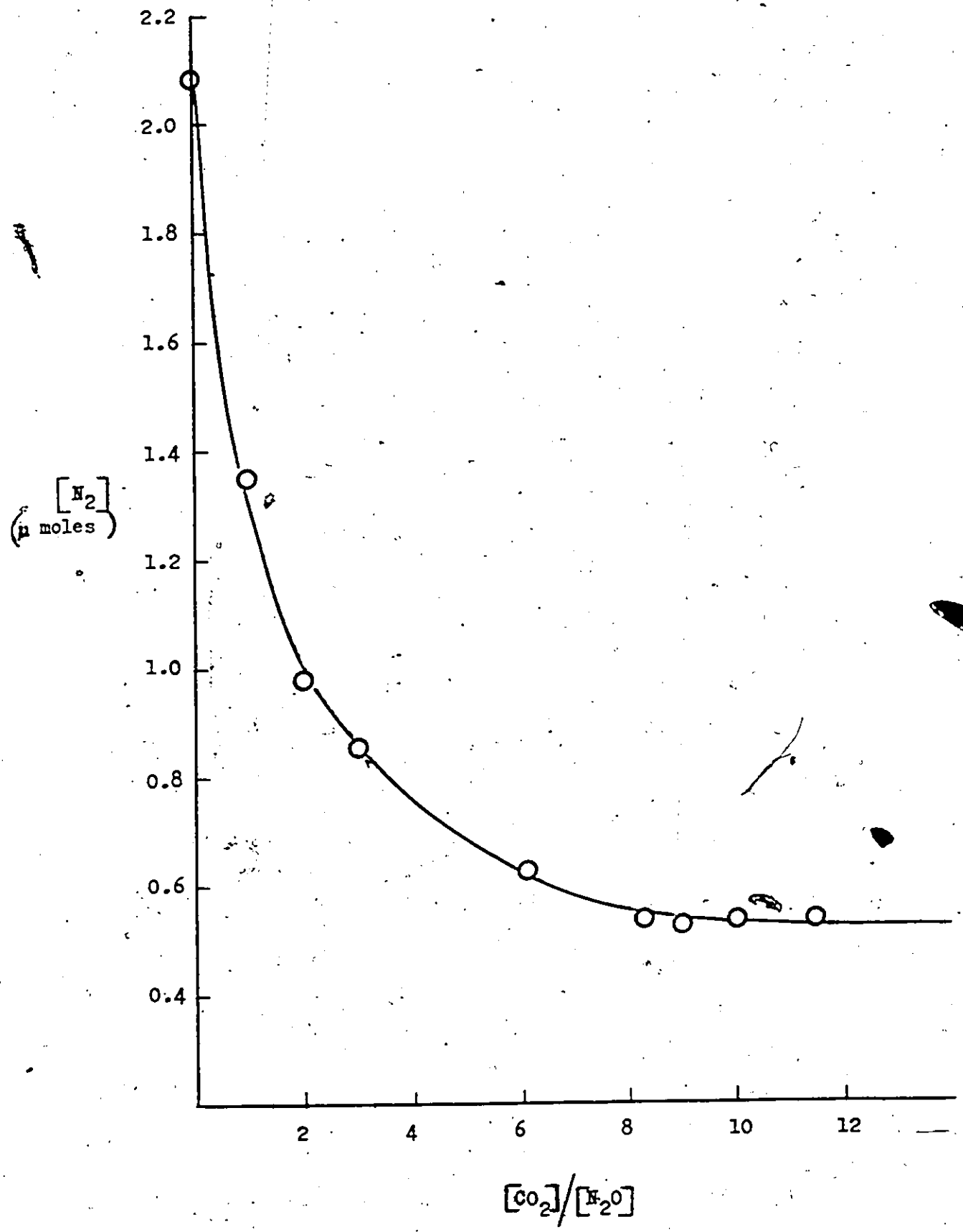
2.2
2.0
1.8
1.6
1.4
1.2
1.0
0.8
0.6
0.4
[N2]
(μ moles)
2
4
6
8
10
12
[CO2]/[N2O]

TABLE 4.13

Inert Gas Effect of Helium on HI Photolysis

[Temp: 25°C][$\lambda \rightarrow$ 2537 Å][Time 1000 seconds]

$\frac{[He]}{[HI]_o}$	$[HI]_o$ (μmoles)	$[I_2]_i$ (μmoles)	$[I_2]_T$ (μmoles)	$[I_2]_p$ (μmoles)	E_{abs} (μeinsteins)	$\frac{k_7}{k_2}$
2.5	70.0	5.70	17.6	11.9	17.3	6.1
5.0	70.1	5.70	16.6	10.9	17.3	7.9
10.0	70.0	5.70	15.8	10.1	17.3	9.5
15.0	70.1	5.70	15.6	9.90	17.3	10.1
25.0	70.0	5.70	15.2	9.51	17.3	10.9
30.0	70.0	5.70	15.1	9.41	17.3	11.2
50.0	70.0	5.70	15.0	9.30	17.3	11.4
100	70.0	5.70	14.9	9.20	17.3	11.8

$$H^{\cdot} + N_2O \rightarrow NO^{\cdot} + NH \qquad (4.5)$$

$$OH^{\cdot} + HI \rightarrow H_2O + I^{\cdot} \qquad (4.6)$$

$$H^{\cdot} + I_2 \rightarrow HI + I^{\cdot} \qquad (4.7)$$

$$NH + 3HI \rightarrow NH_4I + I_2 \qquad (4.8)$$

$$6HI + NO \rightarrow NH_4I + H_2O + \frac{5}{2} I_2 \qquad (4.9)$$

$$OH^{\cdot} + H_2 \rightarrow H_2O + H^{\cdot} \qquad (4.10)$$

Throughout the whole experimental area covered, with various mixtures of gaseous hydrogen iodide and nitrous oxide, the photolysis led to mixtures of hydrogen, nitrogen and iodine along with unreacted hydrogen iodide. There was no significant experimental evidence for the formation of nitric oxide (NO) or ammonium iodide (NH_4I).

For the production of nitric oxide and subsequently ammonium iodide, light of wavelength below a critical value must be employed. Oldershaw and Porter (115) have reported the formation of nitric oxide as a product in the photolysis of HI in the presence of N_2O in the wavelength range of 2350-3000 Å, but their uncertainties are so large (Table 4.14) that it is doubtful whether any great significance can be attached to their findings.

Tomalesky and Sturm (116) have reported the formation of nitric oxide and ammonium iodide in the photolysis of HI in the presence of N_2O employing the exciting light from a Xenon flash lamp. The energetics of reaction (4.5) require either a high temperature or translationally energetic hydrogen atoms having an average critical energy. Reaction (4.5)

TABLE 4.14

Nitric Oxide (NO) Production in Photolysis of $HI + N_2O$ (115)

λ (nm)	$(\frac{NO}{N_2})$
235	0.09 ± 0.02
250	0.10 ± 0.02
270	0.005 ± 0.01
300	0.005 ± 0.01

occurs with an endothermic intake of about 34.0 kcal $mole^{-1}$, thus the hot hydrogen atoms with an average initial energy of 57 kcals $mole^{-1}$, were obviously very efficient in bringing about reaction (4.5). One must therefore assume that the probability of the $H + N_2O \rightarrow NO + NH$ reaction occurring, decreases considerably as the wavelength of the exciting radiation is increased in the region 2537 Å - 3660 Å. Tomalesky and Sturm further pointed out, that another source of nitric oxide could have been through the processes

$$N_2O \xrightarrow{h\nu} N_2 + O$$

$$O + N_2O \rightarrow 2NO$$

at the shortest wavelengths employed.

In our system, Nessler's test was conducted on half of the aqueous washings of the reaction vessel after it had been removed from the vacuum system. Many runs had been performed in this vessel at 25°C using all three wavelengths of 2537 Å, 3130 Å and 3660 Å. Among these runs over one hundred of them had been performed using the 2537 Å wavelength. On addition of Nessler's reagent (117) to the solution (washings) from the reaction vessel, a yellow colouration developed and on standing for over fifteen minutes, a light yellow precipitate was thrown down, indicating the presence of the ammonium ion (NH_4^+). The second portion of the washings from the reaction vessel was tested spectrophotometrically for absorption of the ammonium ion. By comparing the resulting spectrum with that of a known concentration of pure NH_4I (Figures 4.10 and

Figure 4.10

The ultra-violet spectrum of an aqueous solution of pure ammonium iodide (NH_4I)

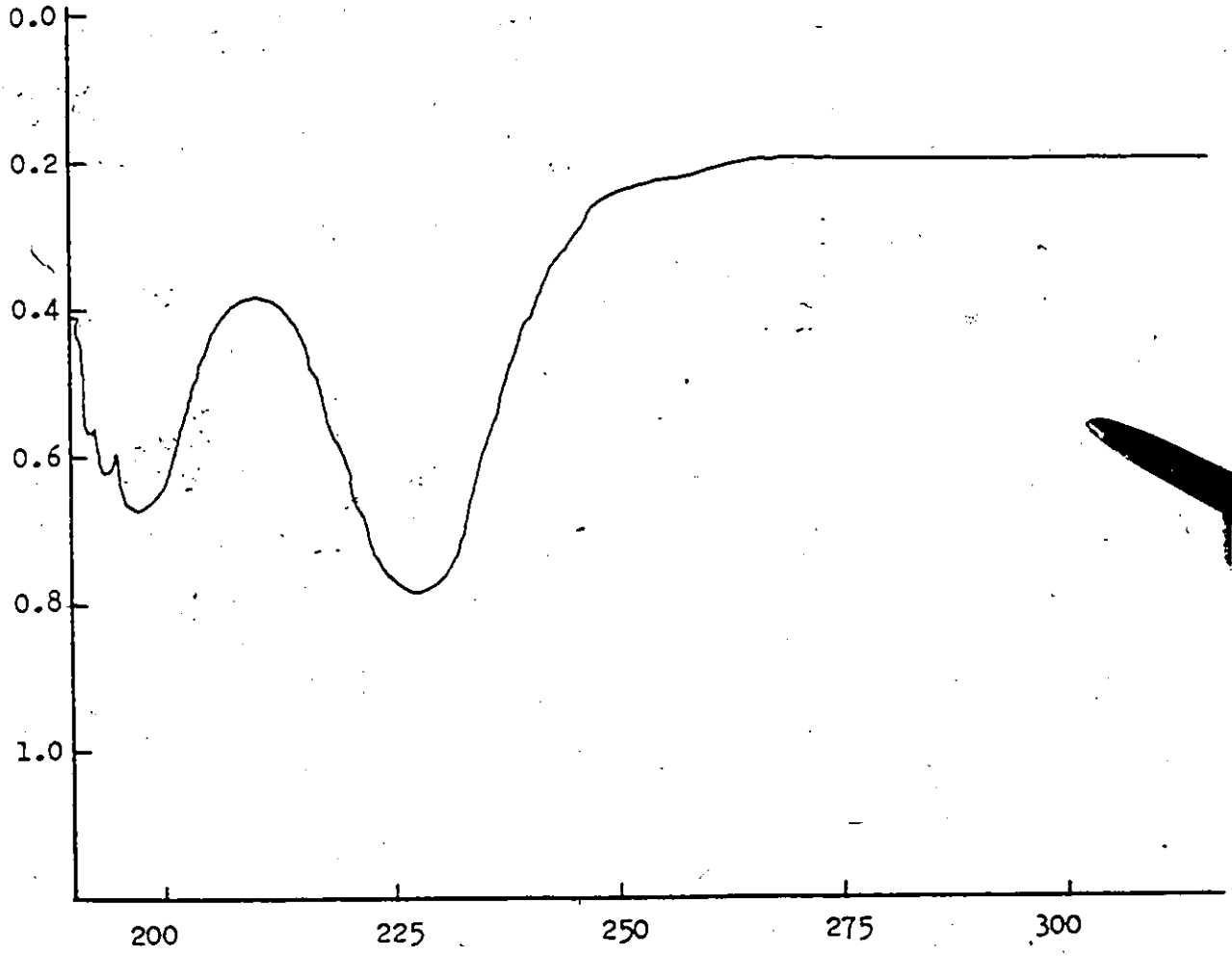
0.0
0.2
0.4
0.6
0.8
1.0
ABSORBANCE
200
225
250
275
300
WAVELENGTH (MILLIMICRONS)

4.11), the presence of the ammonium ion was confirmed. From the calculated molar extinction coefficient, of the NH_4^+ ion, derived from the spectrum of pure ammonium iodide, the molar concentration of the NH_4^+ ion in the washings from the reaction vessel, was calculated and thus the number of moles in the total volume of the washings was obtained. From Figures 4.10 and 4.11 for the spectra of the NH_4^+ ion from the two different sources, the calculations were as follows:

$$O.D. = \log \frac{I_o}{I} = 0.78 - 0.20 = 0.58$$

(where 0.20 units of $\log \frac{I_o}{I}$ represented the zero position).

$$0.58 = \varepsilon C l = \varepsilon \times 4.68 \times 10^{-5} \times 1.0$$

$$\therefore \quad \varepsilon = 1.24 \times 10^4$$

Thus the molar concentration of NH_4^+ ion from the reaction vessel washings is given as,

$$C = \frac{1.35 - 0.20}{1.24 \times 10^4} = 9.27 \times 10^{-5} \text{ M}$$

Taking into consideration the dilution factor before the spectrum was run and the volume used for Nessler's test, the total volume was shown to contain 3.71×10^{-6} moles. Therefore for the hundred or more runs carried out under the 2537 Å radiation between a time period of 300 to 900 seconds for each run, less than 0.05 μmole of NH_4I is averaged per run.

The vapour pressure of ammonium iodide at 25°C is 1.12×10^{-6} mm (Hg), 6.31×10^{-8} mm at 5°C and 2.51×10^{-10} mm

Figure 4.11

The ultra-violet spectrum of the aqueous washings from the reaction vessel after many photolyses of HI and N_2O mixtures

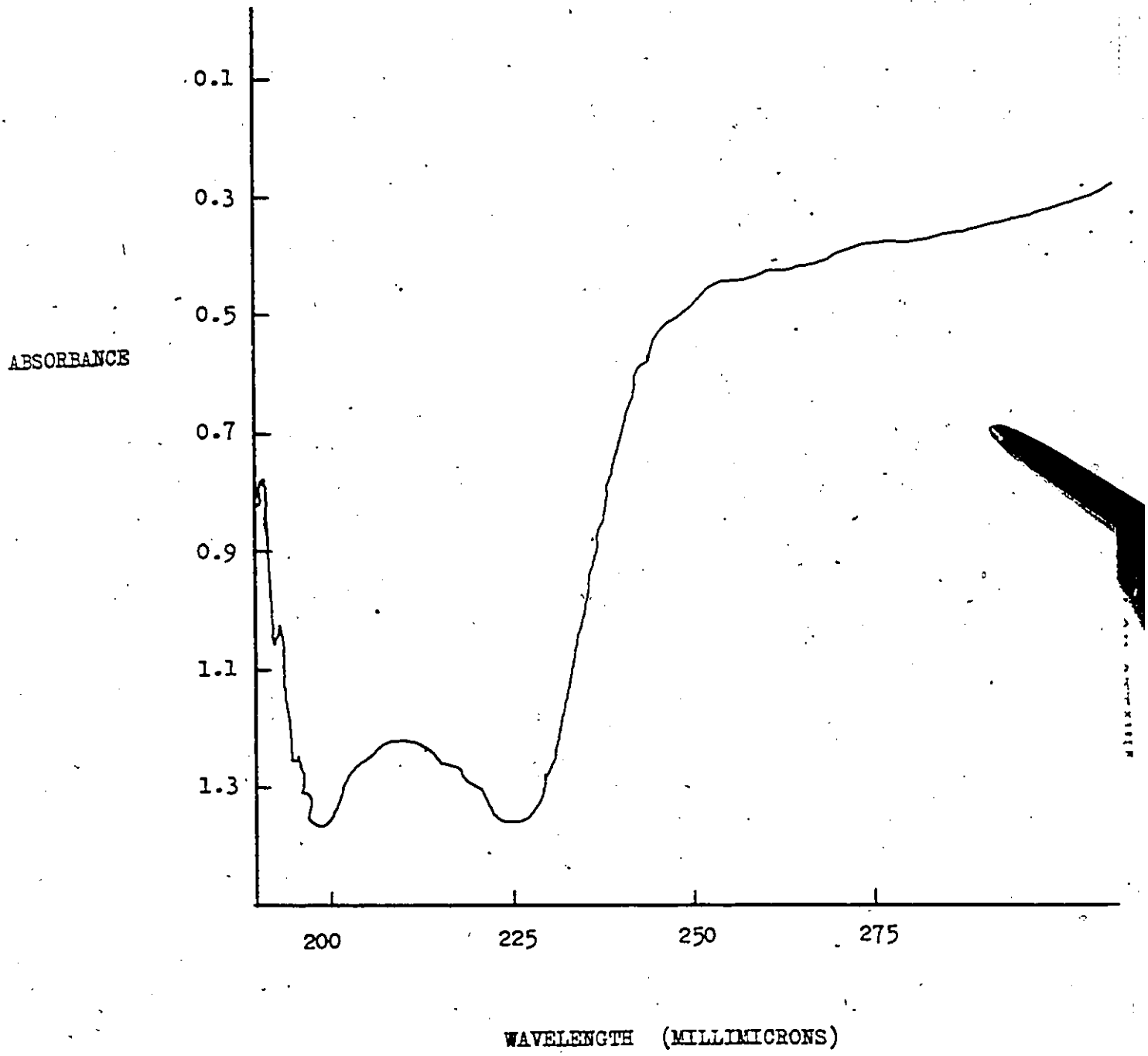
0.1
0.3
0.5
0.7
0.9
1.1
1.3
ABSORBANCE
200
225
250
275
WAVELENGTH (MILLIMICRONS)

at -20.5°C. These values were obtained from Figure 4.12. Because of these very low vapour pressures, the probability of pumping away any NH_4I formed was highly unlikely. It can therefore be correctly stated that the $H + N_2O \rightarrow NO + NH$ reaction is of negligible significance at or below 25°C under radiation of 2537 Å, 3130 Å or 3660 Å.

The absorption of monochromatic light by HI at the three wavelengths 2537 Å, 3130 Å and 3660 Å can be represented by two processes,

(a) $HI + h\nu(\lambda) \rightarrow H^{\cdot *} + I^{\cdot}\ (^2P_{3/2})$

producing an H atom possessing some average initial translational kinetic energy, and

(b) $HI + h\nu(\lambda)$ $\xrightarrow{\text{(i)}}$ $H^{\cdot *} + I^{\cdot *}\ (^2P_{1/2})$

$HI + h\nu(\lambda)$ $\xrightarrow{\text{(ii)}}$ $H^{\cdot} + I^{\cdot}\ (^2P_{1/2})$

giving an energetic H atom with less kinetic energy than that in case (a), and/or a thermal hydrogen atom (see Table 2.2). The possibility of (b)(i) and/or (b)(ii) occurring will depend on the excess energy of the photon over the H-I bond dissociation energy.

The pertinent reactions which seem to be involved in the HI/N_2O photochemical system at the temperatures and wavelengths used, are:

(4.2)	$H^{\cdot}+HI \rightarrow H_2+I^{\cdot}$	ΔH_o^o	-32.8 kcals mole^{-1}
(4.3)	$H^{\cdot}+N_2O \rightarrow N_2+OH^{\cdot}$	ΔH_o^o	-62.3 kcals mole^{-1}
(4.4)	$I^{\cdot}+I^{\cdot}+M \rightarrow I_2+M$	ΔH_o^o	-36.2 kcals mole^{-1}

Figure 4.12

Logarithmic plot of saturated vapour pressure of ammonium iodide (NH_4I) versus temperature (114)

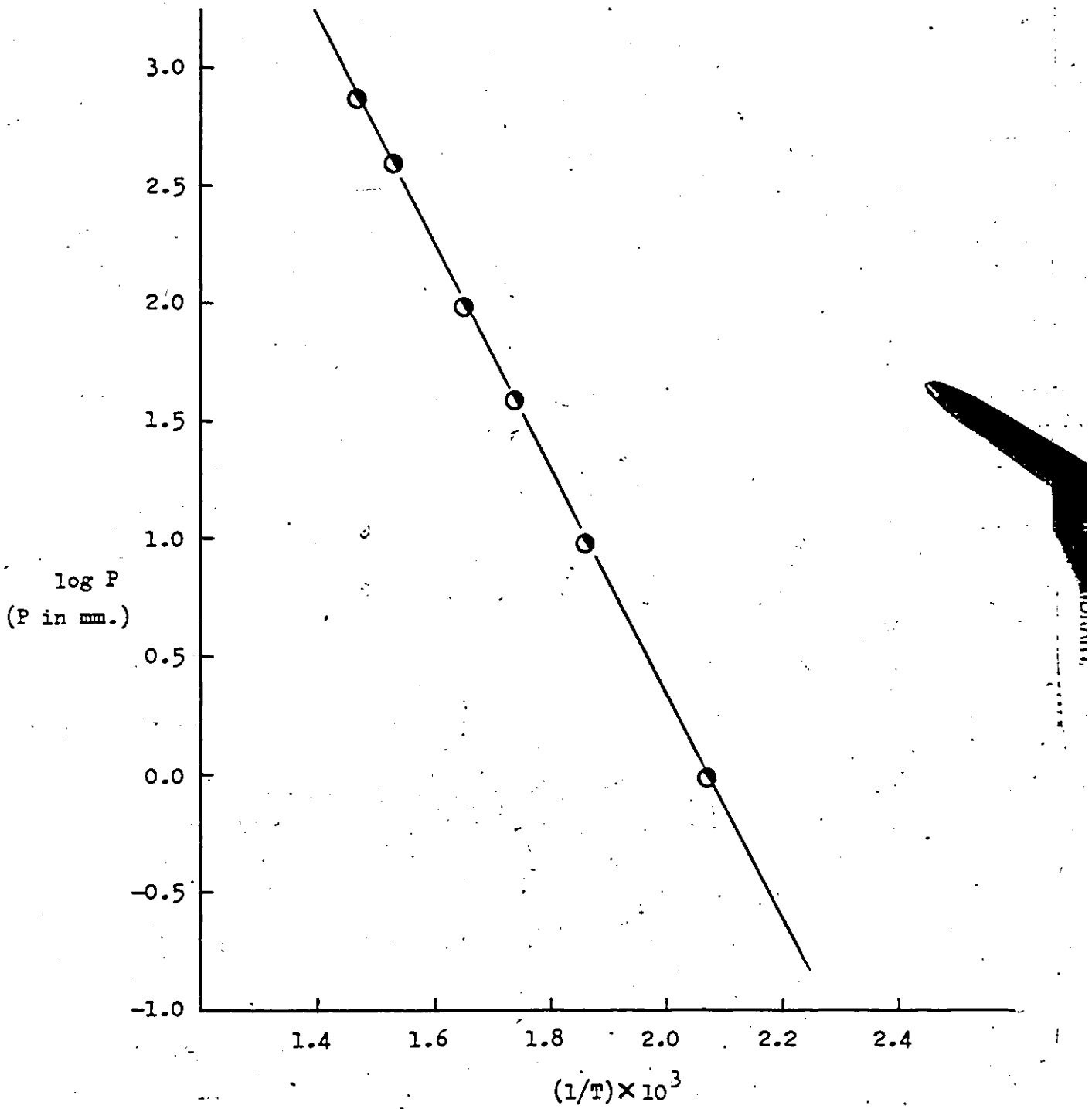
3.0
2.5
2.0
1.5
1.0
0.5
0.0
-0.5
-1.0
log P
(P in mm.)
1.4
1.6
1.8
2.0
2.2
2.4
(1/T)×10³

(4.6) $OH^{\cdot} + HI \rightarrow H_2O + I^{\cdot}$ $\Delta H^{\circ}_{o} = -47.9$ kcals mole^{-1}

(4.7) $H^{\cdot} + I_2 \rightarrow HI + I^{\cdot}$ $\Delta H^{\circ}_{o} = -35.1$ kcals mole^{-1}

It thus appears that reactions (4.2), (4.3) and (4.7) will all compete for both thermal and hot hydrogen atoms, the hot hydrogen atoms having a range of translational kinetic energies. The accumulation of resulting product in each case will then depend on a number of factors, such as the respective reaction cross-section of the individual reactive component, the individual specific rate constants and the initial concentrations of the reactants. Further accumulation of any particular product will only be hindered if a limit or restraint is imposed on the system, and it is this factor which needs to be examined closely in the case of the limiting value of N_2 production and the limiting H_2 quantum yield which were experimentally observed.

A second consideration will be the effect of an added reactive component to the photochemical system, in this case I_2, and the dependence of the H_2 quantum yield (ϕ_{H_2}) as a function of both HI and I_2 concentrations.

Thirdly, an examination of the specific rate constants or ratios of these should clearly indicate the behaviour of the system under changes of the wavelength of the exciting radiation. In addition, the influence of temperature on the kinetics of the HI/N_2O photochemical system should reveal to us the nature of the hydrogen atoms with which we are dealing, i.e., whether we are dealing with thermal

hydrogen atoms in which case we would expect sizeable activation energies, or whether we are dealing with energetic or 'hot' hydrogen atoms having a range of translational kinetic energies, in which case we would expect smaller activation energies.

Fourthly, in view of the potential importance of hot H atoms, the presence of inert foreign gases which are capable of adequate energy transfer, should exert some influence on the kinetic behaviour of the system, and this inert gas effect should be wholly consistent with the mechanism proposed.

If the H' + N_2O reaction (where H' stands for a hydrogen atom of some average kinetic energy) involved the simple billiard ball type of collisions, in which there were fruitful reactions, a continual increase in the yield of N_2 would be expected as increasing amounts of N_2O are added to the photochemical system in which the initial concentration of HI and the photolysis time are both kept constant for each $\frac{[N_2O]_o}{[HI]_o}$ ratio. Since N_2 yields do not continue to increase after a certain value of $\frac{[N_2O]_o}{[HI]_o}$ is reached, it must be assumed that there is some type of modifying process occurring in conjunction with the billiard ball collisions picture. To account for this process, it was necessary to invoke the effect of 'constant partitioning' of energetic hydrogen atoms between the chemical reaction,

$$H' + N_2O \rightarrow N_2 + OH$$

on the one hand, and the moderation process,

$$H^{*'} + N_2O \rightarrow H^{*} + N_2O$$

on the other hand, as a certain ratio of $\frac{[N_2O]_o}{[HI]_o}$ was attained.

The partitioning represents the situation in which the collision of a new born H^* with N_2O first occurs. Following this collision, reaction or deactivation results. On an average these two types of processes will be in a constant ratio when the critical $\frac{[N_2O]_o}{[HI]_o}$ value is reached. For example the processes from the first collision can be represented by,

$$H^{*} + N_2O \xrightarrow{a} \text{(Reaction)}$$

$$H^{*} + N_2O \xrightarrow{b} H^{*'} + N_2O^{*} \text{ (Moderation)}$$

If process b occurs, this could be followed by

$$H^{*'} + N_2O \xrightarrow{c} \text{(Reaction)}$$

$$H^{*'} + N_2O \xrightarrow{d} H^{*} + N_2O^{*} \text{ (Moderation)}$$

No matter how many sets of processes like a or b, or c and d occur, the average fraction of $\frac{a}{b}$, $\frac{c}{d}$, etc., should be a constant for different ratios of $\frac{[N_2O]_o}{[HI]_{constant}}$ at and above the critical value of $\frac{[N_2O]_o}{[HI]_{constant}}$. The ratios of $\frac{a}{b}$ and $\frac{c}{d}$ etc., will all depend on the excess energy of the hot H atom.

If for a given number of experimental runs within a series, (i) the photochemical conversion of HI is kept low, (ii) the photolysis time is the same for each run, and (iii) the initial HI concentration is essentially the same from run to run, then at relatively high concentrations of N_2O, the H atoms produced in the $H' + N_2O$ constant partitioning process, will react with the equivalent quantities of HI in those runs, to produce in each case a constant quantity of H_2. Therefore as the N_2 yields become constant as constant partitioning takes effect at high N_2O concentrations, the H_2 yields will also become constant concomitantly (see Tables 4.1, 4.2 and 4.3).

In the mechanism for the major processes occurring in the HI/N_2O photochemical system,

$$HI + h\nu \xrightarrow{I_a} H^{\cdot\prime} + I^{\cdot}$$

$$H^{\cdot\prime} + HI \xrightarrow{k_2} H_2 + I^{\cdot}$$

$$H^{\cdot\prime} + I_2 \xrightarrow{k_7} HI + I^{\cdot}$$

$$H^{\cdot\prime} + N_2O \xrightarrow{k_3} N_2 + OH^{\cdot}$$

$H^{\cdot\prime}$ is designated as a hydrogen atom having translational energies of between zero and the initial excess energy of the hot H atom. I_a represents the rate of light absorption and k_2 and k_7 are the specific rate constants for their

respective reactions. k_3 is an average rate constant which depends on the excess energy of the hot H atom.

The rate expression for the production of H' can be written as

$$\frac{dH'}{dt} = I_a - k_2[H'][HI] - k_7[H'][I_2] - k_3[H'][N_2O] \qquad (4.11)$$

Assuming steady state conditions, where the rate of accumulation of H' becomes zero, we obtain

$$I_a = [H'](k_2[HI] + k_7[I_2] + k_3[N_2O]) \qquad (4.12)$$

and

$$[H'] = \frac{I_a}{k_2[HI] + k_7[I_2] + k_3[N_2O]} \qquad (4.13)$$

But

$$\frac{d(H_2)}{dt} = k_2[H'][HI] \qquad (4.14)$$

and

$$H' = \frac{d(H_2)}{dt} \cdot \frac{1}{k_2[HI]} \qquad (4.15)$$

$$\frac{d(H_2)}{dt \cdot I_a} = \frac{k_2}{k_2 + k_7\frac{[I_2]}{[HI]} + k_3\frac{[N_2O]}{[HI]}} \qquad (4.16)$$

and

$$\phi_{H_2} = \frac{1}{1 + \frac{k_7}{k_2}\frac{[I_2]}{[HI]} + \frac{k_3}{k_2}\frac{[N_2O]}{[HI]}} \qquad (4.17)$$

on inversion, equation (4.17) becomes

$$\frac{1}{\phi_{H_2}} = 1 + \frac{k_7}{k_2}\frac{[I_2]}{[HI]} + \frac{k_3}{k_2}\frac{[N_2O]}{[HI]} \qquad (4.18)$$

Several predictions can be made from equation (4.18) and these predictions should be observed experimentally.

(i) when $[N_2O] = 0$ and $[I_2] << [HI]$, $\frac{1}{\phi_{H_2}}$ or ϕ_{H_2} should approach unity. This is borne out by the experimental results for low HI conversion in all the Tables where ϕ_{H_2} has been recorded for values of $\frac{[N_2O]}{[HI]} = 0$. A plot of ϕ_{H_2} versus [HI] results in a straight line parallel to the [HI] axis in Figure 4.13,

(ii) $\frac{1}{\phi_{H_2}}$ should increase with increasing $[I_2]$ and/or $[N_2O]$ for a constant value of [HI]. Table 4.8 shows this to be the case with reference to I_2 and Figures 4.1 and 4.2 confirms this prediction for increasing $[N_2O]$.

(iii) For different values of initial HI concentrations and the same $\frac{[N_2O]}{[HI]}$ ratio, ϕ_{H_2} should show an increase. Again Figures 4.1 and 4.2 bear out this prediction. This prediction also accounts for the dependence of the limiting ϕ_{H_2} values on HI concentration.

(iv) Equation (4.18) also suggests that if the $\frac{[N_2O]}{[HI]}$ ratio and the I_2 concentration are both kept constant for a variation of [HI], then there should exist a linear relationship between $\frac{1}{\phi_{H_2}}$ and $\frac{1}{[HI]}$ with a slope equivalent to $\frac{k_7}{k_2}[I_2]$ and an intercept of $\frac{k_3}{k_2}\frac{[N_2O]}{[HI]} + 1$. The constant $[I_2]$ value referred to here, is the S.V.P. value of I_2 at the temperature at which the experiments were conducted.

Figure 4.14 shows a linear plot of $\frac{1}{\phi_{H_2}}$ versus $([HI])^{-1}$ for the data in Table 4.15 for the 2537 Å wavelength. The value

Figure 4.13

Plot of ϕ_{H_2} versus $[HI]_o$ for the photolysis of pure HI (conversion < 8% of HI) at 25°C and 3130 Å

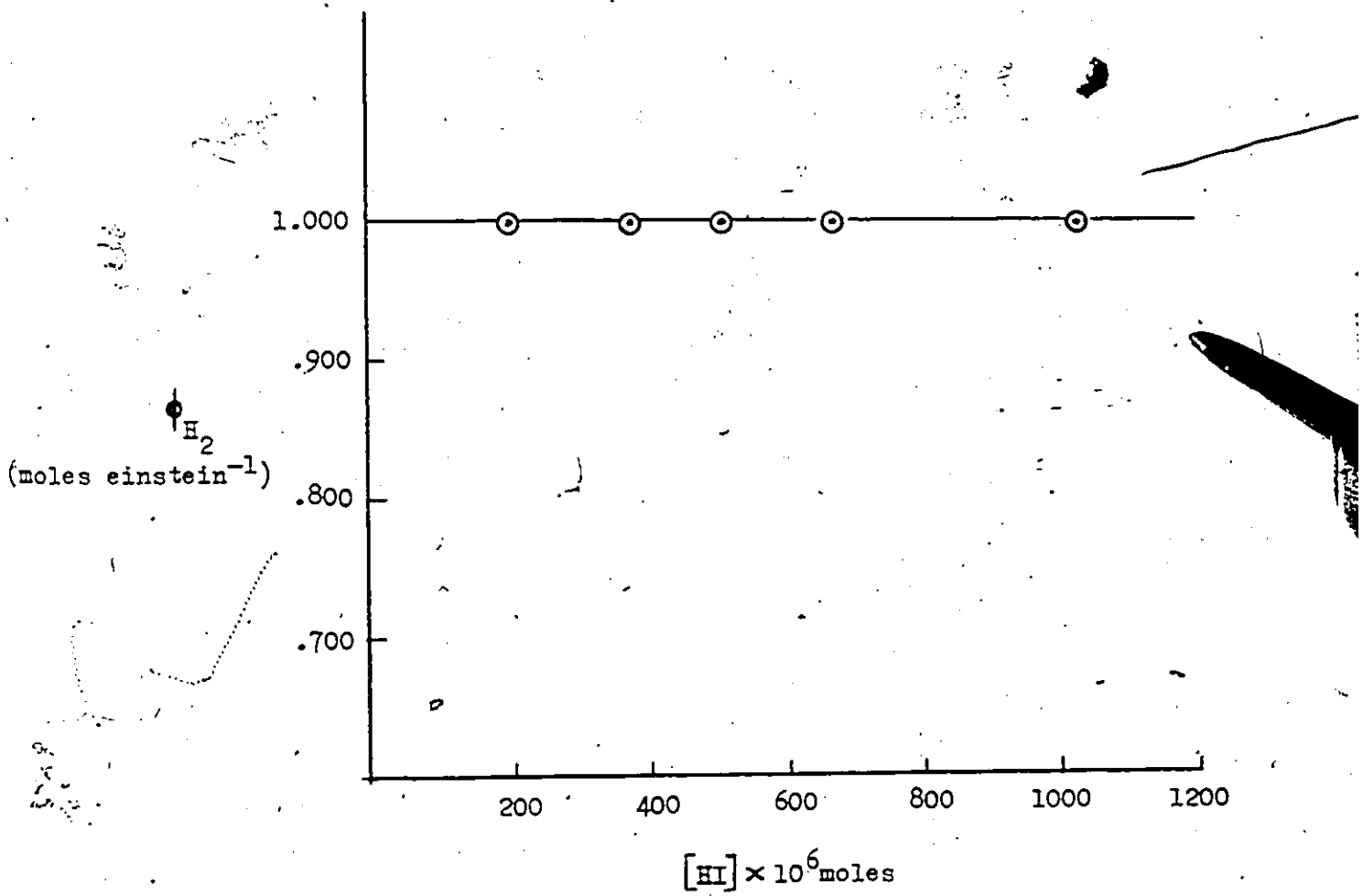
1.000
.900
.800
.700
ϕ_{H_2}
(moles einstein^{-1})
200
400
600
800
1000
1200
[HI] × 10^{6}moles

Figure 4.14

Plot of $\frac{1}{\phi_{H_2}}$ versus $\frac{1}{[HI]}$ for the photolysis of HI/N_2O at 25°C and 2537 Å in the presence of added iodine

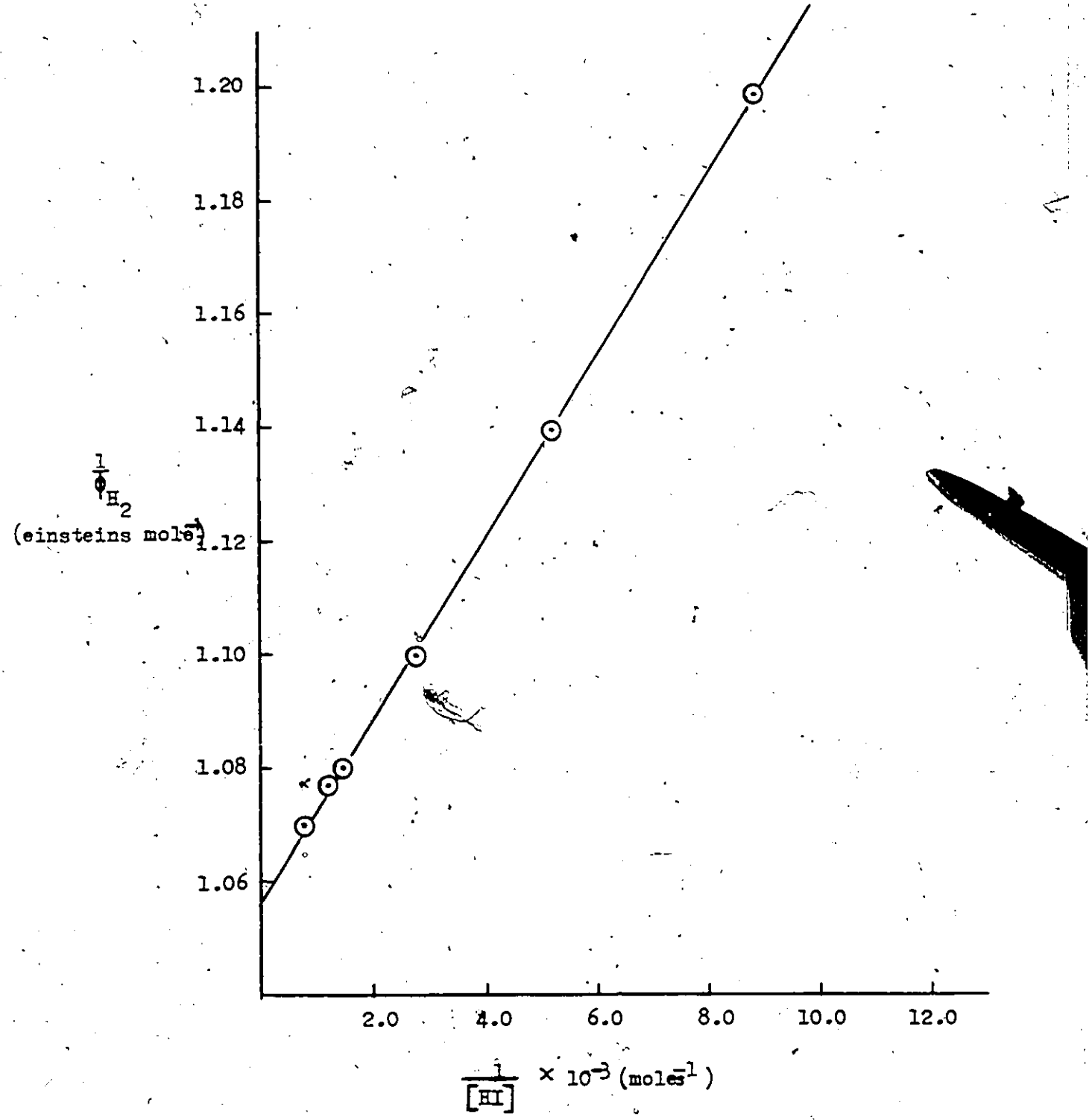
1.20
1.18
1.16
1.14
1.12
1.10
1.08
1.06
$\frac{1}{\Phi_{H_2}}$ (einsteins mole^{-1})
2.0
4.0
6.0
8.0
10.0
12.0
$\frac{1}{[HI]} \times 10^{-3}$ (moles^{-1})

TABLE 4.15

Effect of Added I_2 on ϕ_{H_2} for Various HI Concentrations and Constant $\frac{[N_2O]}{[HI]}$ Ratios at 25°C

$\frac{[N_2O]_o}{[HI]_o}$	$[H_2]$ (μmoles)	$[N_2]$ (μmoles)	$[I_2]_T$ (μmoles)	$[HI]_o$ (μmoles)	$[HI]_f$ (μmoles)	E_{abs} (μeinsteins)	ϕ_{H_2} (moles einstein^{-1})
A. [λ → 2537 Å][Time 450 seconds] (S.V.P. of I_2 ≡ 5.20 μmoles)							
1.0	4.42	0.69	10.8	113	92.9	5.18	0.835
1.0	7.34	0.97	14.1	192	176	8.36	0.878
1.0	15.0	1.41	22.1	360	327	16.5	0.909
1.0	24.9	1.90	32.5	660	607	26.9	0.926
1.0	30.1	2.16	38.0	792	727	32.4	0.930
1.0	50.4	3.44	59.4	1161	1054	54.0	0.935
B. [λ → 3130 Å][Time 2700 seconds]							
1.0	5.73	0.49	11.5	201	192	7.34	0.825
1.0	9.96	0.73	16.1	370	351	11.3	0.881
1.0	14.0	0.84	20.1	597	568	15.4	0.907
1.0	17.9	1.23	24.4	772	735	19.6	0.916
1.0	19.6	1.46	26.2	921	880	21.2	0.922
1.0	22.7	1.69	29.6	1177	1129	24.5	0.928
C. [λ → 3660 Å][Time 21,600 seconds] (Added I_2 = 5.67 μmoles)							
1.0	1.56	0.15	7.58	958	954	1.68	0.929
1.0	2.51	0.17	8.39	1935	1931	2.64	0.950
1.0	4.65	0.20	10.6	3957	3947	4.85	0.960

of $\frac{k_7}{k_2}$ = 3.1 ± 0.1 obtained ($[I_2]$ = 5.20 μmoles) agrees well with Ogg's (80) 'hot atom' value of $\frac{k_7}{k_2}$ = 3.5 ± .3. From the intercept of the plot, a value of $\frac{k_2}{k_3}$ = 17.9 ± .2 was obtained. This value is reflected in the smaller amounts of N_2 compared to those of H_2 produced.

Figure 4.15 gives a second correlation plot of $(\phi_{H_2})^{-1}$ versus $([HI])^{-1}$ for the corresponding data in Table 4.15 for the 3130 Å wavelength. Here $\frac{k_7}{k_2}$ was calculated as 5.9 ± .2. This increase of $\frac{k_7}{k_2}$ at 3130 Å over $\frac{k_7}{k_2}$ at 2537 Å certainly suggests that hot atom reactions are occurring. From the intercept on the $(\phi_{H_2})^{-1}$ axis, we determined $\frac{k_2}{k_3}$ as 19.6 ± 0.6.

There is thus an increase in both $\frac{k_7}{k_2}$ and $\frac{k_2}{k_3}$ as λ becomes greater. For $\frac{k_2}{k_3}$, this seems to indicate that the $H' + N_2O$ reaction becomes less favoured as the average translational kinetic energy of the H atom decreases. As the H atoms become more thermal, the rate of the $H' + I_2$ reaction increases relative to the rate of the H' + HI reaction, and hence $\frac{k_7}{k_2}$ shows an increase.

Further evidence for the increase in $\frac{k_7}{k_2}$ and $\frac{k_2}{k_3}$ with decreasing translational kinetic energy of the hot hydrogen atom, came from a third correlation plot of $(\phi_{H_2})^{-1}$ against $([HI])^{-1}$ with λ = 3660 Å, where the values obtained for $\frac{k_7}{k_2}$ and $\frac{k_2}{k_3}$ from Figure 4.16 were respectively 8.5 ± 1.0 and 32.1 ± 1.7.

At the lower temperatures of 5°C and -20.5°C, the

Figure 4.15

Plot of $\frac{1}{\phi_{H_2}}$ versus $\frac{1}{[HI]}$ for the photolysis of HI/N_2O at 25°C and 3130 Å in the presence of added I_2

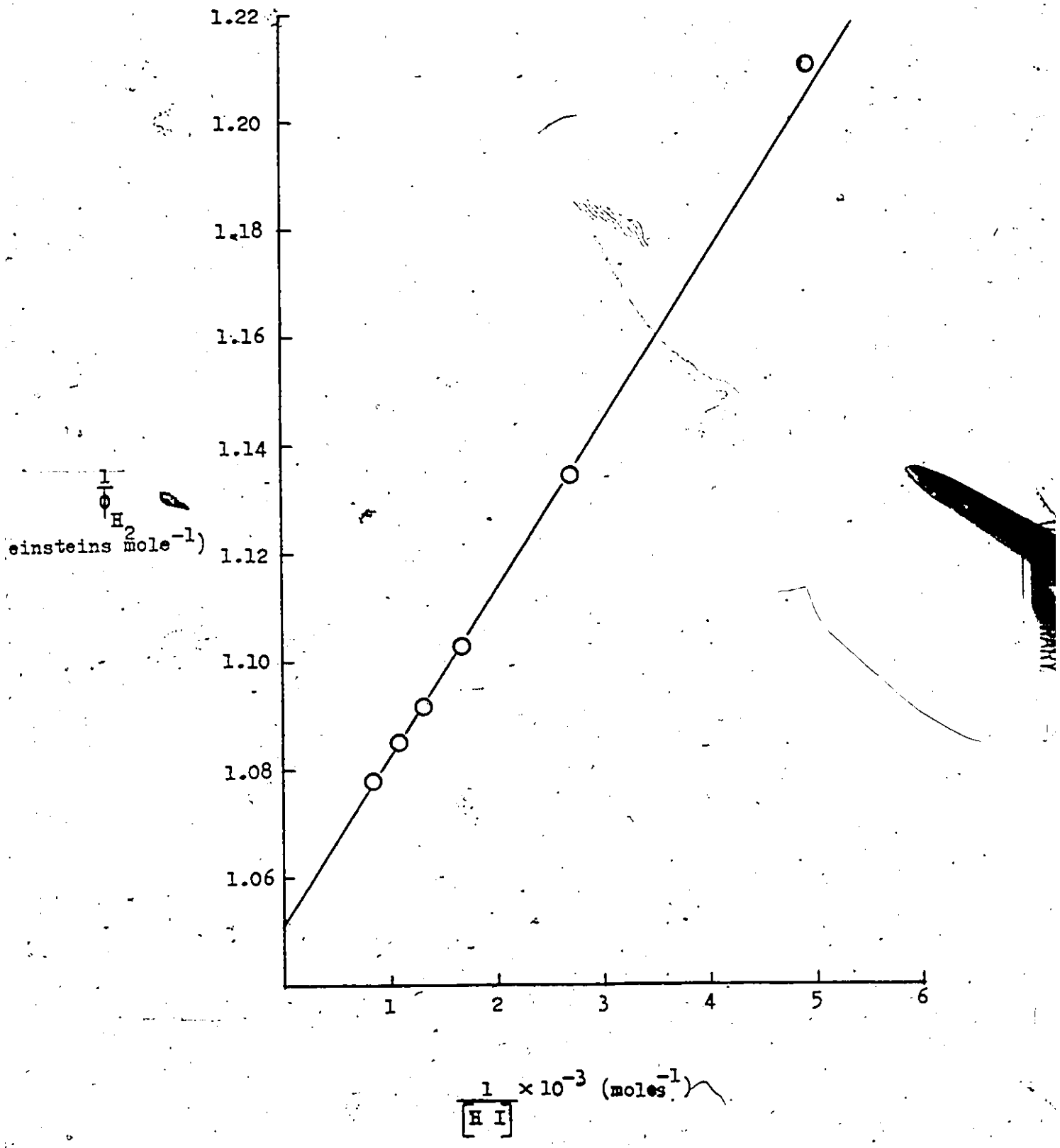
1.22
1.20
1.18
1.16
1.14
1.12
1.10
1.08
1.06
1
2
3
4
5
6
$\frac{1}{\phi_{H_2}}$ einsteins mole^{-1})
$\frac{1}{[HI]} \times 10^{-3}$ (moles^{-1})

Figure 4.16

Plot of $(\phi_{H_2})^{-1}$ versus $([HI])^{-1}$ for the photolysis of HI/N_2O at 25°C and 3660 Å in the presence of added I_2

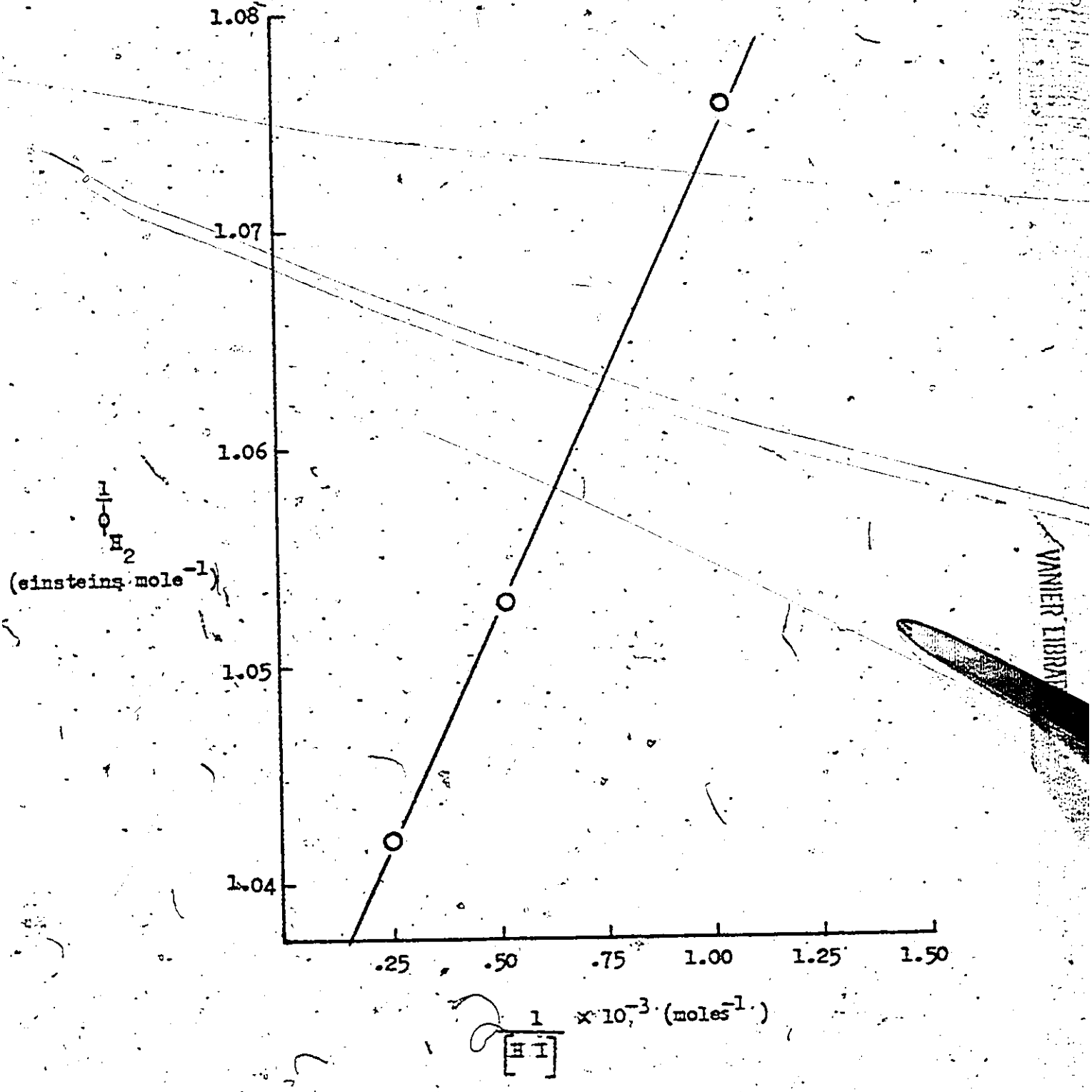

kinetic behaviour of the photochemical system was similar to that at 25°C. The only significant change was the noticeable decrease in N_2 production at the longer wavelengths 3130 Å and 3660 Å, especially so at 3660 Å. The correlation plots in Figure 4.17 produced values of $\frac{k_7}{k_2} = 3.3 \pm .2$ and $\frac{k_2}{k_3} = 18.0 \pm 0.2$ at 5°C, and $\frac{k_7}{k_2} = 3.5 \pm 0.5$, $\frac{k_2}{k_3} = 18.1 \pm .2$ at -20.5°C, both plots being constructed for experiments carried out with the 2537 Å (Table 4.16). Inspection of these two parameters $\frac{k_7}{k_2}$ and $\frac{k_2}{k_3}$ reveal only very small changes within the experimental range and this result was reflected in small activation energies obtained from the slopes of the two Arrhenius plots in Figure 4.18. The calculations gave $E_2 - E_7 = 0.42 \pm 0.40$ kcal mole^{-1} and $E_3 - E_2 = 0.04 \pm 0.04$ kcal mole^{-1}.

The postulation was earlier made, that the N_2 producing reaction, i.e.,

$$H^{\cdot} + N_2O \rightarrow N_2 + OH^{\cdot} \qquad (4.3)$$

seemed to be more favoured the hotter the H atoms. If this is so, then at longer wavelengths and low temperatures as the yields of N_2 drop, the activation energy associated with the $\frac{k_2}{k_3}$ ratio should show an increase over the value obtained with the use of the 2537 Å radiation. The higher the energy of atoms or radicals participating in reactions, the smaller the dependence of these reactions on temperature (79,81,83).

The progression of $\frac{k_7}{k_2}$ and $\frac{k_2}{k_3}$ to higher values, became more evident as a shift was made to longer wavelengths.

Figure 4.17

Plots of $(\phi_{H_2})^{-1}$ versus $([HI])^{-1}$ for the photolysis of HI/N_2O at (i) 5°C, (ii) -20.5°C and 2537 Å

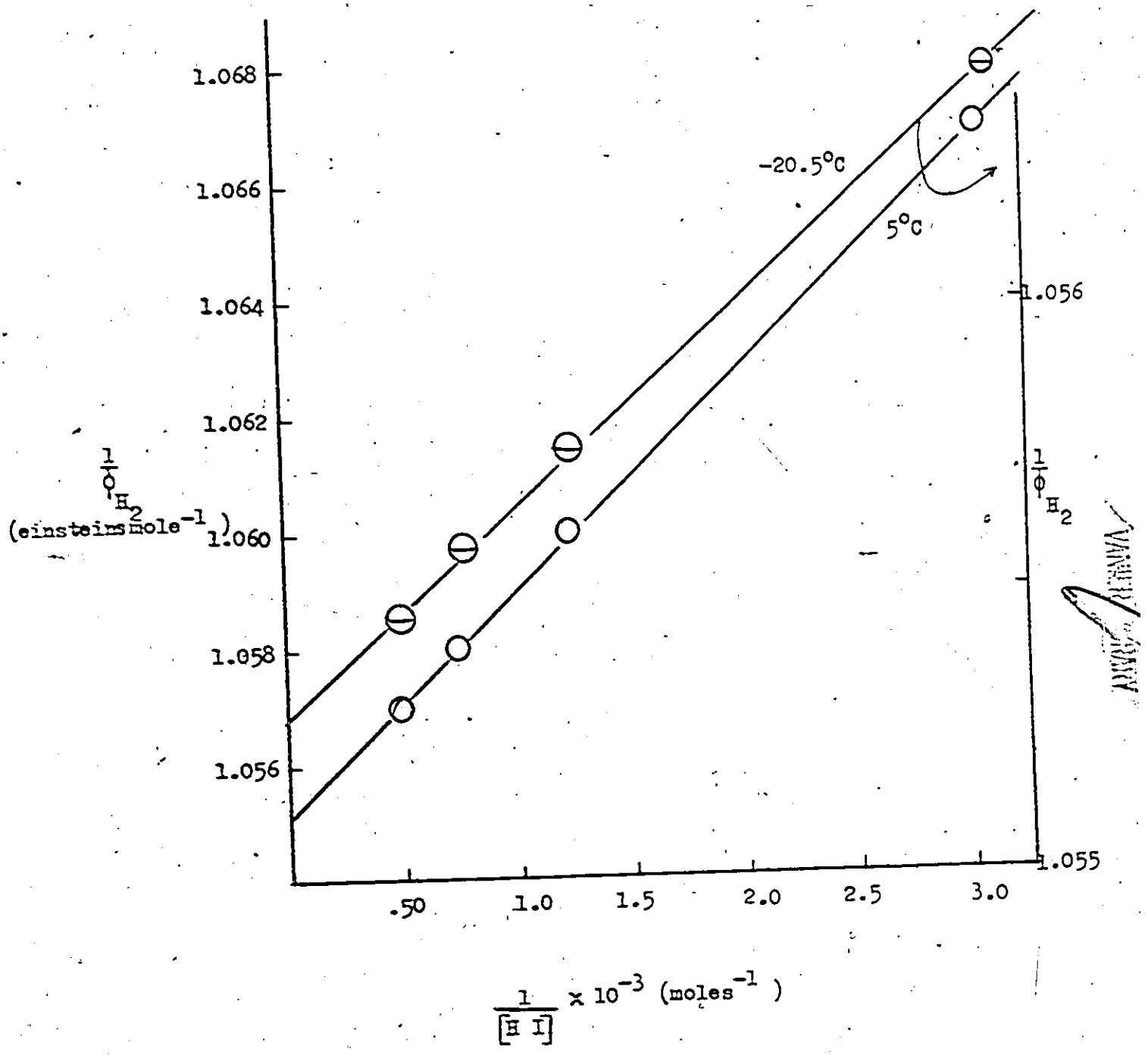
1.068
1.066
1.064
1.062
1.060
1.058
1.056
1.056
1.055
-20.5°C
5°C
.50
1.0
1.5
2.0
2.5
3.0
$\frac{1}{\Phi_{H_2}}$ (einsteins mole^{-1})
$\frac{1}{\Phi_{H_2}}$
$\frac{1}{[H\ I]} \times 10^{-3}$ (moles^{-1})

TABLE 4.16

Effect of Added I_2 and ϕ_{H_2} for Various HI Concentrations and Constant $\frac{[N_2O]}{[HI]}$ Ratios at 5°C and -20.5°C with the 2537 Å Wavelength

(S.V.P. of I_2 ≡ 5.20 moles)

$\frac{[N_2O]_o}{[HI]_o}$	$[H_2]$ (μmoles)	$[N_2]$ (μmoles)	$[I_2]_f$ (μmoles)	$[HI]_o$ (μmoles)	$[HI]_f$ (μmoles)	ϕ_{H_2} (moles einstein^{-1})
A. [Time 300 seconds][Temp: 5°C]						
1.0	15.0	0.91	16.0	326	294	0.937
1.0	19.1	1.09	20.2	806	766	0.943
1.0	20.7	1.15	21.9	1290	1246	0.945
1.0	24.0	1.34	25.4	1968	1918	0.946
B. [Time 300 seconds][Temp: -20.5°C]						
1.0	15.1	0.77	16.00	319	288	0.946
1.0	19.1	1.03	20.2	798	758	0.947_2
1.0	20.7	1.10	21.9	1281	1237	0.947_4
1.0	24.0	1.27	25.4	1913	1863	0.947_5

Figure 4.18

Arrhenius plots for $\frac{k_7}{k_2}$ and $\frac{k_2}{k_3}$ at 2537 Å

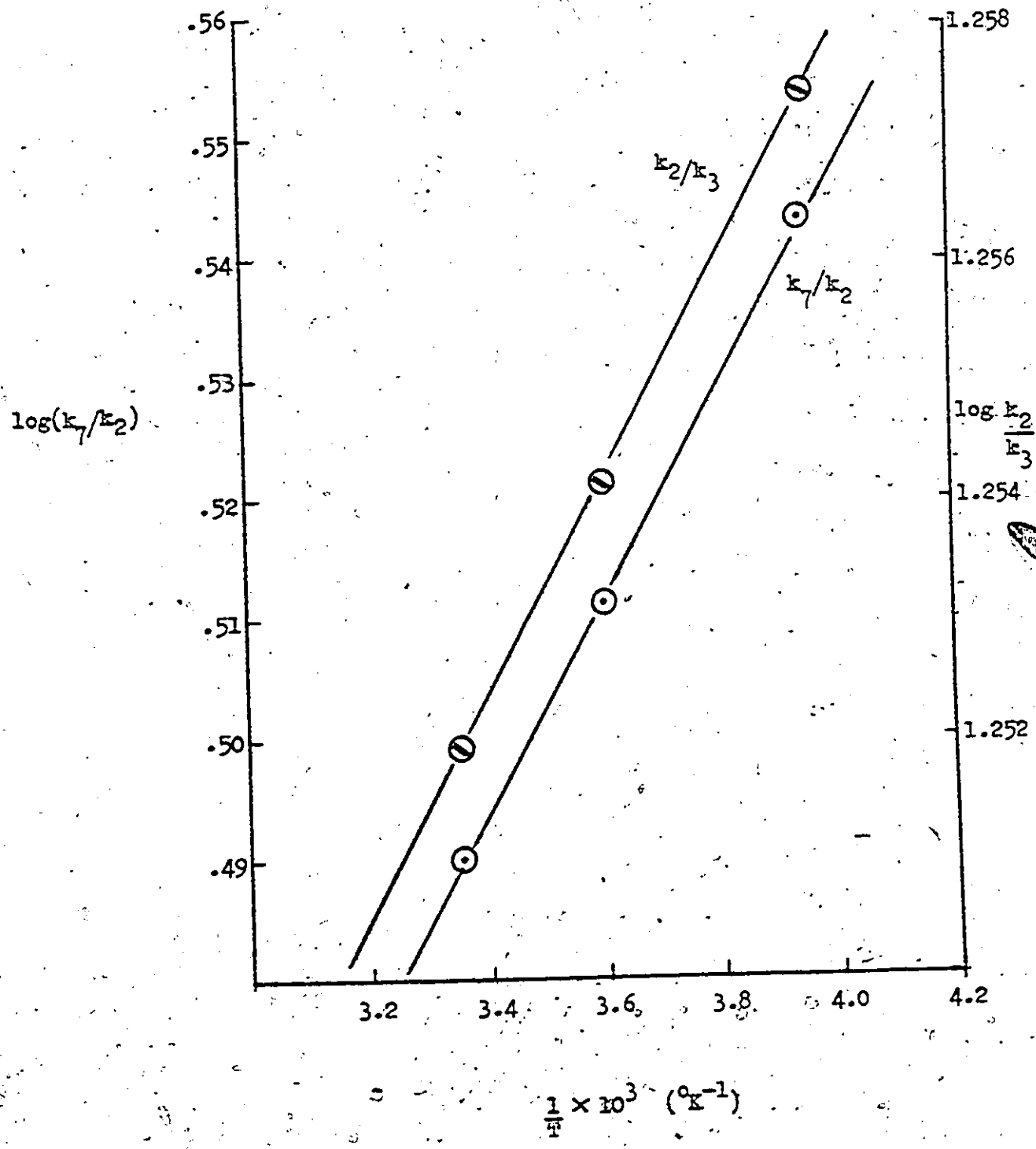
.56
.55
.54
.53
.52
.51
.50
.49
log(k7/k2)
1.258
1.256
1.254
1.252
log k2/k3
k2/k3
k7/k2
3.2
3.4
3.6
3.8
4.0
4.2
1/T × 10^3 (°K^-1)

This is shown in Table 4.19 for the results obtained with the 3130 Å and 3660 Å wavelength at 25°C, 5°C and -20.5°C. A summary of the results obtained at 25°C with the 2537 Å wavelength has also been entered in this Table. The calculated $\frac{k_7}{k_2}$, $\frac{k_2}{k_3}$ and apparent activation energies were obtained from Figures 4.19 - 4.22 for data entered in Tables 4.17 and 4.18. The $E_2 - E_7$ values are in good agreement with those obtained by other authors (76,83,96). E_2 is generally regarded as being approximately 0.0 kcal mole^{-1}.

The Effect of Added I_2

The proposed mechanism governing the kinetics of the HI/N_2O photochemical system, and the subsequently derived equation,

$$\frac{1}{\phi_{H_2}} = 1 + \frac{k_7}{k_2}\frac{[I_2]}{[HI]} + \frac{k_3}{k_2}\frac{[N_2O]}{[HI]} \qquad (4.18)$$

show that if the I_2 content is increased in the system for any given time period, the number of H atoms available for reaction with HI molecules decreases and consequently ϕ_{H_2} decreases.

If a known quantity of I_2 is injected into the HI photochemical system in the absence of N_2O, the relationship between the three terms ϕ_{H_2}, [HI] and $[I_2]$ can be expressed as:

$$\frac{1}{\phi^o_{H_2}} = 1 + \frac{k_7}{k_2}\frac{[I_2]}{[HI]} \qquad (4.19)$$

Figure 4.19

Plots of $(\phi_{H_2})^{-1}$ against $([HI])^{-1}$ for the photolysis of HI/N_2O at (i) 5°C, (ii) -20.5°C and 3130 Å

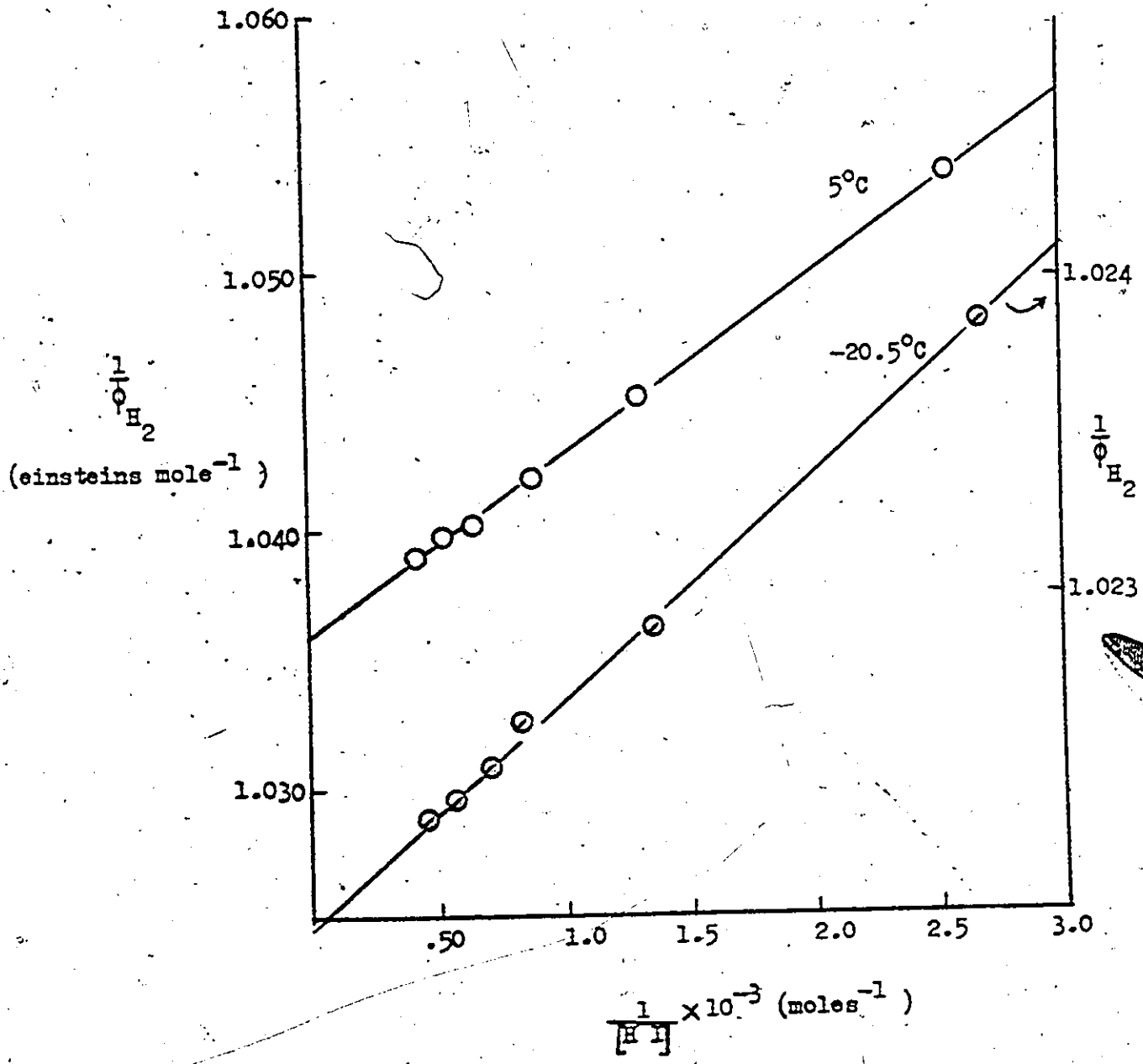

Figure 4.20

Arrhenius plots for $\frac{k_7}{k_2}$ and $\frac{k_2}{k_3}$ at 3130 Å

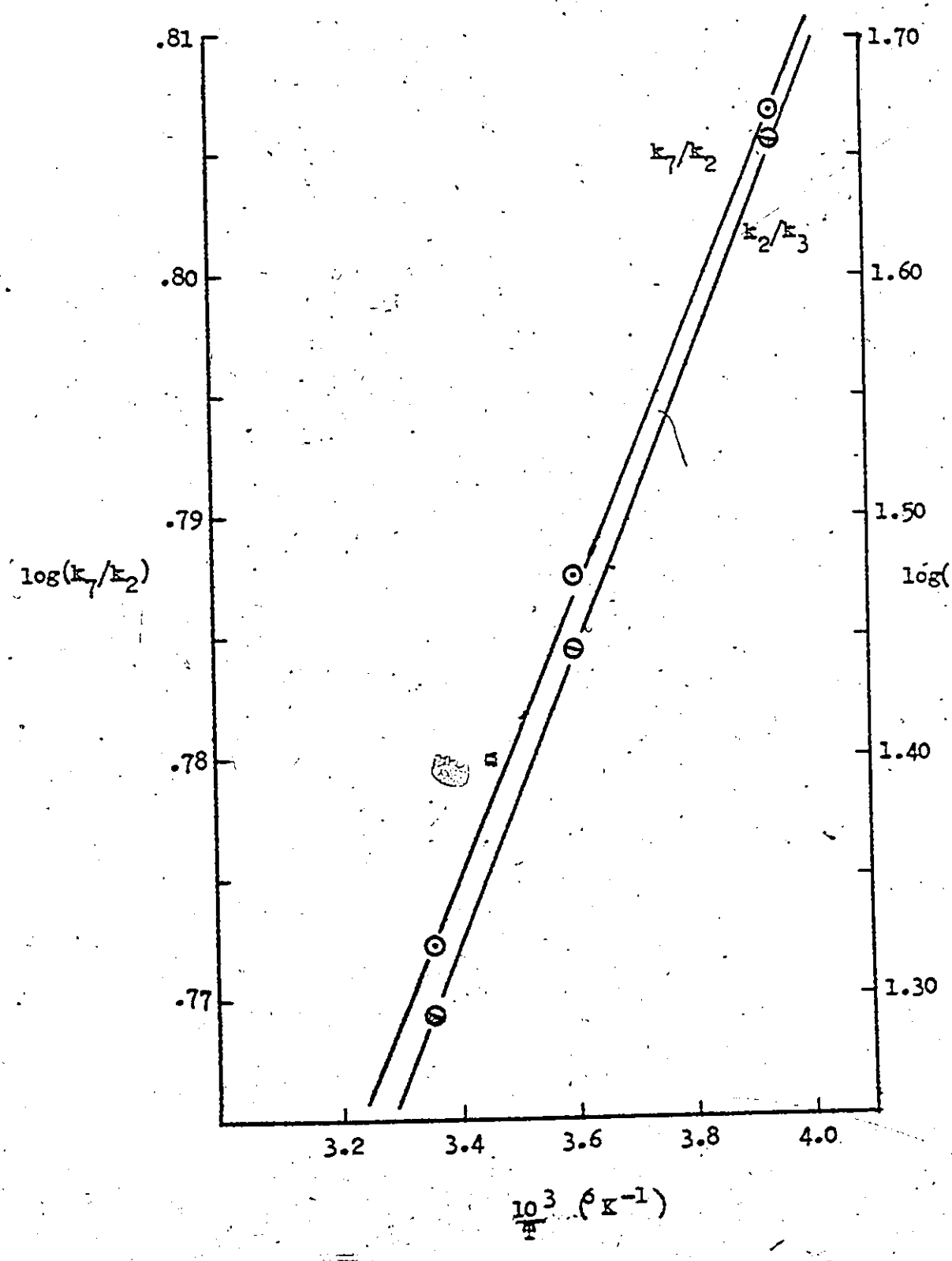
.81
.80
.79
.78
.77
log(k7/k2)
1.70
1.60
1.50
1.40
1.30
log(k2/k3)
k7/k2
k2/k3
3.2
3.4
3.6
3.8
4.0
10^3/T (°K^-1)

Figure 4.21

Plots of $(\phi_{H_2})^{-1}$ against $([HI])^{-1}$ for the photolysis of HI/N_2O at (i) 5°C, (ii) -20.5°C and 3660 Å

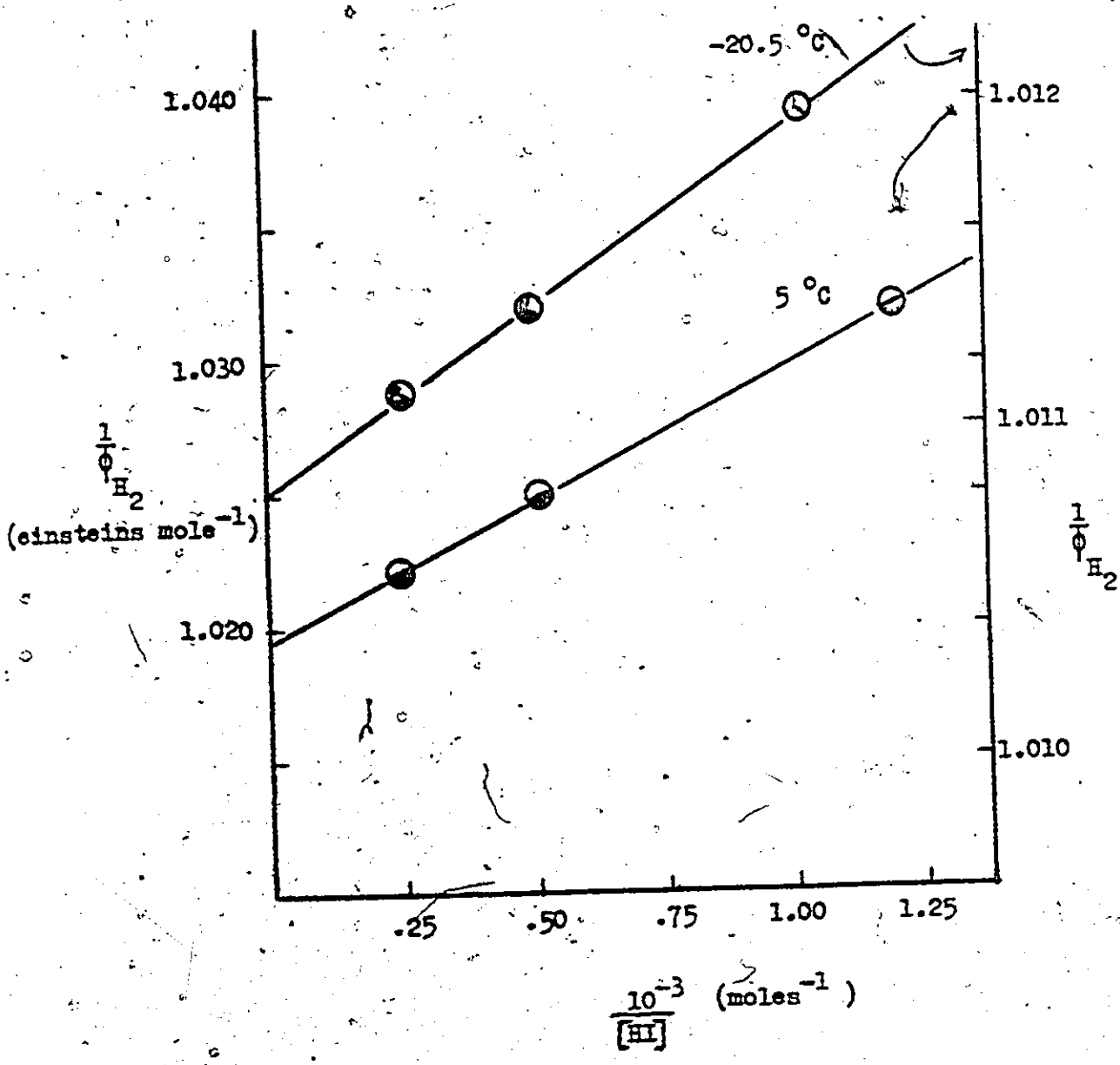
-20.5 °C
5 °C
1.040
1.030
1.020
1.012
1.011
1.010
$\frac{1}{\phi_{H_2}}$
(einsteins mole^{-1})
.25
.50
.75
1.00
1.25
$\frac{10^{-3}}{[HI]}$ (moles^{-1})

Figure 4.22

Arrhenius plots for $\frac{k_7}{k_2}$ and $\frac{k_2}{k_3}$ at 3660 Å

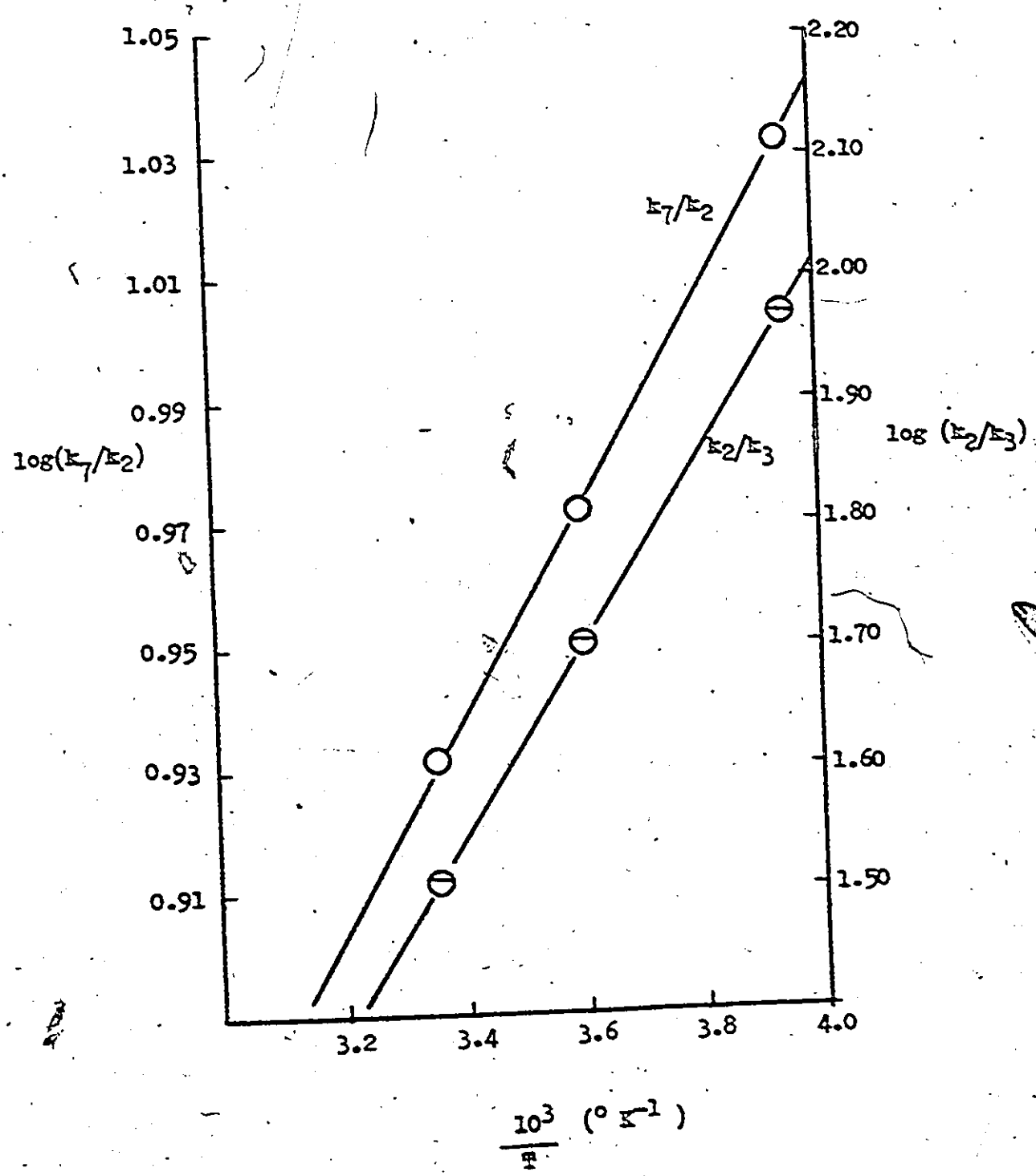
1.05
1.03
1.01
0.99
0.97
0.95
0.93
0.91
log(k7/k2)
2.20
2.10
2.00
1.90
1.80
1.70
1.60
1.50
log (k2/k3)
k7/k2
k2/k3
3.2
3.4
3.6
3.8
4.0
10^3 / T (°K^-1)

TABLE 4.17

Effect of Added I_2 on ϕ_{H_2} for Various HI Concentrations and Constant $\frac{[N_2O]}{[HI]}$ Ratios at 5°C and -20.5°C with the 3130 Å Wavelength

(S.V.P. of I_2 ≡ 5.20 moles)

$\frac{[N_2O]}{[HI]_o}$	$[H_2]$ (μmoles)	$[N_2]$ (μmoles)	$[I_2]$ (μmoles)	$[HI]_o$ (μmoles)	$[HI]_f$ (μmoles)	ϕ_{H_2} (moles einstein^{-1})
A. [Time 2700 seconds][Temp: 5°C]						
1.0	10.8	0.43	11.3	390	368	0.948_7
1.0	18.6	0.78	19.4	769	730	0.956_7
1.0	23.3	0.85	24.3	1153	1105	0.959_6
1.0	27.0	0.97	28.1	1541	1487	0.961
1.0	30.1	1.09	31.3	1926	1864	0.961_7
1.0	36.9	1.32	38.4	2338	2262	0.962_5
B. [Time 2700 seconds][Temp: -20.5°C]						
1.0	10.8	0.15	11.1	374	352	0.976_7
1.0	18.1	0.36	18.5	739	703	0.977_6
1.0	23.3	0.43	23.8	1070	1022	0.977_9
1.0	25.0	0.48	25.5	1415	1364	0.978
1.0	28.6	0.61	29.2	1772	1715	0.978_1
1.0	34.2	0.72	34.9	2154	2084	0.978_2

TABLE 4.18

Effect of Added I_2 on ϕ_{H_2} for Various HI Concentrations and Constant $\frac{[N_2O]}{[HI]}$ Ratios at 5°C and -20.5°C with the 3660 Å Wavelength

$\frac{[N_2O]_o}{[HI]_o}$	$[N_2]$ (μmoles)	$[H_2]$ (μmoles)	$[I_2]$ (μmoles)	$[HI]_o$ (μmoles)	$[HI]_f$ (μmoles)	ϕ_{H_2} (moles einstein^{-1})
A. [Temp: 5°C][Time 21,600 seconds]						
1.0	0.03	1.54	1.59	833	830	0.969
1.0	0.04	2.61	2.68	1961	1956	0.975_6
1.0	0.09	4.76	4.87	3992	3982	0.978_4
B. [Temp: -20.5°C][Time 21,600 seconds]						
1.0	0.01	1.71	1.73	975	972	0.988_2
1.0	0.02	2.62	2.65	1951	1946	0.988_7
1.0	0.03	4.75	4.80	3880	3871	0.989

TABLE 4.19

Summary of $\frac{k_7}{k_2}$, $\frac{k_2}{k_3}$ Values and Apparent Activation Energies E_2-E_7 and E_3-E_2

Wavelength (Å)	Temperature (°C)	$\frac{k_7}{k_2}$	$\frac{k_2}{k_3}$	$E_{Apparent}$ $E_{A(i)}$ (kcal mole^{-1})	$E_{A(ii)}$ (kcal mole^{-1})
2537	25	3.1± .1	17.9± .2		
2537	5	3.3± .2	18.0± .2	0.42±.40	.04±.04
2537	-20.5	3.5± .5	18.1± .2		
3130	25	5.9± .2	19.6± .6		
3130	5	6.1± .9	27.8± .3	.55±.50	2.88±.31
3130	-20.5	6.4±1.4	45.4± .5		
3660	25	8.5±1.0	32.1±1.7		
3660	5	9.4±2.5	50.1±4.3	.71±.72	3.69±.44
3660	-20.5	10.8±1.0	92.6±9.4		

$E_{A(i)}$ corresponds to E_2-E_7 and $E_{A(ii)}$ corresponds to E_3-E_2

where the equations,

$$HI + h\nu \xrightarrow{I_a} H^{\cdot\prime} + I^{\cdot}$$

$$H^{\cdot\prime} + HI \xrightarrow{k_2} H_2 + I^{\cdot}$$

$$H^{\cdot\prime} + I_2 \xrightarrow{k_7} HI + I^{\cdot}$$

$$I^{\cdot} + I^{\cdot} + M \rightarrow I_2$$

govern the relationship in equation (4.19) under steady state conditions for the production and disappearance of H atoms in the absence of N_2O. Equation (4.18) can be rewritten as:

$$\frac{1}{\phi'_{H_2}} = 1 + \frac{k_7}{k_2}\frac{[I_2]}{[HI]} + \frac{k_3}{k_2}\frac{[N_2O]}{[HI]} \qquad (4.18')$$

where ϕ'_{H_2} represents ϕ_{H_2} in the presence of both added I_2 and added N_2O. Equations (4.18') and (4.19) can be combined for constant concentrations of HI and I_2, giving,

$$\left(\frac{1}{\phi'_{H_2}} - \frac{1}{\phi^{o}_{H_2}}\right) = \frac{k_3}{k_2}\frac{[N_2O]}{[HI]} \qquad (4.20)$$

The quantum yield can then be observed in the presence and absence of N_2O for a set of experimental runs (Table 4.20) and by plotting $(\frac{1}{\phi'_{H_2}} - \frac{1}{\phi^{o}_{H_2}})$ against $\frac{[N_2O]}{[HI]}$, $\frac{k_3}{k_2}$ can be determined. Figure 4.23 shows a reasonably good linear plot for the two sets of variables, resulting in a slope of $\frac{k_3}{k_2} = \frac{10}{165}$ or $\frac{k_2}{k_3} = 16.5$. This value of 16.5 ± 2.0 for $\frac{k_2}{k_3}$ is fairly close to the value of 19.6 ± .6 obtained from the use of equation (4.18) in the kinetic analysis of the experimental

TABLE 4.20

Variation of ϕ_{H_2} with $\frac{[N_2O]}{[HI]}$ Ratios in the Presence of I_2 at 3130 Å

[Added I_2 = 5.70 μmoles][Time 2700 seconds][Temp: 25°C]

$\phi^{\circ}_{H_2}$ (H_2 in the presence of I_2; $[N_2O] = 0.0$) = 0.903 moles einstein^{-1}

ϕ'_{H_2} (H_2 in the presence of I_2; $[HI]_o$ = 184 μmoles)

$\frac{[N_2O]_o}{[HI]_o}$	$[H_2]$ (μmoles)	$[N_2]$ (μmoles)	$[I_2]_T$ (μmoles)	$[HI]_o$ (μmoles)	$[HI]_f$ (μmoles)	E_{abs} (μeinsteins)	ϕ'_{H_2} (moles einstein^{-1})
1.00	5.97	0.37	12.6	184	171	7.30	0.818
2.05	5.92	0.69	12.7	183	170	7.33	0.808
3.05	5.63	0.73	12.7	183	171	7.34	0.767
4.08	5.51	0.86	12.7	184	170	7.35	0.750
5.16	5.18	0.97	12.9	182	168	7.40	0.700
6.17	4.97	0.98	12.9	185	171	7.40	0.672

$\frac{[N_2O]_o}{[HI]_o}$	$\left(\frac{1}{\phi'_{H_2}} - \frac{1}{\phi^{\circ}_{H_2}}\right)$ (einsteins mole^{-1})
1.00	0.115
2.05	0.130
3.05	0.197
4.08	0.257
5.16	0.321
6.17	0.381

Figure 4.23

Plot of $(\frac{1}{\phi'_{H_2}} - \frac{1}{\phi^{o}_{H_2}})$ versus $\frac{[N_2O]_o}{[HI]_o}$ at 25°C and 3130 Å.

$\phi^{o}_{H_2} \rightarrow \phi_{H_2}$ in the presence of added I_2;
$[N_2O] = 0.0$.

$\phi'_{H_2} \rightarrow \phi_{H_2}$ in the presence of both added I_2 and N_2O.

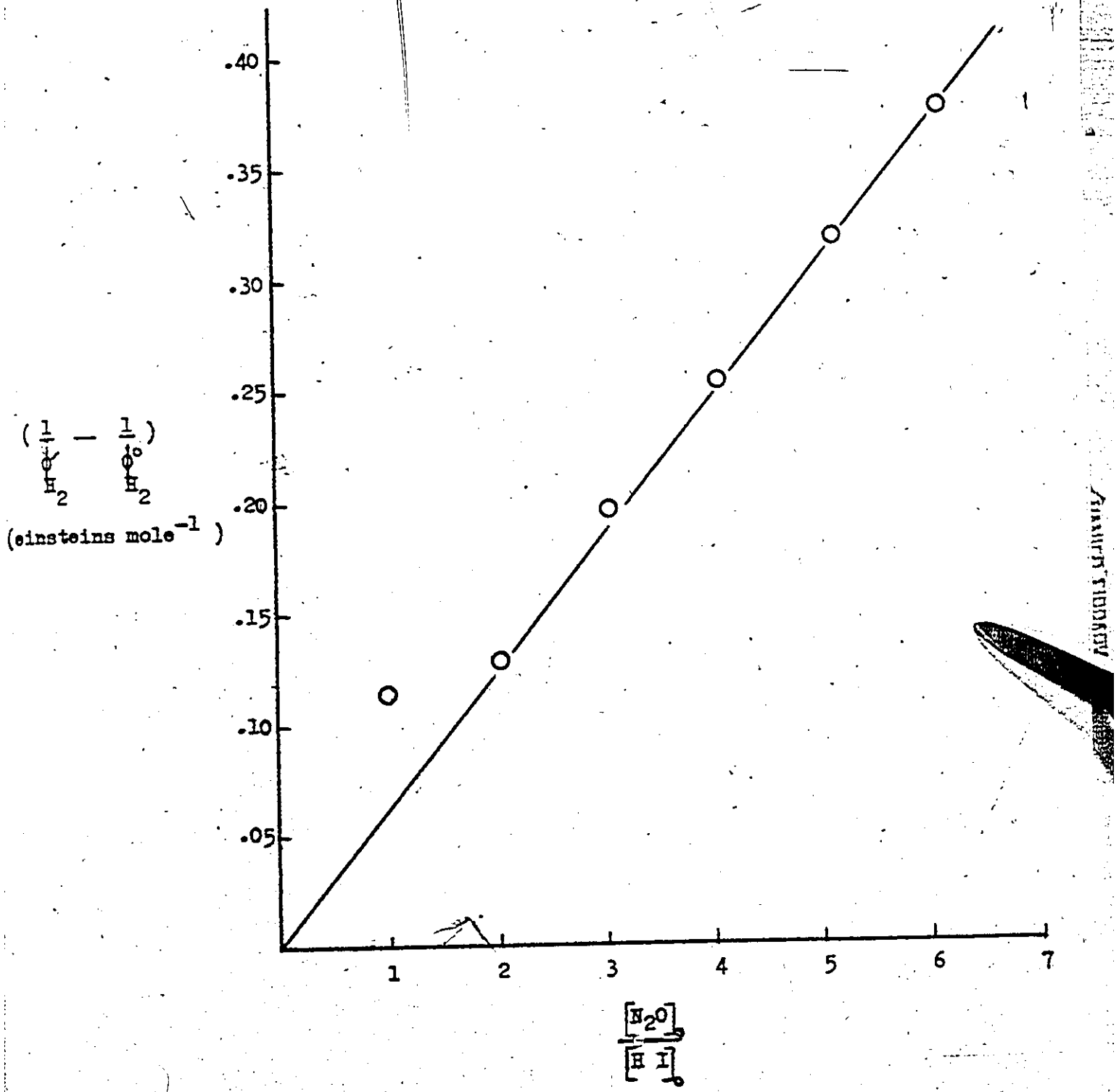
.40
.35
.30
.25
.20
.15
.10
.05
1
2
3
4
5
6
7
$\left(\frac{1}{\phi_{H_2}} - \frac{1}{\phi^{\circ}_{H_2}}\right)$
(einsteins mole^{-1})
$\frac{[N_2O]}{[H\ I]}$

results at 25°C and 3130 Å. The added I_2 has its greatest effect on the $H^{\cdot\prime} + N_2O \rightarrow N_2 + OH^{\cdot}$ reaction when the $\frac{[N_2O]_o}{[HI]_o}$ ratio is relatively low. This is shown in Figure 4.23 for $\frac{[N_2O]_o}{[HI]_o} = 1.00$. The point corresponding to this ratio shows an appreciable deviation from the straight line. The $I_2 + H^{\cdot\prime} \rightarrow HI + I^{\cdot}$ reaction is enhanced by the added I_2, while the level of each of the two reactions

$$H^{\cdot\prime} + HI \rightarrow H_2 + I^{\cdot}$$

$$H^{\cdot\prime} + N_2O \rightarrow N_2 + OH^{\cdot}$$

is reduced.

Effect of CO_2 on $\frac{k_7}{k_2}$ and $\frac{k_2}{k_3}$ (2537 Å)

CO_2 causes a reduction in the quantum yield of H_2 when it is added to the HI/N_2O photochemical system. A similar CO_2 effect was observed by Penzhorn and Darwent (96) in the photolysis of HI, and by Steer and Knight (111) in the photolysis of mercaptan systems. Woolley and Cvetanovic (98) also found a similar effect in the photolysis of H_2S with the 2490 Å wavelength.

In the presence of CO_2, the hot H atoms may be deactivated according to equation (4.21), and there exists the

$$H^{\cdot *} + CO_2 \rightarrow H^{\cdot} + CO_2 \qquad (4.21)$$

possibility of various types of hot H atoms resulting. The hot H atoms found in the primary process with about 20 or 42 kcals $mole^{-1}$ of translational kinetic energy (depending on whether $I^*(^2P_{1/2})$ or $I(^2P_{3/2})$ is formed) may require several collisions with CO_2 before complete deactivation. In the experiments conducted, a 150-200 fold excess of CO_2 produced a pressure independent yield of H_2. It is very likely therefore that the H atoms encountering HI, I_2 and N_2O molecules in the presence of this excess of CO_2, will be displaying the reactivity of 'hot' H atoms whose energies have been degraded.

Figures 4.24 and 4.25 show the results of plots of $(\phi_{H_2})^{-1}$ against $([HI])^{-1}$ for the 2537 Å wavelength. The ϕ_{H_2} values were determined at 25°C, 5°C and -20.5°C in the presence of a 40-fold excess of CO_2 (Table 4.21). The values of $\frac{k_7}{k_2}$ and $\frac{k_2}{k_3}$ obtained here (Table 4.22) are larger than those previously discussed for this work, for non-thermalized H atoms. The probable reasons for these higher values are (1) the deactivated hot H atoms show a higher reactivity towards the halogen I_2 than to HI, and (2) the reaction $H^{\cdot} + N_2O \rightarrow N_2 + OH^{\cdot}$, becomes less facile for thermalized or near-thermalized H atoms. However, some of the $\frac{k_7}{k_2}$ values (those at 25°C and 5°C) are not in the range of 10 → 14, a range generally accepted as indicative of thermal H atoms; from this it might be inferred that some of the H atoms reacting with HI, I_2 and N_2O have not lost all of their trans-

Figure 4.24

Plot of $(\phi_{H_2})^{-1}$ against $\frac{1}{[HI]}$ for the photolysis of HI + N_2O at (i) 25°C, (ii) 5°C and 2537 Å in the presence of carbon dioxide (CO_2).

$$\frac{[CO_2]}{[HI]_o} = 40$$

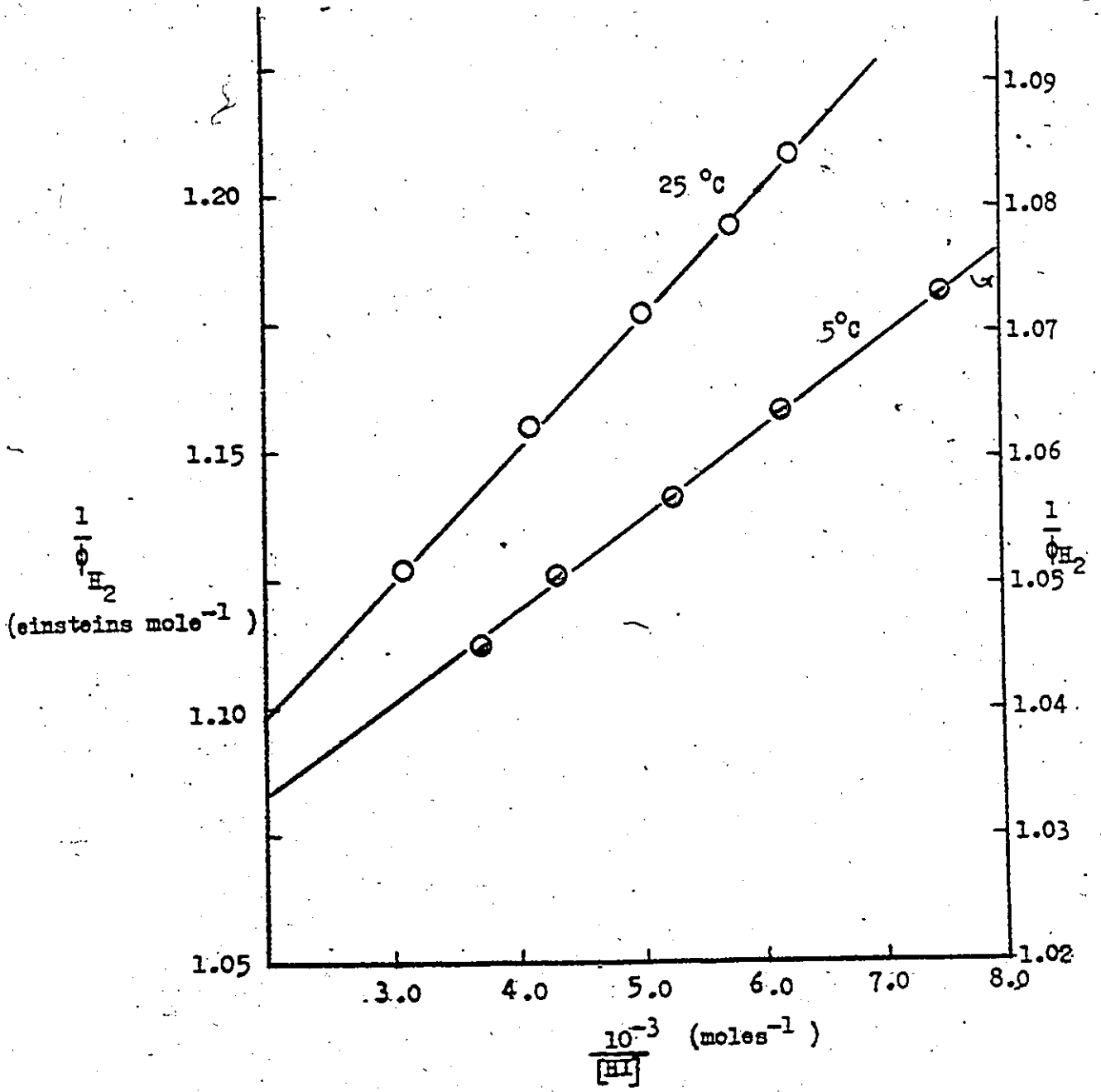
25 °C
5°C
1.20
1.15
1.10
1.05
1.09
1.08
1.07
1.06
1.05
1.04
1.03
1.02
3.0
4.0
5.0
6.0
7.0
8.0
$\frac{1}{\phi_{H_2}}$ (einsteins mole^{-1})
$\frac{1}{\phi_{H_2}}$
$\frac{10^{-3}}{[HI]}$ (moles^{-1})

Figure 4.25

Plot of $(\phi_{H_2})^{-1}$ versus $([HI])^{-1}$ for the photolysis of HI + N_2O at -20.5°C and 2537 Å in the presence of CO_2.

$$\frac{[CO_2]}{[HI]_o} = 40$$

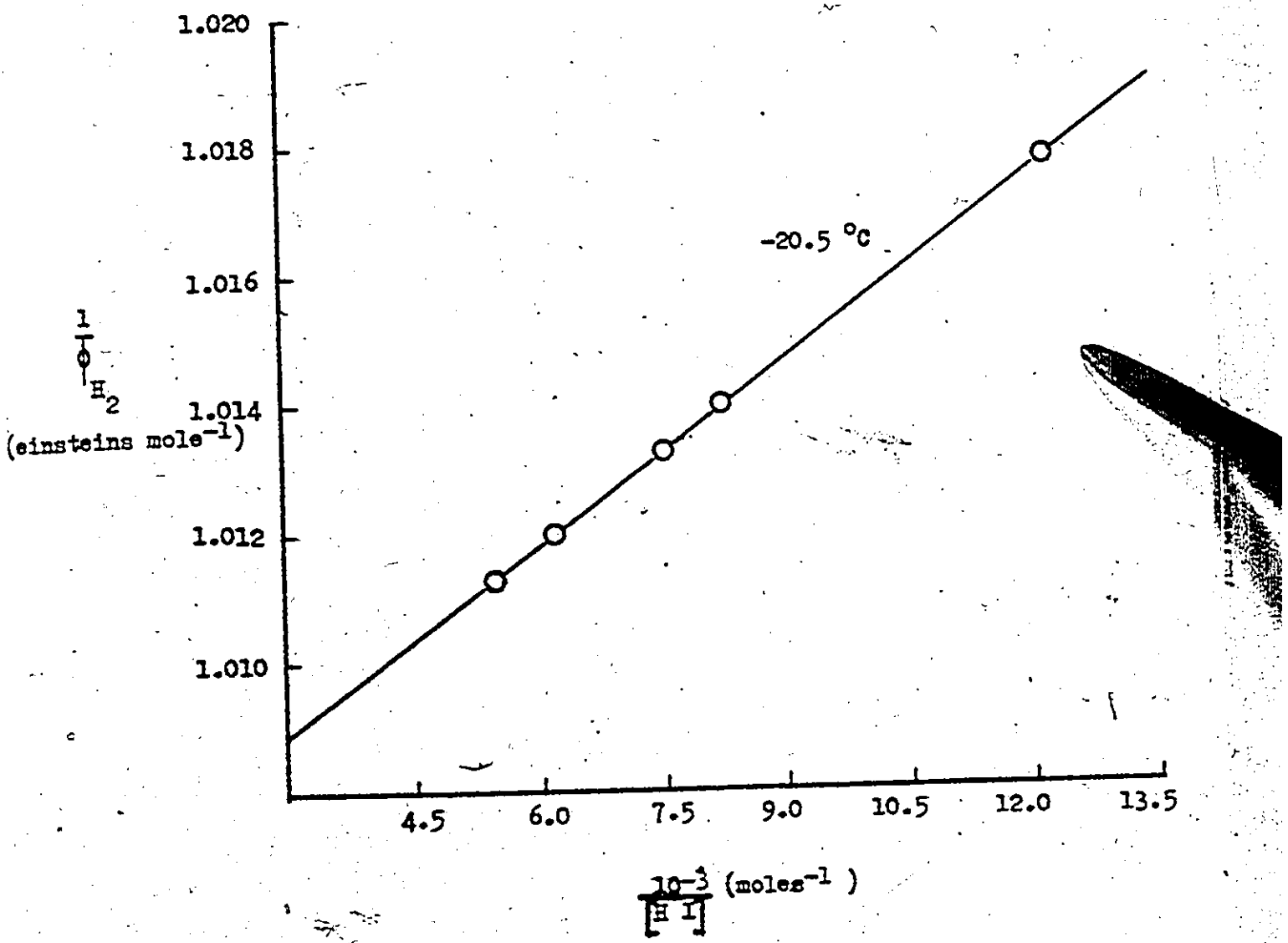
1.020
1.018
1.016
1.014
1.012
1.010
$\frac{1}{\phi_{H_2}}$
(einsteins mole^{-1})
-20.5 °C
4.5
6.0
7.5
9.0
10.5
12.0
13.5
$\frac{10^{-3}}{[HI]}$ (moles^{-1})

TABLE 4.21

The Effect of Added CO_2 (in the presence of added I_2) on ϕ_{H_2} at 2537 Å in the Photolysis of HI + N_2O

$\frac{[N_2O]_o}{[HI]_o}$	$\frac{[CO_2]}{[HI]_o}$	$[H_2]$ (μmoles)	$[N_2]$ (μmoles)	$[HI]_o$ (μmoles)	E_{abs} (μeinsteins)	ϕ_{H_2} (moles einstein^{-1})
A. [Temp: 25°C][Time 300 seconds][$[I_2]_i$ = 5.56 μmoles]						
1.0	40.0	5.70	0.32	160	6.90	0.826
1.0	40.2	6.40	0.33	174	7.67	0.835
1.0	40.2	6.96	0.34	200	8.20	0.849
1.0	40.1	10.0	0.36	244	11.6	0.866
1.0	40.0	11.8	0.39	325	12.2	0.887
B. [Temp: 5°C][Time 300 seconds][$[I_2]_i$ = 5.56 μmoles]						
1.0	40.2	5.18	0.07	133	5.55	0.932
1.0	40.1	5.40	0.08	163	5.74	0.940
1.0	40.1	5.81	0.10	191	6.14	0.947
1.0	40.5	8.65	0.11	233	9.09	0.952
1.0	40.1	10.8	0.14	270	11.3	0.957
C.						
1.0	40.6	3.30	0.03	81.8	3.35	0.982
1.0	40.3	5.02	0.04	121	5.09	0.986
1.0	40.1	5.14	0.04	133	5.21	0.987
1.0	40.3	5.40	0.05	163	5.47	0.988
1.0	40.4	6.10	0.06	182	6.17	0.989

TABLE 4.22

Effect of CO_2 on $\frac{k_7}{k_2}$ and $\frac{k_2}{k_3}$ ($\lambda \rightarrow 2537$ Å)

$\frac{[CO_2]}{[HI]_o}$	Temperature (°C)	$\frac{k_7}{k_2}$	$\frac{k_2}{k_3}$	$E_{Apparent}$ $E_{A(i)}$	$E_{A(ii)}$ kcal mole^{-1}
40.1	25	5.2± .8	22.9±1.2		
40.3	5	6.5±1.2	52.6±2.8	1.9±1.1	6.3±.8
40.4	-20.5	9.3±2.9	16.7±4.2		

$E_{A(i)}$ represents E_2-E_7 and $E_{A(ii)}$ represents E_3-E_2

lational kinetic energy prior to their encounter with HI, I_2 and N_2O molecules.

As the excess energy of the hot H atom becomes degraded, a temperature effect becomes prominent and the N_2 producing reaction becomes less productive. The inert gas effect in combination with the low temperature of -20.5°C gave the highest values of $\frac{k_7}{k_2}$ and $\frac{k_2}{k_3}$ obtained in all the experiments.

Table 4.23 taken from a recent review by Holmes and Armstrong (118) lists several values for $(\frac{k_7}{k_2})$ for the reactivity of thermalized H atoms with HI and I_2. Figure 4.24 shows the temperature effect on $\frac{k_7}{k_2}$ and on $\frac{k_2}{k_3}$.

The composite apparent activation energy (E_3-E_2) for the processes

$$H^{\cdot} + HI \xrightarrow{k_2} H_2 + I^{\cdot}$$

$$H^{\cdot} + N_2O \xrightarrow{k_3} N_2 + OH^{\cdot}$$

was estimated as 6.3 ± 0.8 kcals $mole^{-1}$ in the presence of the excess CO_2. From the kinetics of the thermal hydrogen-nitrous oxide reaction in silica vessels, Melville reported the value of E_a the activation energy for the $H + N_2O \rightarrow N_2 + OH$ reaction as 7.0 kcals $mole^{-1}$. The calculation of E_a was based on the high pressure temperature coefficient. Melville's value for E_a, and that obtained in this study can be considered close if E_2 is very small.

Fenimore and Jones (120) have obtained a rate

TABLE 4.23

Values of $(\frac{k_7}{k_2})_\infty$ From The Photolysis of HI

$(\frac{k_7}{k_2})_\infty$	T ($^\circ$C)	Reference
11.2	53	83
11.7	69	83
11.9	102	83
13.5	114	82
9.01	154	82
7.00	155	80
4.69	198	82
11.40	200	83
10.20	393.6	75
14±4	394	76
8.85	437.1	75
8.20	464.7	75
12±2	527	76

constant of $4.0 \times 10^{11} \exp\left(-\frac{16000}{RT}\right)$ ℓ mole^{-1} sec^{-1} over the temperature range 1000°C to 1500°C for the reaction

$$H + N_2O \rightarrow N_2 + OH$$

The value of 16.0 kcal mole^{-1} is a surprisingly large activation energy for such an exothermic reaction (ΔH°_o = -62.3 kcal mole^{-1})

Henrici and Bauer (121) in order to get the best fit for their data in the reaction of hydrogen and nitrous oxide, behind incident shock waves over the temperature range 1700°K-2600°K, used a value of

$$k_3 = 4.0 \times 10^{13} \exp\left(-\frac{12000}{RT}\right) \text{ cm}^3 \text{ mole}^{-1} \text{ sec}^{-1}$$

for $H + N_2O \xrightarrow{k_3} OH + N_2$

Besides the indirect method of arriving at k_3, there were inconsistencies in their experimental work in the lower temperature range, which could not be reconciled within the frame-work of the assumed mechanism.

<u>The Inhibition Efficiencies of Helium, Carbon Dioxide and Nitrous Oxide in HI Photolysis (2537 Å)</u>

Helium, because of its smaller mass, is a better moderator of hot H atoms than CO_2. From a simple billiard ball collision type of approach, it would take eleven times as many collisions between a CO_2 molecule and an H atom to effect the same amount of energy transfer between a helium atom and an H atom, momentum being conserved in each case.

For the photolysis of HI in the presence of N_2O, Figure 4.8 shows that the H_2 yield falls by some 60% with increasing helium, whereas the H_2 yields falls only by about 30% with increasing CO_2, indicating the greater efficiency of He atoms in moderating hot H atoms. In the region where the inhibition effect of CO_2 starts to level off, the corresponding effect of He on the I_2 (or H_2) production, occurs at a smaller ratio of $\frac{[M]}{[HI]}$.

Examination of Tables 4.9 and 4.13 for the photolysis of HI in the presence of CO_2 and He, shows that as the $\frac{[\text{inert gas}]}{[HI]}$ ratio increases to high values, $\frac{k_7}{k_2}$ tends towards a limiting value. In the process of $\frac{[CO_2]}{[HI]}$ or $\frac{[He]}{[HI]}$ being made larger, $\frac{k_7}{k_2}$ increases from approximately 3.5 to an average value of 12.0. The smaller value of $\frac{k_7}{k_2}$ is associated with the reaction of 'hot' H atoms with HI and I_2, and the larger value, with the reaction of thermal hydrogen atoms with HI and I_2. Figure 4.27 shows the relationship between the experimentally determined values of $\frac{k_7}{k_2}$ (in the presence of CO_2 and He) and the curve obtained by Holmes and Rodgers (83) in their study on the hot atom effects in the gas-phase photolysis of HI.

On the hard spheres collision theory model for atoms and small molecules, both CO_2 and N_2O would be expected to demonstrate similar capabilities for moderating energetic species like hot hydrogen atoms. However, Tables 4.24, 4.25 and Figure 4.28 show that this is not the case. Therefore,

Figure 4.26

Arrhenius plots for $\frac{k_7}{k_2}$ and $\frac{k_2}{k_3}$ at 2537 Å in the presence of the inert gas effect of CO_2.

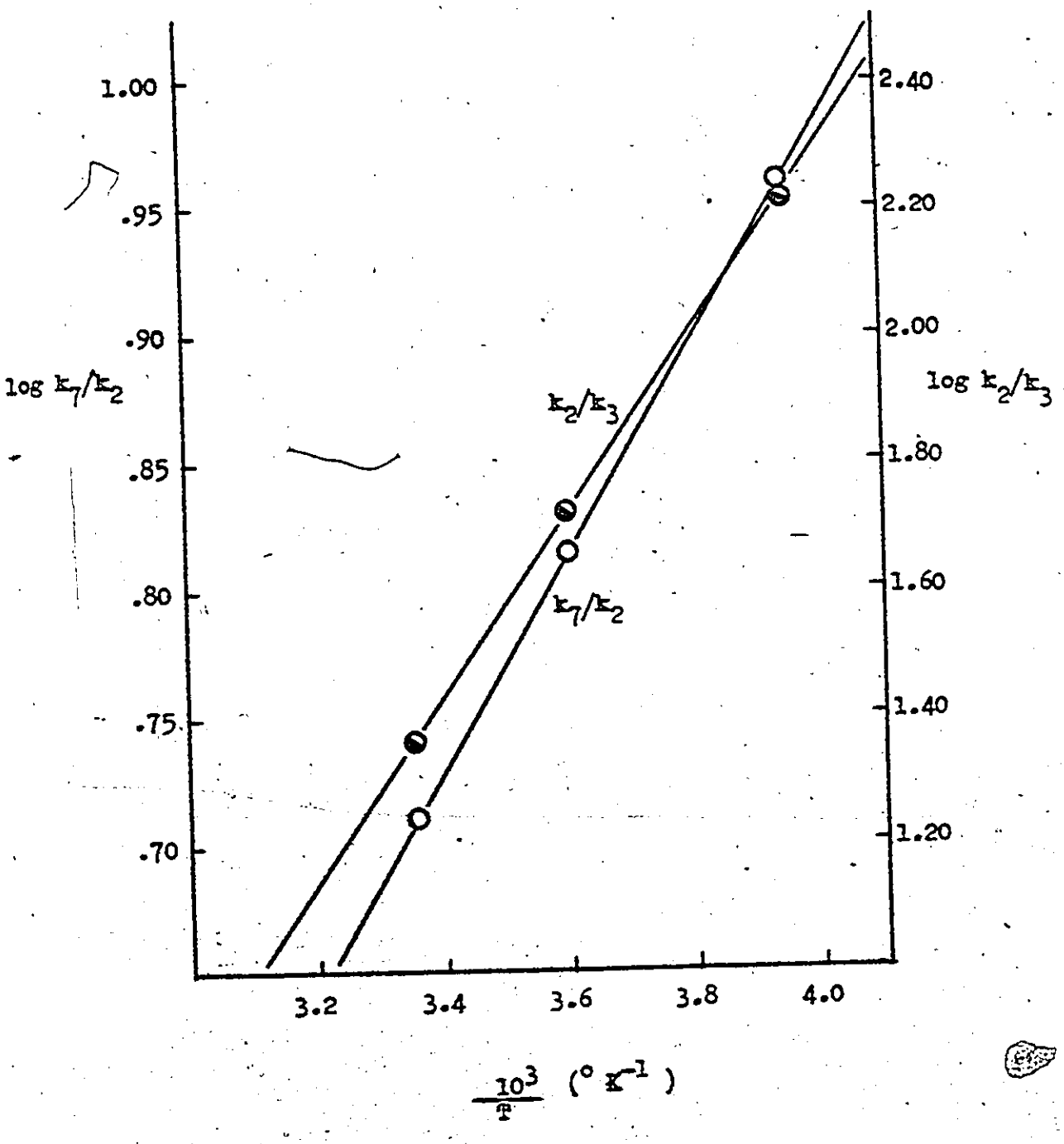
1.00
.95
.90
.85
.80
.75
.70
log k_1/k_2
2.40
2.20
2.00
1.80
1.60
1.40
1.20
log k_2/k_3
k_2/k_3
k_1/k_2
3.2
3.4
3.6
3.8
4.0
$\frac{10^3}{T}$ ($^\circ K^{-1}$)

Figure 4.27

$\frac{k_7}{k_2}$ as a function of $\frac{[\text{inert gas}]}{[HI]}$ ratio at 25°C and 2537 Å

⊖ CO_2

⊖ Helium

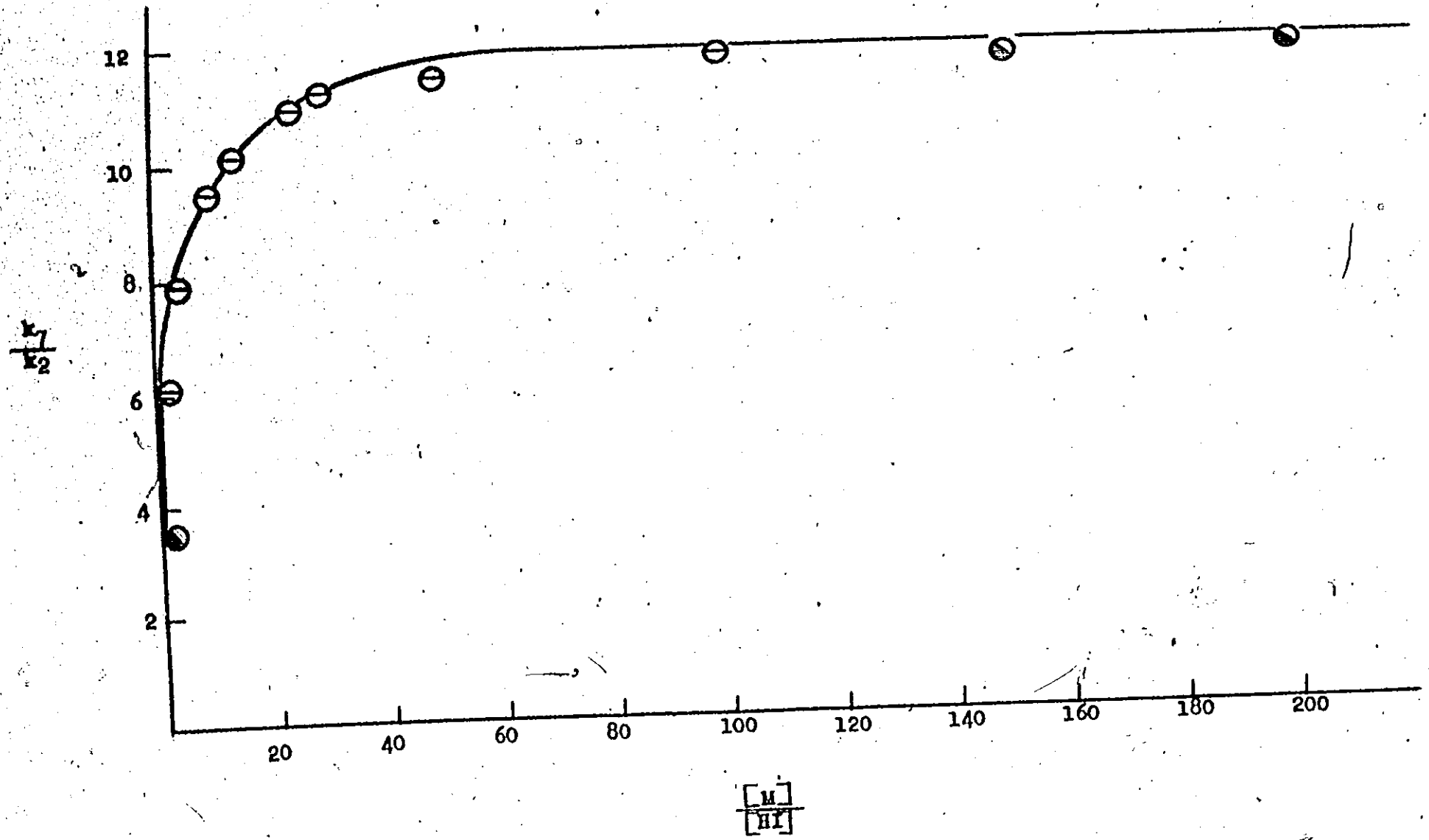
12
10
8
6
4
2
$\frac{k_1}{k_2}$
20
40
60
80
100
120
140
160
180
200
$\frac{[M]}{[HI]}$

TABLE 4.24

Effect of CO_2 on HI Photolysis at 25°C and 2537 Å

[Time 900 seconds]

$\frac{[CO_2]}{[HI]_o}$	$[H_2]$ (μmoles)	$[I_2]$ (μmoles)	$[HI]_o$ (μmoles)	$[HI]_f$ (μmoles)	$[CO_2]$ (μmoles)	ϕ_{H_2} (moles einstein^{-1})
0.0	16.0	16.0	105	73.0	105	1.000
5	14.5	14.5	104	75.1	521	0.905
15	13.3	13.4	105	78.3	1575	0.830
20	12.9	13.0	105	79.0	2083	0.805
30	12.2	12.2	105	80.7	3128	0.763
50	11.3	11.3	104	81.3	5205	0.707
100	10.3	10.3	104	83.4	10,400	0.645
150	10.1	10.1	105	84.8	15,750	0.630
200	10.1	10.1	104	83.7	20,800	0.630

TABLE 4.25

Effect of N_2O on Photolysis of HI at 25°C and 2537 Å

[Time 900 seconds]

$\frac{[N_2O]_o}{[HI]_o}$	$[H_2]$ (μmoles)	$[N_2]$ (μmoles)	$[I_2]$ (μmoles)	$[HI]_o$ (μmoles)	$[HI]_f$ (μmoles)	$[N_2O]_o$ (μmoles)	ϕ_{H_2} (moles einstein^{-1})
0.0	16.0	0.00	16.0	105	73.1	0.0	1.000
1.0	14.6	0.65	15.3	104	73.3	104	0.910
2.0	13.6	1.20	14.8	104	74.5	210	0.850
3.0	12.7	1.62	14.3	104	75.4	313	0.794
4.0	12.3	1.85	14.1	105	76.7	420	0.769
5.0	12.0	1.97	14.0	105	76.9	527	0.755
6.0	11.9	1.98	13.8	105	77.4	630	0.744
7.0	11.8	1.98	13.8	104	76.5	729	0.738
8.0	11.8	1.98	13.8	105	76.4	840	0.738
9.0	11.8	1.98	13.8	105	76.5	945	0.738
10.0	11.8	1.98	13.8	104	76.5	1041	0.738
11.0	11.8	1.98	13.8	104	76.3	1145	0.738

Figure 4.28

Plot of ϕ_{H_2} versus $\frac{[M]}{[HI]}$ ratio for inhibition of H_2 production by N_2O and CO_2 at 25°C and 2537 Å

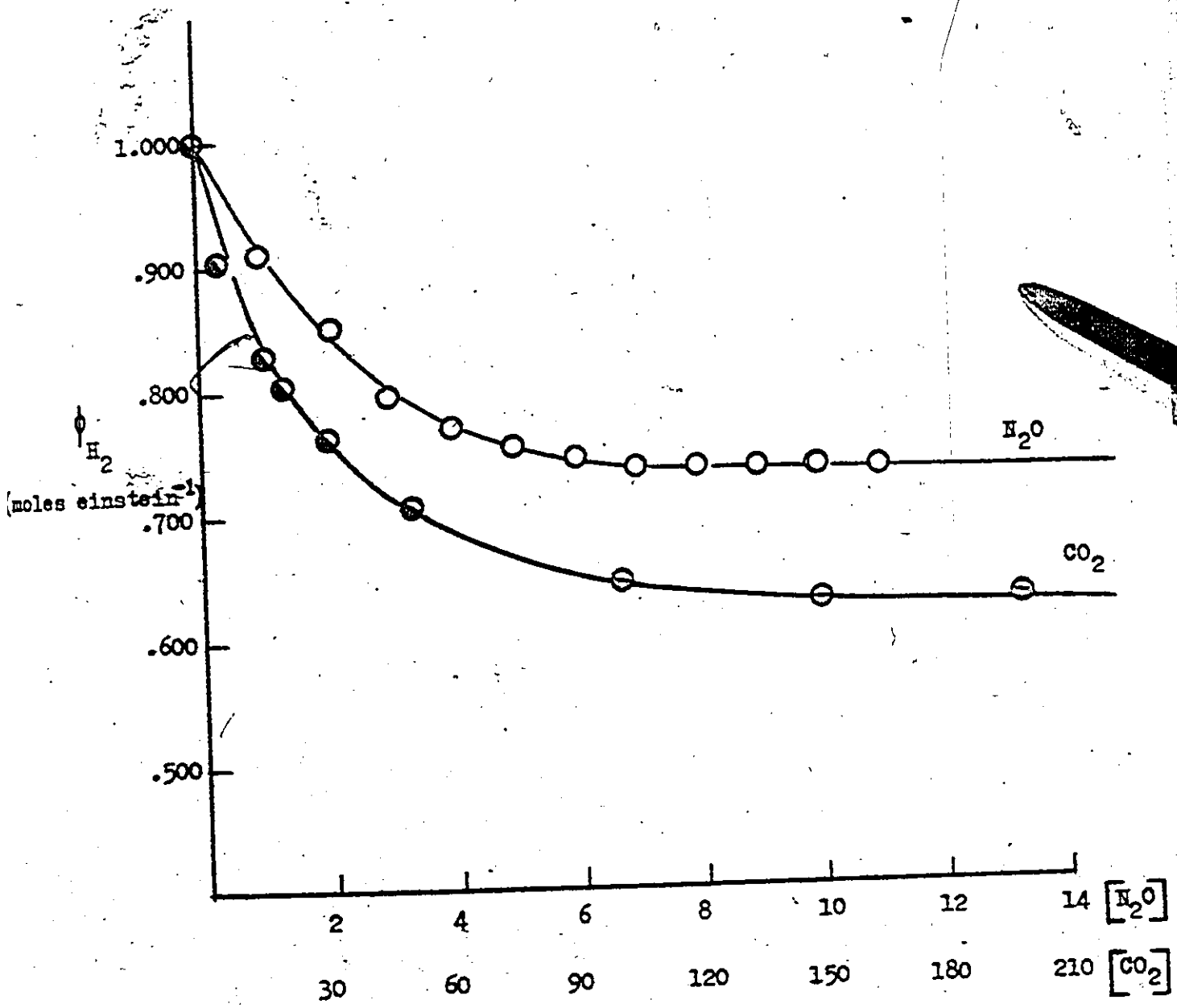
1.000
.900
.800
.700
.600
.500
ϕ_{H_2}
(moles einstein^{-1})
N_2O
CO_2
2
4
6
8
10
12
14 $[N_2O]$
30
60
90
120
150
180
210 $[CO_2]$

$$\frac{[H]}{[HI]}$$

there must be some other factor which serves to distinguish these two molecules insofar as their moderation efficiencies for hot H atoms are concerned.

The molecule of nitrous oxide is linear and unsymmetrical. It may have the structure N–N–O which lies between the two canonical forms N-N≡O and N≡N-O. Its electron structure is probably similar to that of carbon dioxide, which according to Mulliken (122) is

$$\sigma^2\sigma^2\sigma^2\sigma^2\sigma^2\sigma^2\sigma^2\ \pi^4\pi^4$$

corresponding to a $^1\Sigma$ state for a diatomic molecule. A definite prediction as to the nature of the upper electron state is difficult.

Manning and Noyes (123) in their work on 'the photochemical decomposition of nitrous oxide sensitized by mercury vapour', gave some indication of the existence of a definite compound $NO \cdot N_2O$ (N_3O_2) stable at liquid air temperature. It is therefore possible that collisions between N_2O molecules and H' atoms could result in some type of very short life linear complex such as

$$[N{=}{=}N{=}{=}{=}O{-}{-}{-}{-}H]^{\cdot}$$

If we now compare this assumed sticky collision with a similar type of collision between H and CO_2, giving $[COOH]^{\cdot}$, we can discuss the relative inhibition efficiencies in terms of inelastic collisions of the first kind. An inelastic collision of the first kind is an encounter between an atom,

(molecule) and an energetic species (e.g. electron, atom or molecule) in which kinetic energy is converted into excitation energy. When the excitation energy of an atom or molecule is converted into kinetic energy, i.e., heat, the encounter is called a collision of the second kind.

The lowest rotational and vibrational states of CO_2 are energetically lower than those of N_2O (124) and therefore these states are more accessible to kinetic energy transfer to rotational and vibrational forms. Thus an overall transfer of energy into the three most available forms (translational, rotational and vibrational) will favour the CO_2 molecule and this should be reflected in its greater hot atom moderation capacity.

Intensity Variation

Equation (4.16) shows that if the HI, I_2 and N_2O concentrations are kept constant for different series of time-yield experimental runs, while I_a is varied from series to series, then $\frac{d(H_2)}{dt} \cdot \frac{1}{I_a}$ should remain constant. That is,

$$\frac{d(H_2)}{dt} \cdot \frac{1}{I_a} = \frac{1}{1 + \frac{k_7}{k_2}\frac{[I_2]}{[HI]} + \frac{k_3}{k_2}\frac{[N_2O]}{[HI]}} \qquad (4.17)$$

$$= \frac{1}{1 + \frac{k_7}{k_2} K_a + \frac{k_3}{k_2} K_b} \qquad (4.22)$$

$$= \frac{1}{1 + A + B} = K \qquad (4.23)$$

where K_a, K_b, A, B and K are all constants.

Since $I_a \propto I_o$ or $I_a = \rho I_o$, then

$$\frac{d(H_2)}{dt} \cdot \frac{1}{I_a} = \frac{dH_2}{dt} \cdot \frac{1}{\rho I_o}$$

$$\therefore \quad \frac{d(H_2)}{dt} \frac{1}{I_o} = \rho K = \delta \qquad (4.24)$$

(ρ and δ are also constants).

Experimental

Indian-ink solutions of different dilutions were employed as filters in order to assist us in varying the initial light intensities (I_o). The stock quantity was of the Leroy grade. The strengths of these prepared solutions were adjusted by examining them spectrophotometrically to determine how much light they absorbed, and hence the percentage of light which would be allowed to pass at 2537 Å could be regulated by effecting greater dilution or by the strengthening of the filter solutions.

The indian-ink solution was placed in an actinometer cell in a position between the focussing lens and the quartz window of the insulated box housing the reaction vessel. The actinometer cell's diameter was larger than the width of the window, thus ensuring that each ray of light passing through the quartz glass window of the reaction vessel cage, would have passed through the indian-ink

solution. For each time-course run (with a particular I_o value), a fresh solution of the prepared diluted stock solution of indian-ink was used. This was merely a precautionary method, although it was shown that the same solution of indian-ink could be used more than twice with a given set of initial concentrations of HI and N_2O and still produce the same results. Each run was conducted at -20.5°C.

Results and Conclusion

The results of the three sets of experiments at three different initial intensities are shown in Table 4.26, and from the data in this table, three pairs of graphs have been constructed. Figures 4.29, 4.30 and 4.31 show the straight line plots of $[H_2]$ and $[N_2]$ versus time, and from these straight lines, the values of the slopes $\frac{dH_2}{dt}$ (R_{H_2}) and $\frac{dN_2}{dt}$ (R_{N_2}) were obtained.

The S.V.P. of I_2 at -20.5°C is very small (0.104 μmoles for the volume of the reaction vessel used), and by using the 2537 Å wavelength in conjunction with a relatively large initial concentration of HI (> 520 μmoles), the S.V.P. of I_2 is reached very quickly (less than four seconds), and the assumption concerning the constancy of the I_2 concentration during a time-course run, is therefore justified. The quickly attained S.V.P. of I_2 at -20.5°C also allows the time-yield graphs to be linear even in the region of the graphs' origin.

TABLE 4.26

Rate of Hydrogen Production at Different Light Intensities

at -20.5°C (2537 Å)

$\frac{[N_2O]_o}{[HI]_o}$	Time (seconds)	$[H_2]$ (μmoles)	$[N_2]$ (μmoles)	$[I_2]$ (μmoles)	$[HI]_o$ (μmoles)	$[HI]_f$ (μmoles)	$[N_2O]_o$ (μmoles)
A. Intensity, $I_o = 11.14 \times 10^{-8}$ einsteins sec^{-1}							
2.81	300	8.17	0.58	8.81	515	498	1448
2.80	900	24.6	1.71	26.4	523	471	1466
2.80	1200	33.1	2.29	33.4	523	452	1465
2.80	1800	49.1	3.42	52.6	523	417	1458
2.80	2700	74.0	5.14	79.3	520	361	1446
B. Intensity, $I_o = 13.14 \times 10^{-9}$ einsteins sec^{-1}							
2.83	300	0.98	0.12	1.16	522	519	1477
2.81	900	2.95	0.37	3.38	523	516	1469
2.81	1200	3.90	0.49	4.42	524	515	1482
2.83	1800	5.87	0.74	6.67	525	512	1476
2.82	2700	8.75	1.11	9.93	525	505	1481
C. Intensity, $I_o = 27.72 \times 10^{-10}$ einsteins sec^{-1}							
2.81	900	0.61	0.12	0.78	526	525	1479
2.83	1800	1.22	0.24	1.50	526	523	1489
2.82	2400	1.62	0.33	1.98	523	519	1474
2.84	2700	1.83	0.37	2.26	523	519	1486
2.82	3600	2.44	0.49	2.97	525	519	1480

D. Constancy of (R_{H_2}/I_o). $\varepsilon_{HI}(2537\ Å) = 80.0$ litres $mole^{-1}$ cm^{-1}

R_{H_2} (moles sec^{-1})	I_o (einsteins sec^{-1})	(R_{H_2}/I_o) (moles $einstein^{-1}$)	I_a (einsteins sec^{-1})
27.0×10^{-9}	11.14×10^{-8}	0.242	2.79×10^{-8}
32.4×10^{-10}	13.14×10^{-9}	0.245	3.33×10^{-9}
66.7×10^{-11}	27.72×10^{-10}	0.241	6.81×10^{-10}

Figure 4.29

Time course plots for H_2 and N_2 production at $-20.5^{\circ}C$ for $I_o = 11.14 \times 10^{-8}$ einsteins sec^{-1}

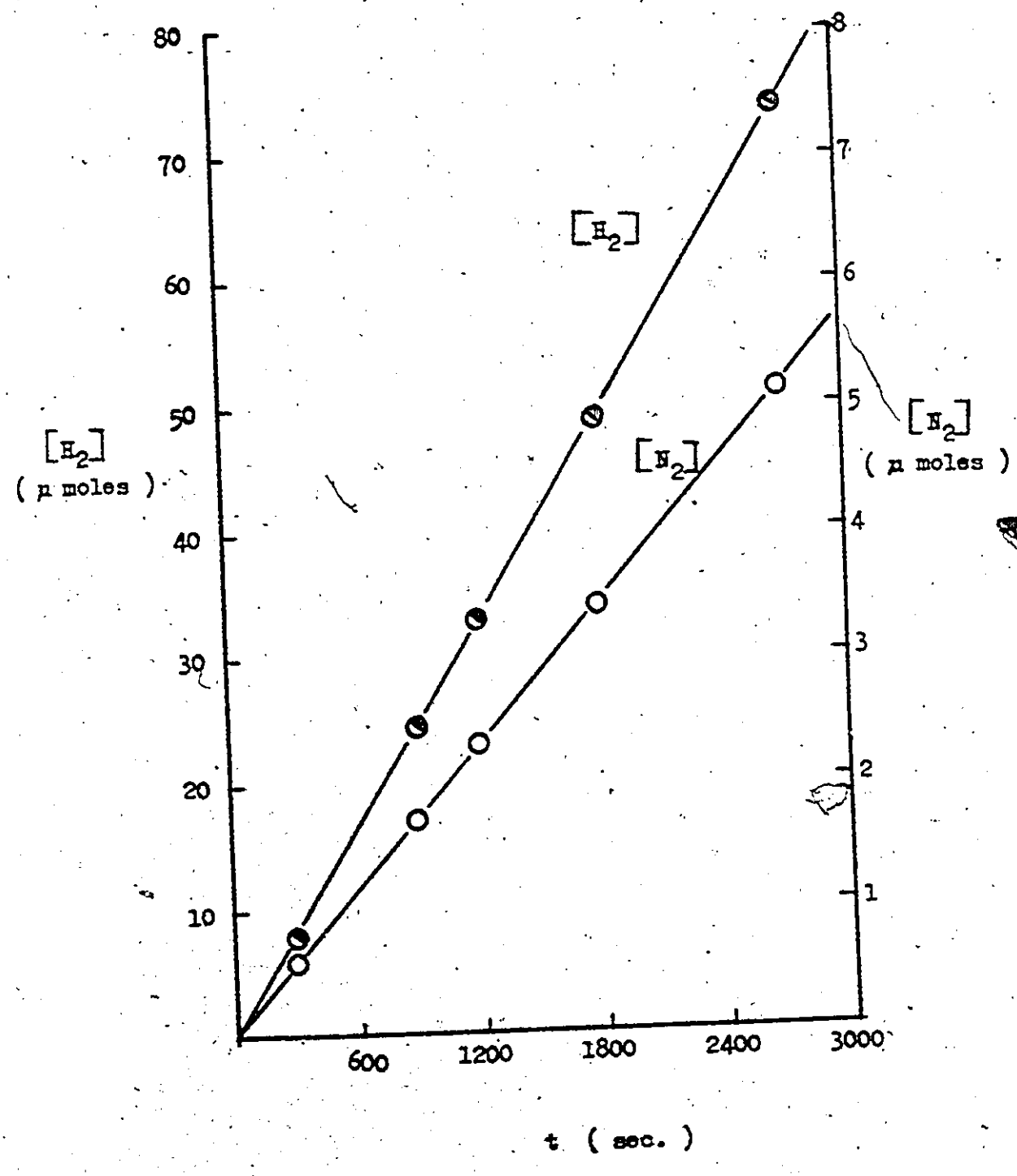
80
70
60
50
40
30
20
10
8
7
6
5
4
3
2
1
[H2]
(μ moles)
[H2]
[N2]
[N2]
(μ moles)
600
1200
1800
2400
3000
t (sec.)

Figure 4.30

Time course plots for H_2 and N_2 production at $-20.5^{\circ}C$ for $I_o = 13.14 \times 10^{-9}$ einsteins sec^{-1}

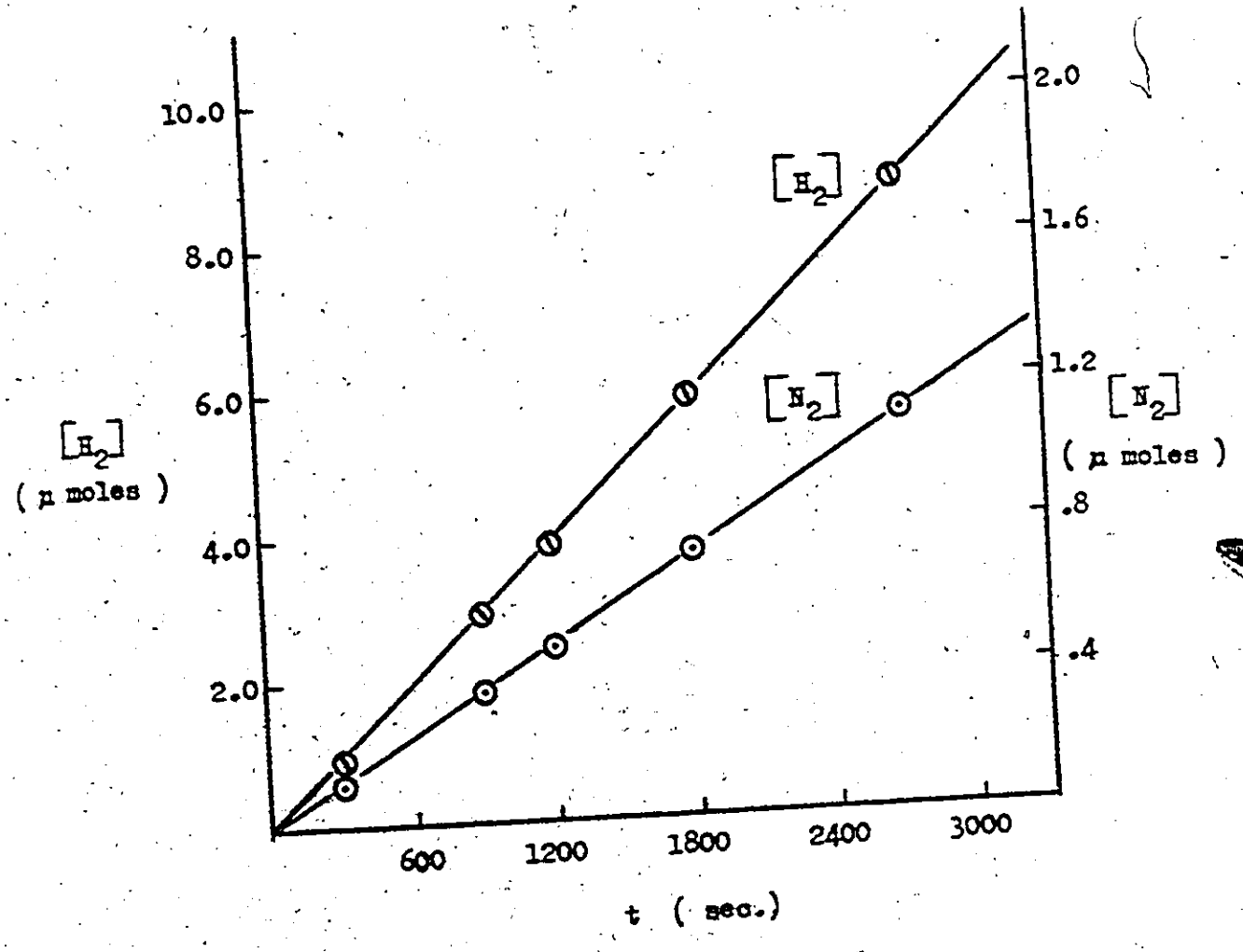
10.0
8.0
6.0
4.0
2.0
[H2]
(μ moles)
2.0
1.6
1.2
.8
.4
[N2]
(μ moles)
[H2]
[N2]
600
1200
1800
2400
3000
t (sec.)

Figure 4.31

Time course plots for H_2 and N_2 production at -20.5°C for $I_o = 27.72 \times 10^{-10}$ einsteins sec^{-1}

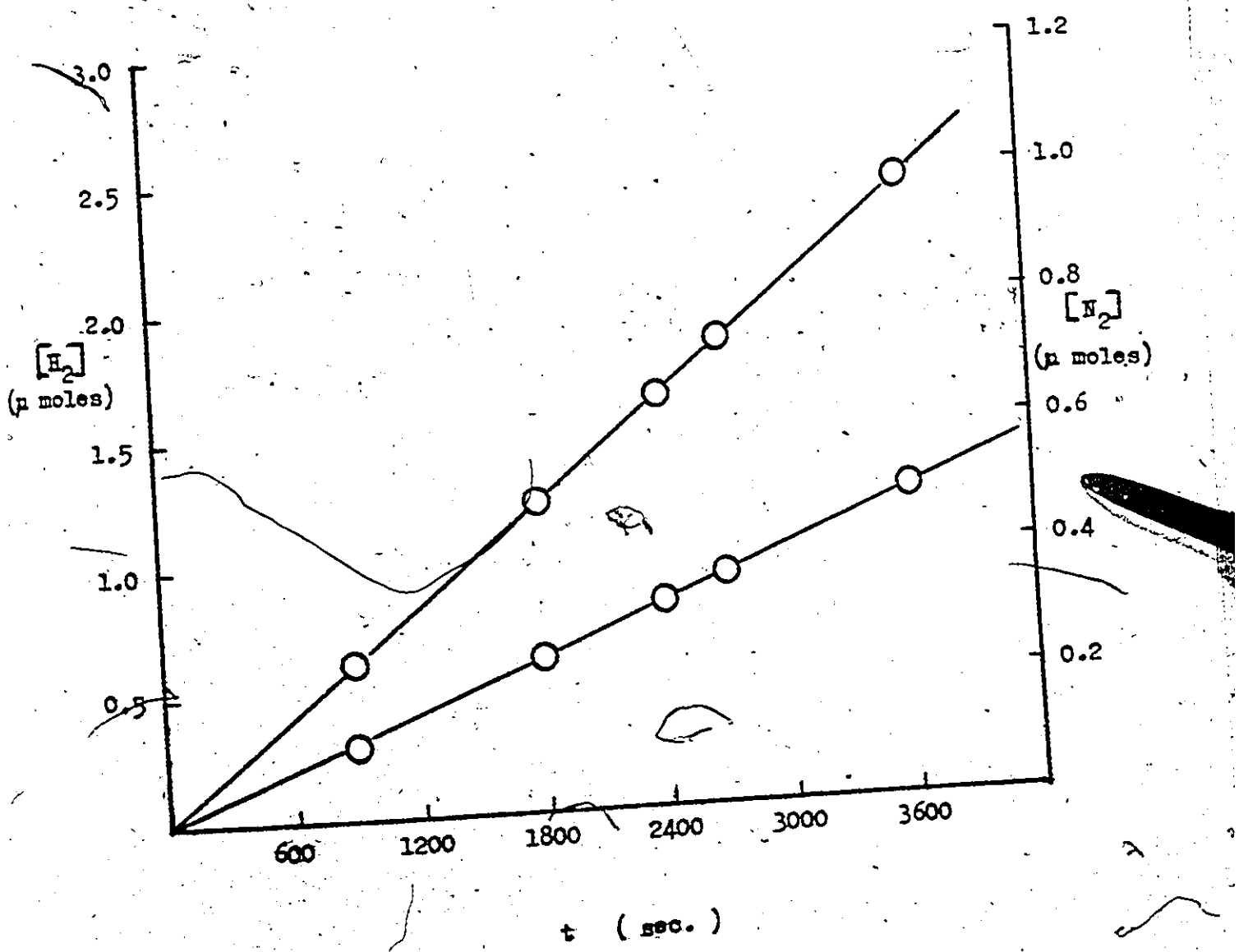
3.0
2.5
2.0
1.5
1.0
0.5
[H2]
(μ moles)
1.2
1.0
0.8
0.6
0.4
0.2
[N2]
(μ moles)
600
1200
1800
2400
3000
3600
t (sec.)

The extinction coefficient with which HI absorbs in the region of 2537 Å was taken as 80.0 from the HI absorption curve in the work of Romand (70). The calculation of the different I_o values were then effected, and the $\frac{R_{H_2}}{I_o}$ ratios were determined. Table 4.26 shows the relative constancy of the $\frac{R_{H_2}}{I_o}$ values. The fact that these ratios (or $\frac{R_{H_2}}{I_a}$ ratios) are constant, supports not only the tenability of equation (4.16) in dealing with the kinetics of the HI/N_2O photochemical system, but also shows that in general the experimental results are in good agreement with the theory.

Hot Atom Treatment of the HI/N_2O Photochemical System

In addition to the classical mechanism

$$H^{\cdot} + HI \xrightarrow{k_2} H_2 + I^{\cdot} \qquad (4.2)$$

$$H^{\cdot} + I_2 \xrightarrow{k_7} HI + I^{\cdot} \qquad (4.7)$$

describing the fate of thermal H atoms, a number of reactions can be written in order to account for the hot atom processes. Such appropriate reactions are,

$$HI \xrightarrow[I_a]{h\nu} H^{\cdot *} + I^{\cdot} \qquad (4.1)$$

$$H^{\cdot *} + HI \xrightarrow{k_{25}} H_2 + I \qquad (4.25)$$

$$H^{\cdot *} + I_2 \xrightarrow{k_{26}} HI + I \qquad (4.26)$$

$$H^{\cdot *} + N_2O \xrightarrow{k_{27}} N_2 + OH \qquad (4.27)$$

$$H^{\cdot *} + N_2O \xrightarrow{k_{28}} H^{\cdot} + N_2O \qquad (4.28)$$

where $H^{\cdot *}$ is a hot H atom, hot enough to react with N_2O, and $H^{\cdot}$ represents all other H atoms. k_{25}, k_{26}, k_{27} and k_{28} are average specific rate constants. From the above reactions, the following rate expressions can be formulated,

$$\frac{dN_2}{dt} = k_{27}[H^*][N_2O] \qquad (4.29)$$

$$\frac{dH_2}{dt} = k_{28}[H^*][N_2O] + k_{25}[H^*][HI] \qquad (4.30)$$

Dividing equation (4.30) by equation (4.29), one obtains:

$$\frac{dH_2}{dN_2} = \frac{k_{28}[N_2O] + k_{25}[HI]}{k_{27}[N_2O]} \qquad (4.31)$$

we have assumed here, that conversions used were low enough (typically in the range of 7%) to avoid very significant scavenging of thermalized hydrogen atoms by I_2. Equation (4.31) can be rewritten as,

$$\frac{[H_2]_1 - [H_2]_o}{[N_2]_1 - [N_2]_o} = \frac{k_{28}}{k_{27}} + \frac{k_{25}}{k_{27}} \frac{[HI]}{[N_2O]} \qquad (4.32)$$

but $[H_2]_o$ and $[N_2]_o$ are both equal to zero, and therefore,

$$\frac{[H_2]}{[N_2]} = \frac{k_{28}}{k_{27}} + \frac{k_{25}}{k_{27}} \frac{[HI]}{[N_2O]} \qquad (4.33)$$

Application of equation (4.33) to the data in Table 4.27 led to the linear plots in Figure 4.32. The slope (S) of each plot $\frac{k_{25}}{k_{27}}$ gives the ratio of the number of hot hydrogen atoms reacting with HI, to the number involved

TABLE 4.27

Product and Reactants Ratios in the Photolysis of Mixtures of HI and N_2O at 25°C

$\frac{[HI]_o}{[N_2O]_o}$	$[H_2]$ (μmoles)	$[N_2]$ (μmoles)	$\frac{[H_2]}{[N_2]}$
A. [λ → 2537 Å][Average $[HI]_o$ = 651 μmoles]			
0.90	24.7	1.80	13.7
0.50	23.7	2.88	8.22
0.33	22.6	3.90	5.80
0.25	21.6	4.91	4.40
0.20	21.0	5.47	3.84
B. [λ → 2537 Å][Average $[HI]_o$ = 373 μmoles]			
0.79	14.8	1.33	11.1
0.50	14.4	1.81	7.93
0.33	13.7	2.46	5.58
0.25	13.1	3.12	4.21
0.20	12.6	3.65	3.45
0.17	12.2	4.05	3.01
C. [λ → 3130 Å][Average $[HI]_o$ = 510 μmoles]			
1.00	13.45	0.99	13.6
0.49	13.21	1.22	10.8
0.33	13.17	1.35	9.76

Figure 4.32

Plot of product ratios against reactants ratios in the photolysis of HI + N_2O mixtures at 25°C

- θ HI + N_2O at 2537 Å (Average $[HI]_o$ = 651 μmoles)
- θ HI + N_2O at 2537 Å (Average $[HI]_o$ = 373 μmoles)
- θ HI + N_2O at 3130 Å (Average $[HI]_o$ = 510 μmoles)

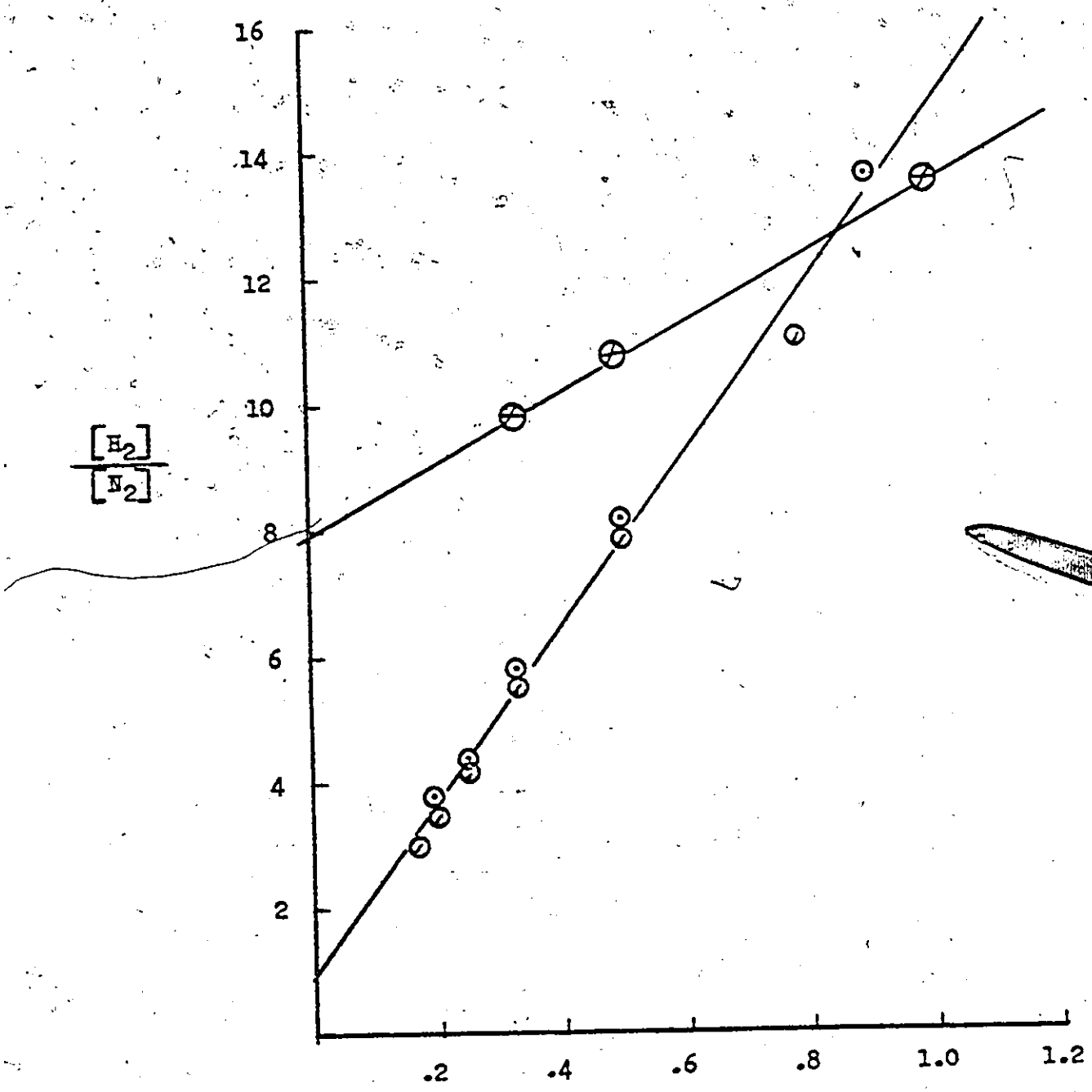
16
14
12
10
8
6
4
2
.2
.4
.6
.8
1.0
1.2
$\frac{[H_2]}{[N_2]}$
$\frac{[HI]}{[H_2O]}$

in reaction with N_2O. The intercept (I) $\frac{k_{28}}{k_{27}}$ gives the ratio of the number of hot hydrogen atoms which are deactivated in collisions with N_2O, to the number which react with N_2O, and the net probability of reaction (4.27) is $P=(1+I)^{-1}$. The respective slopes were calculated as $S_{(2537\ \mathring{A})} = 11.0$ and $S_{(3130\ \mathring{A})} = 5.6$. The intercepts obtained were $I_{(2537\ \mathring{A})} = 0.95$ and $I_{(3130\ \mathring{A})} = 7.9$. Figure 4.32 shows that the net probability P increases with the initial energy of the hydrogen atoms produced by photolysis, and the chance that reaction will occur between a hot H atom and a nitrous oxide molecule relative to the moderation process between these two entities, works out to be 50% at 2537 $\mathring{A}$ and 11% at 3130 $\mathring{A}$. These values seem reasonable in the light of the relatively large exothermicity of the $H + N_2O \rightarrow N_2 + OH$ reaction ($\Delta H^o_o = -62.3$ kcal $mole^{-1}$). Oldershaw et al (125) obtained a value of 12% for the net probability P of $H^* + N_2O \rightarrow OH + N_2$ occurring at 2790 $\mathring{A}$ and a value of about 3% for P at 3130 $\mathring{A}$. The latter value appears to be smaller than what would be expected, and could be a result of experimental errors involved in the measurements of the tiny fractions of N_2 which the authors obtained after degassing H_2 and N_2 from involatile products at liquid nitrogen temperature.

A comparison of $\frac{k_{25}}{k_{27}}$ at both wavelengths of 2537 $\mathring{A}$ and 3130 $\mathring{A}$, indicates that there are approximately twice as many hot atom reactions occurring with the former wavelength as with the latter wavelength.

Moderation of 'Hot' H Atoms by CO_2 and He in the Photolysis of HI (2537 Å)

Two assumptions will be made here, (a) that the moderation that occurs, only does so in collisions with the inert gas and (b) that hot H atoms react principally with hydrogen iodide. There is little change in $R(k_7/k_2)$ with small inert gas additions and the HI quantum yields are very close to two, so that this approximation can be permitted.

The fraction of collisions that occur with the moderating gas can be expressed as

$$\frac{\sigma_M M}{\sigma_M[M] + \sigma_R[HI]} = \frac{1}{(1 + \sigma_R[HI]/\sigma_M[M])} \qquad (4.34)$$

where σ_M and σ_R are the cross-sections for moderation and reaction respectively. When an atom makes N cooling collisions before it becomes thermalized, then the chance that it will do so without reacting, is given by,

$$(1 - \gamma)^* = \left[\frac{1}{1 + \sigma_R[HI]/\sigma_M[M]}\right]^N \qquad (4.35)$$

For the estimation of N, it is necessary that the maximum fraction of the translational energy transferred during a collision, be known. This is expressed as,

$$\frac{\Delta E}{E} = 4\, M_A M_B/(M_A + M_B)^2 \qquad (4.36)$$

where M_A and M_B are the masses of the colliding bodies A and B. Expression (4.36) was derived for a direct collision between A and B along their line of centers (see Appendix 2).

*(γ is the fraction of hot H atom reactions).

In addition, the initial energy of the hot atom, and the minimum energy of the hot atoms must be known. For the 2537 Å wavelength, the initial energy is 42.0 kcal $mole^{-1}$ and the minimum energy is identified with the activation energy of k_2 (E_7 is considered as approximately zero kcal $mole^{-1}$).

$$H^{\cdot} + HI \xrightarrow{k_2} H_2 + I^{\cdot}$$

$$H^{\cdot} + I_2 \xrightarrow{k_7} HI + I^{\cdot}$$

The value of E_2-E_7 obtained in the studies with CO_2 as the inert gas was 1.9 ± 1.10 kcal $mole^{-1}$, and we have chosen the lower value of 0.80 kcal $mole^{-1}$ for the subsequent calculations. The choice of the lower value of E_2-E_7 can be regarded as permissible, since the subsequent treatment is not sensitive to reasonable variations in this value. The value of 0.35 kcal $mole^{-1}$ for E_2-E_7 obtained by Holmes and Rodgers (83) in their studies with He as the inert gas, will be used in calculating the number of collisions N between He and hot H atoms to achieve the required level of moderation (0.35 kcal $mole^{-1}$).

For the calculation of N, the number of moderating collisions, it was necessary to derive another expression which related N, $\frac{\Delta E}{E}$, $E_{(initial)}$ and $E_{(minimum)}$. The expression obtained (see Appendix 3) is shown in equation (4.37)

$$(1 - \frac{\Delta E}{E})^N = \frac{E_{min}}{E_{init}} \qquad (4.37)$$

It therefore requires 5 collisions with helium to moderate hot hydrogen atoms from 42 to 0.35 kcal and 43 collisions with CO_2 for the moderation of hot hydrogen atoms from 42 to 0.80 kcal.

For the classical reactions,

$$H^{\cdot} + HI \xrightarrow{k_2} H_2 + I^{\cdot} \qquad (4.2)$$

$$H^{\cdot} + I_2 \xrightarrow{k_7} HI + I^{\cdot} \qquad (4.7)$$

and the hot atom reactions,

$$H^{\cdot *} + HI \xrightarrow{k_{25}} H_2 + I^{\cdot} \qquad (4.25)$$

$$H^{\cdot *} + I_2 \xrightarrow{k_{26}} HI + I^{\cdot} \qquad (4.26)$$

$$H^{\cdot *} + M \xrightarrow{k_{21'}} H^{\cdot} + M \qquad (4.21')$$

(where M represents the inert gases CO_2 and He), the rate expressions are as follows,

$$\frac{dH^*}{dt} = I_a - k_{25}[H^*][HI] - k_{26}[H^*][I_2] - k_{21'}[H^*][M] \qquad (4.38)$$

$$\frac{dH}{dt} = k_{21'}[H^*][M] - k_2[H][HI] - k_7[H][I_2] \qquad (4.39)$$

$$\frac{dH_2}{dt} = k_2[H][HI] + k_{25}[H^*][HI] \qquad (4.40)$$

assuming one steady state treatment for 'hot' hydrogen atoms and another for thermal hydrogen atoms, we obtain,

$$[H^*] = \frac{I_a}{k_{25}[HI] + k_{26}[I_2] + k_{21'}[M]} \qquad (4.41)$$

and $$[H] = \frac{k_{21'}[H^*][M]}{k_2[HI] + k_7[I_2]} \qquad (4.42)$$

Combination of equations (4.40), (4.41) and (4.42) gives,

$$\frac{dH_2}{dt} = \frac{k_2[HI]I_a\, k_{21'}[M]}{(k_2[HI]+k_7[I_2])(k_{25}[HI]+k_{28}[I_2]+k_{21'}[M]} + \frac{k_{25}[HI]\, I_a}{k_{25}[HI]+k_{26}[I_2]+k_{21'}[M]} \qquad (4.43)$$

i.e. $$\frac{dH_2}{dt} = \frac{k_{25}[HI]\cdot I_a}{k_{25}[HI]+k_{26}[I_2]+k_{21'}[M]} + \frac{k_2[HI]\, I_a\, k_{21'}[M]}{k_{25}[HI]+k_{26}[I_2]+k_{21'}[M]} \cdot \frac{I_a}{(1\ \frac{k_7}{k_2}\ \frac{[I_2]}{[HI]})} \qquad (4.44)$$

Multiplying the first term of the right hand side by

$$\frac{k_{25}[HI] + k_{26}[I_2]}{k_{25}[HI] + k_{26}[I_2]} ,$$

gives,

$$\frac{dH_2}{dt} = \frac{\gamma\, I_a}{(1+R_o\frac{[I_2]}{[HI]})} + \frac{(1-\gamma)I_a}{(1+R_\infty\frac{[I_2]}{[HI]})} \qquad (4.45)$$

where $$\gamma = \frac{k_{25}[HI]+k_{26}[I_2]}{k_{25}[HI]+k_{26}[I_2]+k_{21'}[M]} \qquad (4.46)$$

and is identified with the fraction of hydrogen atoms that undergo hot atom reactions. $(1-\gamma)$ is identified with the fraction of hot hydrogen atoms undergoing moderation. R_o is $\frac{k_{26}}{k_{25}}$ the ratio of the rate constants for the hot reactions

and R_∞ is $\frac{k_7}{k_2}$ the ratio of the thermal rate constants.

It can be seen that if all of the atoms reacted hot, γ would become unity and equation (4.45) would be reduced to the first term. With an infinite amount of moderator present, there would be no hot atom reactions, γ would be zero and equation (4.45) would be reduced to the second term. Both of these limiting equations are of the form

$$I_{abs}xt-(I_2)_f = R\frac{[HI]_i}{4}\ln\frac{[HI]_i}{[HI]_i-2[I_2]_f} - \frac{[I_2]_f}{2} \qquad (4.47)$$

Equation (4.47) is the integrated solution for the rate equation

$$\frac{dI_2}{dt} = \frac{I_{abs}}{(1+R\frac{[I_2]}{[HI]})} = \frac{dH_2}{dt} \qquad (4.48)$$

An adequate evaluation of the parameters of equation (4.45) can be found by interpreting the results in terms of equation (4.47),

i.e. $$\frac{I_{abs}}{(1+R\frac{[I_2]}{[HI]})} = \frac{\gamma I_{abs}}{(1+R_o\frac{[I_2]}{[HI]})} + \frac{(1-\gamma)\ I_{abs}}{(1+R_\infty\frac{[I_2]}{[HI]})} \qquad (4.49)$$

With R_o, R_∞ and $\frac{[I_2]}{[HI]}$ fixed, changes in $\frac{[\text{inert gas}]}{[HI]}$ values should allow us to follow the variation of γ with R, where R is obtained from the formula

$$\frac{1}{\phi_{H_2}} = 1 + R\frac{[I_2]}{[HI]} \qquad (4.50)$$

Here $[I_2]$ is the S.V.P. of $I_2 \equiv 5.20$ μmoles at 25°C.

On re-arranging equation (4.49), an expression for γ turns out to be,

$$\gamma = \frac{(R_\infty - R)(1 + R_o \frac{[I_2]}{[HI]})}{(R_\infty - R_o)(1 + R \frac{[I_2]}{[HI]})} \qquad (4.51)$$

Using $R_\infty = 12$, $R_o = 3.5$ and the R values from Tables 4.9 and 4.13 for corresponding $\frac{[\text{inert gas}]}{[HI]}$ ratios, two sets of γ values were calculated, one set with reference to CO_2 as the inert gas and the other with reference to He. Table 4.28 shows these values and illustrates the relative effect which these gases have in varying $\frac{[M]}{[HI]}$ proportions, on the HI photochemical system with the 2537 Å wavelength.

A combination of equations (4.35) and (4.51) allows the determination of $\frac{\sigma_R}{\sigma_M}$ ratios for both the HI/CO_2 and HI/He systems. The ratios of cross-sections found are also presented in Table 4.28 alongside the γ values. The mean $\frac{\sigma_R}{\sigma_M}$ value for the HI/He system was calculated as 0.50 and agrees well with the value of 0.49 quoted by other authors (71) for a similar system. For moderation by CO_2, the mean value of $\frac{\sigma_R}{\sigma_M}$ was determined as 0.70, indicating that the CO_2 molecule has a smaller cross-section for moderation of hot H atoms than helium.

Although this method of estimating ratios of cross-sections is only approximate, it is still able to give us an adequate evaluation of the relative efficiencies of inert gases in moderating hot H atoms.

TABLE 4.28

Variation of $\frac{k_7}{k_2}$ Values with $\frac{[\text{inert gas}]}{[HI]}$ Ratios at 25°C and 2537 Å

A.

$\frac{[He]}{[HI]}$	$\frac{[HI]}{[He]}$	[HI] (μmoles)	$\frac{k_7}{k_2}$	γ	$\frac{\sigma_R}{\sigma_M}$
2.5	0.40	70.0	6.1	0.60	0.51
5.0	0.20	70.1	7.9	0.38	0.50
10.0	0.10	70.0	9.5	0.22	0.50
15.0	0.07	70.1	10.1	0.16	0.50
25.0	0.04	70.0	10.9	0.09	0.50
30.0	0.03	70.0	11.2	0.07	0.50

B.

$\frac{[CO_2]}{[HI]}$	$\frac{[HI]}{[CO_2]}$	[HI] (μmoles)	$\frac{k_7}{k_2}$	γ	$\frac{\sigma_R}{\sigma_M}$
2.5	0.40	48.2	3.5	1.00	0.70
5.0	0.20	48.2	3.5	0.99	0.70
10.0	0.10	48.0	3.6	0.94	0.70
15.0	0.07	48.2	4.3	0.86	0.70
20.0	0.05	48.3	4.9	0.76	0.70
30.0	0.03	48.0	6.1	0.58	0.70

Summary on Hot Atom Effects

The equations proposed for the treatment of the hot atom chemistry of photochemically produced hydrogen atoms, do not adequately describe all the details of the processes involved. The results obtained in studies or treatments of this kind are very approximate. For instance, deactivation does not always occur at every collision of the hot atom with the moderating gas. In some cases the deactivating influence of a substance is greater than would be expected from the number of collisions calculated from the kinetic theory employing the normal collision diameters, whereas in other instances it is less. The moderating radius or cross-section of the deactivating molecule or atom is thus generally not identical with the normal values.

APPENDIX 1

SOLUTION OF THE DIFFERENTIAL EQUATION DERIVED FROM THE STEADY STATE CONDITION FOR THE PROCESSES:

$$HI + h\nu \xrightarrow{I_a} H^{\cdot} + I^{\cdot}$$

$$H^{\cdot} + HI \xrightarrow{k_2} H_2 + I^{\cdot}$$

$$H^{\cdot} + I_2 \xrightarrow{k_7} HI + I^{\cdot}$$

The steady state condition for the three processes gives

$$\frac{dI_2}{dt} = \frac{E_{abs}}{\{1 + \frac{k_7}{k_2}\frac{[I_2]}{[HI]}\}} = \frac{dH_2}{dt}$$

Let $[I_2] = x$; $[HI]_i = y_i$; $[HI]_f = y_f$; $\frac{k_7}{k_2} = R$ (a constant);

E_{abs} = # Einsteins Absorbed.

Then $$y_f = y_i - 2x$$

$$dy_f = dy_i - 2dx$$

or $$dx = -\frac{dy_f}{2}$$

$$\int dx = \int \frac{E_{abs}\, dt}{\{1 + R\frac{x}{y}\}}$$

or $$\int (1 + R\frac{x}{y})dx = \int E_{abs}\, dt$$

i.e. $$\int dx + R\int \frac{x}{y}\, dx = \int E_{abs}\, dt$$

$$\text{or} \qquad \int dx + \frac{R}{2} \int \frac{y_i - y_f}{y_f} (- dy_f/2) = \int E_{abs}\, dt$$

$$\text{or} \qquad \int \frac{dy_f}{2} - \frac{R}{4} \int \frac{(y_i - y_f)}{y_f}\, dy_f = \int E_{abs}\, dt$$

$$\text{i.e.} \qquad - \int_{y_i}^{y_f} \frac{dy_f}{2} - \frac{R}{4} \int_{y_i}^{y_f} \frac{(y_i - y_f)}{y_f}\, dy_f = \int_o^t E_{abs}\, dt$$

$$\text{i.e.} \qquad - 1/2 \int_{y_i}^{y_f} dy_f - \frac{R}{4} \int_{y_i}^{y_f} \left(\frac{y_i}{y_f} - 1\right) dy_f = \int_o^t E_{abs}\, dt$$

$$\text{i.e.} \qquad \frac{2x_f}{2} - \frac{R}{4}\, y_i [\ln y_f]_{y_i}^{y_t} - \frac{R}{4}(2x_f) = E_{abs} \times t$$

$$\text{or} \qquad x_f - \frac{R}{4}\, y_i \ln y_f + \frac{R}{4}\, y_i \ln y_i - \frac{Rx_f}{2} = E_{abs}\, t$$

$$\text{i.e.} \qquad E_{abs}\, t - x_f = \frac{R}{4}\, y_i \ln \frac{y_i}{y_f} - \frac{R}{2}\, x_f$$

$$\text{i.e.} \qquad E_{abs}\, t - [I_2]_f = R\left[\frac{[HI]_i}{4} \ln \frac{[HI]_i}{[HI]_i - 2[I_2]_f} - \frac{[I_2]_f}{2}\right]$$

where 'i' denotes initial and 'f' denotes final.

APPENDIX 2

THE MAXIMUM FRACTION OF TRANSLATIONAL KINETIC ENERGY WHICH CAN BE TRANSFERRED BETWEEN A MOVING SPECIES OF MASS M_1 AND A STATIONARY SPECIES OF MASS M_2 IN A DIRECT COLLISION ALONG THEIR LINE OF CENTRES

Let V_1 be the velocity of M_1 before collision, V_2 the velocity of M_2 after collision and V the velocity of M_1 after collision. Then for the conservation of momentum,

$$M_1V_1 = M_2V_2 + M_1V \tag{1}$$

and using the principle of the conservation of energy, we have,

$$1/2\ M_1V_1^2 = 1/2\ M_2V_2^2 + 1/2\ M_1V^2 \tag{2}$$

$$= 1/2\ M_2V_2^2 + 1/2\ M_1\left(\frac{M_1V_1 - M_2V_2}{M_1}\right)^2 \tag{3}$$

$$= 1/2\ M_2V_2^2 + 1/2\ \frac{M_1}{M_1^2}\left(M_1^2V_1^2 - 2M_1M_2V_1V_2 + M_2^2V_2^2\right) \tag{4}$$

$$\text{i.e. } 1/2\ M_1V_1^2 = 1/2\ M_2V_2^2 + 1/2\ M_1V_1^2 - M_2V_1V_2 + 1/2\ \frac{M_2^2V_2^2}{M_1} \tag{5}$$

$$\text{i.e. } M_2V_2V_1 = 1/2\ M_2V_2^2 + 1/2\ \frac{M_2^2}{M_1}V_2^2 \tag{6}$$

$$\text{and hence } V_1V_2 = 1/2\left(V_2^2 + \frac{M_2}{M_1}V_2^2\right) \tag{7}$$

$$V_1 = 1/2\ \frac{V_2}{M_1}\left(M_1 + M_2\right) \tag{8}$$

$$\frac{1/2\ M_2V_2^2}{1/2\ M_1V_1^2} = \frac{4M_1^2M_2V_2^2}{M_1V_2^2(M_1 + M_2)^2} = \frac{4M_1M_2}{(M_1 + M_2)^2}$$

APPENDIX 3

DERIVATION OF EQUATION TO FIND N, THE NUMBER OF COLLISIONS OCCURRING BETWEEN AN ENERGETIC SPECIES AND THE MOLECULES (ATOMS) OF AN INERT GAS, WITHIN A SPECIFIED ENERGY RANGE

Let $\frac{\Delta E}{E}$ ($4M_AM_B/(M_A + M_B)^2$) be the fraction of translational kinetic energy lost during a head-on collision between the moving species M_A and the target molecule or atom of mass M_B, and let the initial energy of the energetic species (M_A) be x_E, and its final energy after a number (N) of moderating collisions be y_E.

The energy lost by the first collision would be

$$\frac{\Delta E}{E} \cdot x_E$$

Energy lost in the second collision would be

$$\frac{\Delta E}{E} (x_E - \frac{\Delta E}{E} \cdot x_E)$$

Energy lost in the third collision would be

$$\frac{\Delta E}{E}\{[x_E - \frac{\Delta E}{E}x_E] - \frac{\Delta E}{E} (x_E - \frac{\Delta E}{E} x_E)\}$$

The energy remaining to the energetic species (M_A) after three (3) collisions is then given by

$$[(x_E - \frac{\Delta E}{E} x_E) - \frac{\Delta E}{E}(x_E - \frac{\Delta E}{E}x_E)] - \frac{\Delta E}{E}[(x_E - \frac{\Delta E}{E} x_E) - \frac{\Delta E}{E}(x_E - \frac{\Delta E}{E} x_E)]$$

and this quantity can be labelled y_E

i.e. $x_E - (\frac{\Delta E}{E})\, x_E - (\frac{\Delta E}{E})\, x_E + (\frac{\Delta E}{E})^2\, x_E - (\frac{\Delta E}{E})\, x_E$

$+ (\frac{\Delta E}{E})^2\, x_E + (\frac{\Delta E}{E})^2\, x_E - (\frac{\Delta E}{E})^3\, x_E = y_E$

or $x_E\, [1 - 3(\frac{\Delta E}{E}) + 3(\frac{\Delta E}{E})^2 - (\frac{\Delta E}{E})^3] = y_E$

i.e. $x_E\, (1 - \frac{\Delta E}{E})^3 = y_E$

By the process of induction, it can be shown that in general,

$$x_E\, (1 - \frac{\Delta E}{E})^N = y_E$$

or $$(1 - \frac{\Delta E}{E})^N = \frac{y_E}{x_E} = \frac{E_{minimum}}{E_{initial}}$$

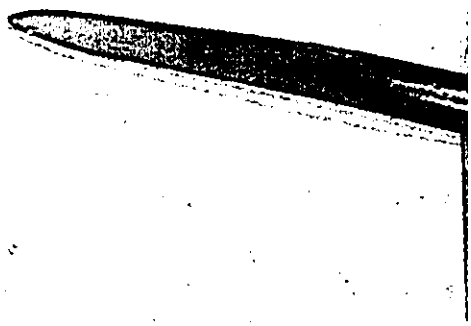

CLAIMS TO ORIGINAL RESEARCH

1. The photolysis of gaseous hydrogen iodide in the presence of nitrous oxide was investigated at 25°C, 5°C and -20.5°C with the 2537 Å, 3130 Å and 3660 Å wavelengths. The same products consisting of H_2, N_2, I_2 and H_2O were obtained at all three temperatures.

2. N_2 yields were lowest at -20.5°C with the 3660 Å wavelength. H_2 production on the other hand, remained almost constant under fixed composition of reactants and a constant λ. The yields of both H_2 and N_2 for any one temperature were highest with the 2537 Å wavelength.

3. A limitation on the production of both H_2 and N_2 was imposed on the photochemical system after a certain $\frac{[N_2O]}{[HI]}$ ratio was reached and this was accounted for by the 'constant partitioning effect' of hot H atoms between reaction and moderation with N_2O.

4. Nitrous oxide inhibited the production of H_2, via the N_2 producing reaction $H^{\cdot} + N_2O \rightarrow N_2 + OH^{\cdot}$.

5. $\frac{k_7}{k_2}$ values and apparent activation energies of E_2-E_7 at different wavelengths were in good agreement with values previously obtained for these parameters. New $\frac{k_2}{k_3}$ and apparent E_3-E_2 values were also estimated.

6. Hot H atom reactions were shown to be unambiguously active in the HI/N_2O photochemical system at each wavelength

by an examination of the effect which added inert gases had on the two rate constant ratios $\frac{k_7}{k_2}$ and $\frac{k_2}{k_3}$ and on N_2 production.

7. Within the limitations of the collision theory for gases, and despite a number of assumptions which were made (such as inelastic collisions between the hot H atoms and the inert gas molecules), parameters such as P, γ and $(\frac{\sigma_R}{\sigma_M})$ seemed to have described the photochemical systems of HI/N_2O, HI/CO_2 and HI/He satisfactorily.

REFERENCES

1. J.W. Draper, Phil. Mag., 1, 368 (1851).
2. J. Stark, Physik. Z., 9, 889 (1908); A. Einstein, Ann. Physik., 37, 832; 38, 881 (1912).
3. M. Bodenstein, Z. Physik. Chem. (Leipzig), 85, 329 (1913).
4. A.N. Terenin, Phys. Rev., 36, 147 (1930); A.N. Terenin and B. Popov, Z. Phys., 75, 338 (1932).
5. K. Watanabe, F.F. Marmo and E.C.Y. Inn, Phys. Rev., 91, 1155 (1953).
6. R.A. Back and D.C. Walker, J. Chem. Phys., 37, 2348 (1962).
7. W.C. Price, R. Bralsford, P.V. Harris and R.G. Ridley, 'Proceedings of the Conference on Molecular Spectroscopy,' Eds. E. Thornton and H.W. Thompson, Pergamon Press, London, 1959, p.54.
8. (a) H. Okabe and J.R. McNesby, J. Chem. Phys., 34, 668 (1961).
   (b) J.R. McNesby, I. Tanaka and H. Okabe, J. Chem. Phys., 36, 605 (1962).
9. E.W.R. Steacie, 'Atomic and Free Radical Reactions,' Reinhold Publishing Co., New York, 1954, p.411.
10. A.C.G. Mitchell and M.W. Zemansky, 'Resonance Radiation and Excited Atoms,' Cambridge Univ. Press, 1961, p.56.
11. A.B. Callear and R.G.W. Norrish, Proc. Roy. Soc. (London), A266, 299 (1962).
12. R.A. Uphaus and H.E. Gunning, J. Chem. Phys., 21, 2229 (1953).

13. Y. Mori, Bull. Chem. Soc., Japan, 34, 1128 (1961).

14. J.E. Cline and G.S. Forbes, J. Am. Chem. Soc., 61, 716 (1939).

15. O.P. Strausz and H.E. Gunning, Can. J. Chem., 39, 2244 (1961).

16. J.D. McGilvery and C.A. Winkler, Can. J. Chem., 30, 194 (1951).

17. W.A. Noyes, Jr., G. Porter and J.G. Jolley, Chem. Rev., 56, 49 (1956).

18. R. Srinivasan, J. Am. Chem. Soc., 81, 1546 (1959).

19. J.C. Anderson and C.B. Reese, Proc. Chem. Soc., 217, (1960).

20. H. Kobsa, J. Org. Chem., 27, 2293 (1962).

21. J. Franck, Trans. Faraday Soc., 21, 536 (1925); E.U. Condon and P.M. Morse, 'Quantum Mechanics,' McGraw Hill, New York, 1929, p.164.

22. K.J. Laidler, The Chemical Kinetics of Excited States, Clarendon Press, Oxford, 1955, p.43.

23. E. Wigner, Nachr. Gotting, Ges., 375 (1927).

24. W.A. Noyes, Jr., and I. Unger, Pure Appl. Chem., 9, 461 (1964).

25. C.F. Goodeve and A.W.C. Taylor, Proc. Roy. Soc. (London), A154, 181 (1936).

26. A.C.G. Mitchell and M.W. Zemansky, 'Resonance Radiation and Excited Atoms,' Cambridge, 1934, Ch.4.

27. H.E. Gunning and O.P. Strausz, in 'Advances in Photochemistry,' Vol. 1, Eds. W.A. Noyes, Jr., G.S. Hammond and J.N. Pitts, Interscience, 1963.

28. (a) O. Stern and M. Volmer, Physik. Z., 20, 183 (1919).
(b) See B. deB. Darwent, J. Chem. Phys., 20, 1673 (1952).

29. V.N. Kondrat'ev, 'Chemical Kinetics of Gas Reactions,' Pergamon Press, London, 1964, p.433.

30. R.B. Cundall and D.G. Milne, J. Am. Chem. Soc., 83, 3902 (1961).

31. H. Spooner, Radiation Res. Suppl., 1, 558 (1959).

32. C.L. Braun, S. Kato and S. Lipsky, J. Chem. Phys., 39, 1645 (1963).

33. R.E. Kellog and R.G. Bennett, J. Chem. Phys., 41, 3042 (1964).

34. H. Ishikawa and W.A. Noyes, Jr., J. Chem. Phys., 37, 583 (1962).

35. M. Kasha, Discussions Faraday Soc., 9, 14 (1950).

36. J.N. Pitts, Jr., F. Wilkinson and G.S. Hammond, "The Vocabulary of Photochemistry," Advances in Photochemistry, Vol. 1, ed. by W.A. Noyes, Jr., G.S. Hammond and J.N. Pitts, Jr., Interscience Publishers, A Division of John Wiley & Sons, New York, p.1.

37. (a) R.S. Mulliken, J. Chem. Phys., 7, 20 (1939).
(b) ibid., 23, 1997 (1955).

38. G. Herzberg, 'Molecular Spectra and Molecular Structure, Spectra of Diatomic Molecules', D. van Nostrand, New York, 1950.

39. H.A. Schwarz, R.R. Williams and W.H. Hamill, J. Am. Chem. Soc., 74, 6007 (1952); R.M. Martin and J.E. Willard, J. Chem. Phys., 40, 2999 (1964).

40. R.G. Gann and J. Dubrin, J. Chem. Phys., 47, 1867 (1967); L.E. Compton and R.M. Martin, J. Chem. Phys., 52, 1613 (1970); G.P. Sturm, Jr., and J.M. White, J. Chem. Phys., 50, 5035 (1969).

41. J.C. Polanyi, J. Chem. Phys., 31, 1338 (1959); J.K. Cashion and J.C. Polanyi, J. Chem. Phys., 35, 600 (1961); N. Basco and R.G.W. Norrish, Can. J. Chem., 38, 1769 (1960).

42. F.P. Lossing, D.G.H. Marsden and J.B. Farmer, Can. J. Chem., 34, 701 (1956).

43. Y. Tanaka, A.S. Jursa and F.J. Leblanc, J. Opt. Soc. Am., 48, 304 (1958).

44. F.S. Feates, B. Knight and E.W.T. Richards, Spectrochim. Acta, 18, 485 (1962).

45. F.J. Comes and E.W. Schlag, Z. Physik. Chem. (Frankfurt), 21, 212 (1959).

46. H. Okabe, J. Opt. Soc. Am., 54, 478 (1964).

47. "Glass Color Filters", Corning Glass Works, Optical Sales Dept., Corning, New York.

48. E.J. Bowen, J. Chem. Soc., 76 (1935), and Chemical Aspects of Light, 2nd Ed., Clarendon, Oxford, 1946, p.276.

49. P.A. Leighton and G.S. Forbes, J. Am. Chem. Soc., 51, 3549 (1929); L.J. Heidt and F. Daniels, J. Am. Chem. Soc., 54, 2384 (1932); E.K. Rideal and J.S. Mitchell, Proc. Roy. Soc. (London), A159, 206 (1937).

50. H. Melville and B.G. Gowenlock, Experimental Methods in Gas Reactions, 2nd Ed., Macmillan and Co., London, 1964.

51. J. Strong, Procedure in Experimental Physics, Prentice Hall, New York, 1939, Ch. 8.

52. W.G. Leighton and G.S. Forbes, J. Am. Chem. Soc., 52, 3139 (1930); G.S. Forbes and L.J. Heidt, J. Am. Chem. Soc., 56, 2363 (1934).

53. C.A. Parker, Proc. Roy. Soc. (London), A220, 104 (1953).

54. W.A. Noyes, Jr., and P.A. Leighton, The Photochemistry of Gases, Reinhold, New York, 1941, p.82.

55. C.M. Masson, V. Boekelheide and W.A. Noyes, Jr., in "Catalytic, Photochemical, Electrolytical Reactions", Technique of Organic Chemistry, Vol. 2, 2nd Ed., A. Weissberger Ed., Interscience Publishers, New York, 1956, p.294.

56. L.P. Zill, Arch. Biochem. Biophys., 59, 473 (1955).

57. K. Porter and D.H. Volman, J. Am. Chem. Soc., 84, 2011 (1962).

58. K. Porter and D.H. Volman, Anal. Chem., 34, 748 (1962).

59. C.G. Hatchard and C.A. Parker, Proc. Roy. Soc. (London), A235, 518 (1956).

60. J. Lee and H.H. Seliger, J. Chem. Phys., 40, 519 (1964).

61. D.S. Herr and W.A. Noyes, Jr., J. Am. Chem. Soc., 62, 2052 (1940).

62. D.S. Weir, J. Am. Chem. Soc., 83, 2629 (1961).

63. A.G. Leiga and H.A. Taylor, J. Chem. Phys., 41, 1247 (1964).

64. M. Zelikoff and L.M. Aschenbrand, J. Chem. Phys., 22, 1685 (1954).

65. S. Cremer and A. Margreiter, Z. Phys. Chem., 199, 90 (1952).

66. G.N. Lewis and M. Randall, "Thermodynamics", p.525, McGraw-Hill Book Co., New York, 1923.

67. C.F. Goodeve and A.W.C. Taylor, Proc. Roy. Soc., (London), A154, 181 (1936).

68. G.K. Rollefson and J.E. Booher, J. Am. Chem. Soc., 53, 1728 (1931).

69. (a) R.S. Mulliken, Phys. Rev., 50, 1017 (1936);
(b) ibid., 51, 310 (1937);
(c) ibid., 57, 500 (1940);
(d) J. Chem. Phys., 8, 382 (1940).

70. J. Romand, Ann. Phys. (Paris), 4, 527 (1948); Compt. Rend., 227, 117 (1948).

71. R.M. Martin and J.E. Willard, J. Chem. Phys., 40, 2999 (1964).

72. For Reviews of the Literature, see (a) W.A. Noyes, Jr., and P.A. Leighton, 'The Photochemistry of Gases,' Reinhold Publishing Corp., New York, 1941.
(b) D.A. Armstrong and J.L. Holmes, 'The Decomposition of Halides and Derivatives', Comprehensive Chemical Kinetics, Ed. C.H. Bamford and C.F.H. Tipper, Elsevier Publishing Company, New York, Volume 4, p.143.

73. E. Warburg, Sitzber. Preuss. Akad. Wiss., 26, 300 (1926).

74. M. Bodenstein and F. Lieneweg, Z. Physik. Chem. (Leipzig), 119, 123 (1926).

75. J.H. Sullivan, J. Chem. Phys., 30, 1292 (1959).

76. J.H. Sullivan, J. Chem. Phys., 36, 1925 (1962).

77. J.L. Holmes and E.V. Sundaram, Trans. Faraday Soc., 62, 910 (1966).

78. K.F. Bonhoeffer and L. Farkas, Z. Physik. Chem., 132, 235 (1928).

79. R.A. Ogg and R.R. Williams, J. Chem. Phys., 11, 214 (1943).

80. R.A. Ogg and R.R. Williams, J. Chem. Phys., 13, 586, (1945).

81. R.A. Ogg and R.R. Williams, J. Chem. Phys., 15, 691 (1947).

82. W.H. Hamill, H.A. Schwarz and R.R. Williams, J. Am. Chem. Soc., 74, 6007 (1952).

83. J.L. Holmes and P. Rodgers, Trans. Faraday Soc., 64, 2341 (1968).

84. R.J. Carter, W.H. Hamill and R.R. Williams, J. Am. Chem. Soc., 77, 6457 (1955).

85. R.M. Martin and J.E. Willard, J. Chem. Phys., 40, 3007 (1964).

86. M.F.A. ElSayed and R. Wolfgang, J. Am. Chem. Soc., 79, 3286 (1957).

87. (a) G.M. Harris and J.E. Willard, J. Am. Chem. Soc., 76, 4678 (1954).

87. (b) J.R. Majer and J.P. Simons, 'Advances in Photochemistry', Vol. II, ed. by W.A. Noyes, Jr., G.S. Hammond and J.N. Pitts, Jr., Interscience Publishers, A Division of John Wiley & Sons, New York, 1964, p.137.

88. (a) R.D. Schultz and H.A. Taylor, J. Chem. Phys., 18, 194 (1950).

(b) F.P. Hudson, R.R. Williams, Jr., and W.H. Hamill, J. Chem. Phys., 21, 1894 (1953).

89. C. Zener, Phys. Rev., 37, 556 (1931).

90. K.E. Shuler and R. Zwanzig, J. Chem. Phys., 33, 1778 (1960).

91. F.H. Mies and K.E. Shuler, J. Chem. Phys., 37, 177 (1962).

92. M. Bodenstein, Z. Physik. Chem., 13, 56 (1894).

93. G.B. Kistiakowsky, J. Am. Chem. Soc., 50, 2315 (1928).

94. E.W.R. Steacie, 'Atomic and Free Radical Reactions', 2nd Ed., Reinhold Publ. Corp., New York, N.Y., 1954.

95. R.S. Mulliken, J. Chem. Phys., 8, 382 (1940).

96. R.D. Penzhorn and B. DeB. Darwent, J. Phys. Chem., 72, 1639 (1968).

97. R.D. Penzhorn and B. DeB. Darwent, 'Abstracts of the Sixth International Conference of Photochemistry', Bordeaux, September 1971.

98. G.R. Woolley and R.J. Cvetanovic, J. Chem. Phys., 50, 4697 (1969).

99. B.G. Dzantiev and A.V. Shishkov, High Energy Chem., 1, 164 (1967).

100. B.G. Dzantiev, A.K. Lyubimova and A.V. Shishkov, High Energy Chem., 3, 438 (1969).

101. C.F. Goodeve and N.O. Stein, Trans. Faraday Soc., 27, 393 (1931).

102. (a) G. Herzberg, 'Electronic Spectra of Polyatomic Molecules', D. van Nostrand Co., Inc., Princeton, N.J., 1966.

(b) G. Porter, Discussions Faraday Soc., 9, 60 (1950).

(c) D.A. Ramsay, J. Chem. Phys., 20, 1920 (1952).

103. J. A. Kerr, Chem. Rev., 487 (1966).

104. V.H. Dibeler and S.K. Liston, J. Chem. Phys., 49, 482 (1962).

105. B. deB. Darwent, R.L. Wadlinger and M.J. Allard, J. Phys. Chem., 71, 2346 (1967).

106. B.G. Dzantiev and A.V. Shishkov, Khim. Vysokikh Energii, 1, 192 (1967).

107. R.L. Wadlinger and B. deB. Darwent, J. Phys. Chem., 71, 2057 (1957).

108. B. deB. Darwent and R. Roberts, Proc. Roy. Soc., (London), A216, 344 (1953).

109. N.O. Stein, Trans. Faraday Soc., 29, 583 (1933).

110. G.S. Forbes, J.E. Cline and B.C. Bradshaw, J. Am. Chem. Soc., 60, 1431 (1938).

111. R.P. Steer and A.R. Knight, Can. J. Chem., 46, 2878 (1968).

112. A. Farkas and H.W. Melville, 'Experimental Methods in Gas Reactions,' Macmillan and Co., London, 1934, p.255.

113. A.I. Vogel, 'A Text Book of Quantitative Inorganic Analysis,' Longmans, London, 1946, p.338, 340.

114. Handbook of Physics and Chemistry, 49th Ed., Chemical Rubber Co., Ohio.

115. G.A. Oldershaw and D.A. Porter, Nature, 223, 490 (1969).

116. R.E. Tomalesky and J.E. Sturm, Trans. Faraday Soc., 7, 1241 (1972).

117. A.I. Vogel, 'A Text Book of Quantitative Inorganic Analysis,' Longmans, London, 3rd Ed., p.783.

118. D.A. Armstrong and J.L. Holmes, 'Comprehensive Chemical Kinetics,' Ed., C.H. Bamford and C.F.H. Tipper, Elsevier Publishing Company, New York, Volume 4, p.143.

119. H.W. Melville, Proc. Roy. Soc., (London) A146, 737 (1934).

120. C.P. Fenimore and G.W. Jones, J.Phys.Chem., 63, 1154 (1959).

121. H. Henrici and S.H. Bauer, J. Chem. Phys., 50, 1133 (1969).

122. R.S. Mulliken, Phys. Rev., 40, 60 (1932).

123. W.M. Manning and W.A. Noyes, Jr., J. Chem. Phys., 54, 3907 (1932).

124. G. Herzberg, (a) 'Molecular Spectra and Molecular Structure, Vol. 2, Infra-red and Raman Spectra of Polyatomic Molecules,' Van Nostrand, 1945.
(b) 'Electronic Spectra of Polyatomic Molecules,' D. Van Nostrand Co., Inc., Princeton, N.J., 1966.

125. G.A. Oldershaw, D.A. Porter and A. Smith, J.C.S., Faraday, 1, 68, 2218 (1972).